MISR overview and observational principles
Data products
Example data applications

David J. Diner
Jet Propulsion Laboratory, California Institute of Technology

Exploring and Using MISR Data
Greenbelt, MD
September 2005

MISR characteristics

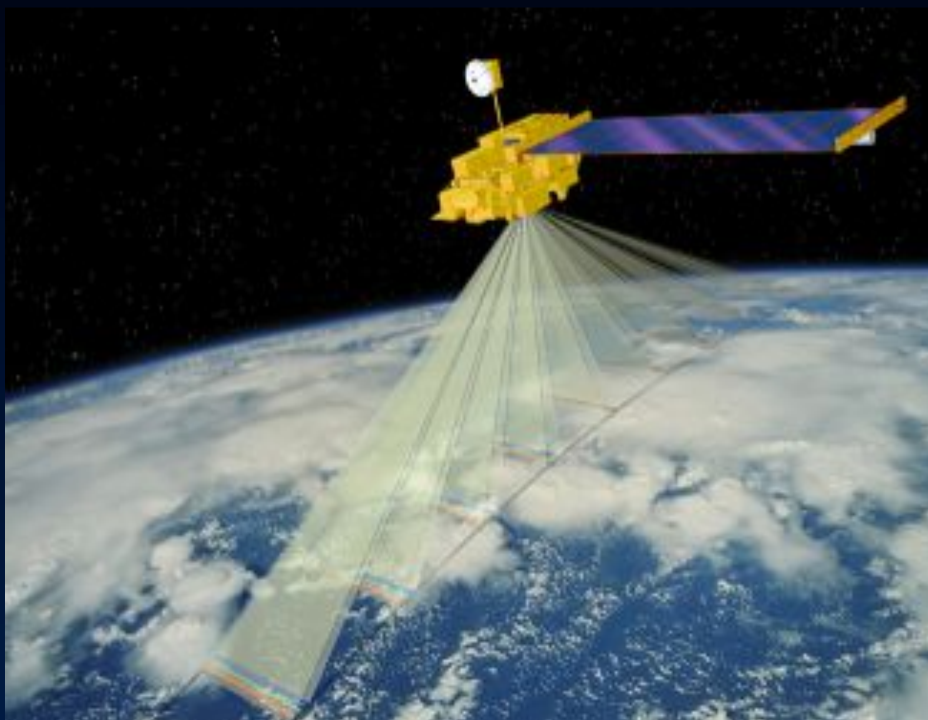

Flies on Terra

9 view angles at Earth surface:
70.5°. 60.0°, 45.6°, 26.1° forward of nadir
nadir
26.1°, 45.6°, 60.0°, 70.5° backward of nadir

Four spectral bands at each angle:
446 nm ± 21 nm
558 nm ± 15 nm
672 nm ± 11 nm
866 nm ± 20 nm

Global Mode (continuous):
275 m sampling in all nadir bands and
red band of off-nadir cameras
1.1 km for the other channels

Local Mode (targeted): 275 m all channels

400-km swath: Complete zonal coverage
9 days at equator, 2 days at poles

14-bit quantization

Radiometrically, geometrically calibrated

AirMISR

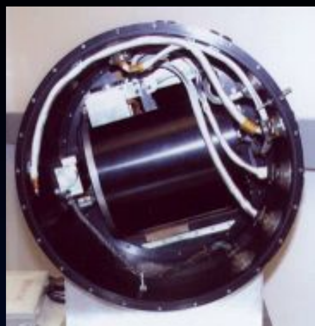

Flies in nose of NASA ER-2

Covers MISR's nine angles

Uses gimballed MISR prototype camera

27.5 m georectified spatial resolution

9 x 11 km area covered at all angles

Data available at LaRC DAAC

46° images near Howland, ME 28 August 2003

Why multi-angle?

1. Change in brightness, color, and contrast with angle helps distinguish different types of surfaces, clouds, and airborne particles (aerosols)

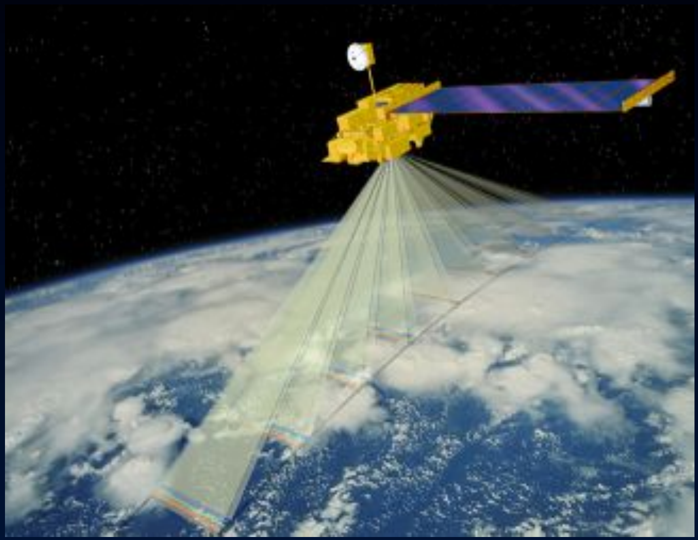

2. Oblique slant paths through the atmosphere enhance sensitivity to aerosols and thin cirrus

3. Changing geometric perspective provides 3-D views of clouds

4. Time lapse from forward to backward views makes it possible to use clouds as tracers of winds aloft

5. Different angles of view enable sunglint avoidance or accentuation

6. Integration over angle is required to estimate hemispherical reflectance (albedo) accurately

Example areas of research

What is the abundance and distribution of different aerosol types, and how are these related to source locations and characteristics?

How does the surface respond to climate change or other disturbances? How does vegetation canopy structure affect photosynthetic and shortwave radiation fluxes?

How does 3-dimensional cloud structure affect our ability to relate cloud hydrological and radiative properties?

New ways of using MISR data are still being discovered.

MISR instrument

Family portrait

The “V-9” optical bench

Undergoing test

JPL’s Space Simulator Facility

MISR on Terra spacecraft

Terra launch
18 December 1999

MISR calibration

Absolute radiometric uncertainty 3%
Relative radiometric uncertainty 2%
Temporal stability 1%
Geolocation uncertainty 50 m
Camera-to-camera registration < 275 m

MISR On-Board Calibrator

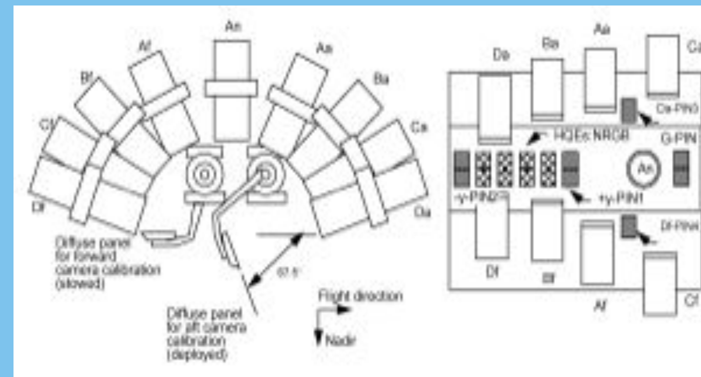

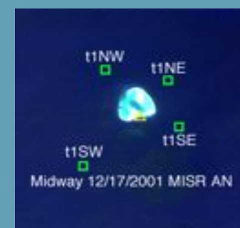

Vicarious calibrations and validations over desert playas and dark water sites

AirMISR

MISR lunar images

Calibration, geolocation, resampling, and co-registration occurs during Level 1 processing

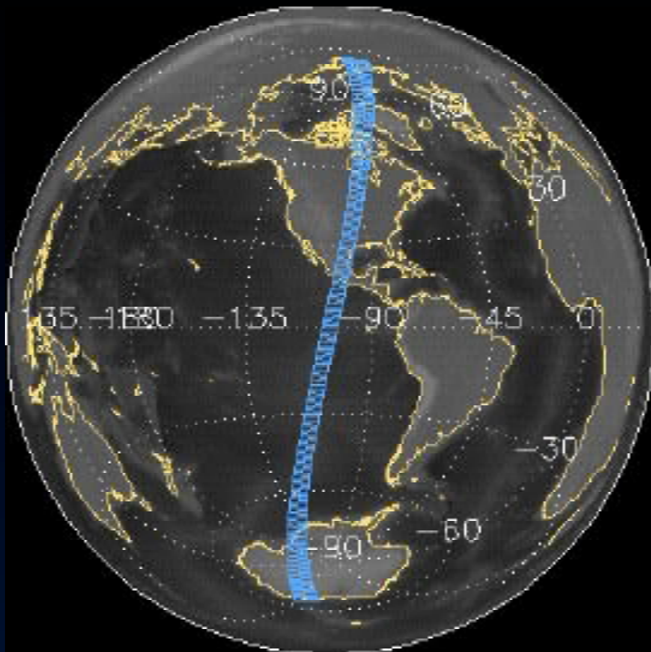

Space Oblique Mercator projection

233 unique paths in 16-day repeat-cycle of Terra orbit

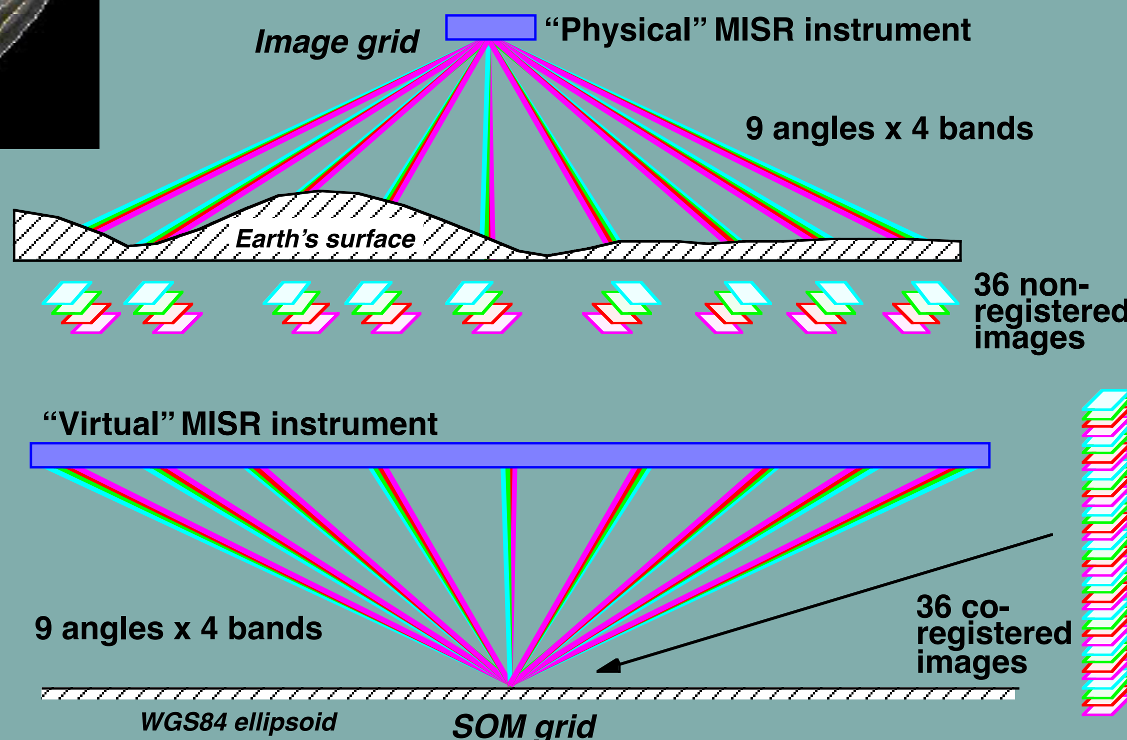

Instrument science modes

Global

- Pole-to-pole coverage on orbit dayside
- Full resolution in all 4 nadir bands, and red band of off-nadir cameras (275-m sampling)
- 4x4 pixel averaging in all other channels (1.1-km sampling)

Local

- Implemented for pre-established targets (1-2 per day)
- Provides full resolution in all 36 channels (275-m sampling)
- Pixel averaging is inhibited sequentially from camera Df to camera Da over targets approximately 300 km in length

Calibration

- Implemented bi-monthly
- Spectralon solar diffuser panels are deployed near poles and observed by cameras and a set of stable photodiodes

Objects along a camera line-of-sight have multiple “locations” on the Space Oblique Mercator grid

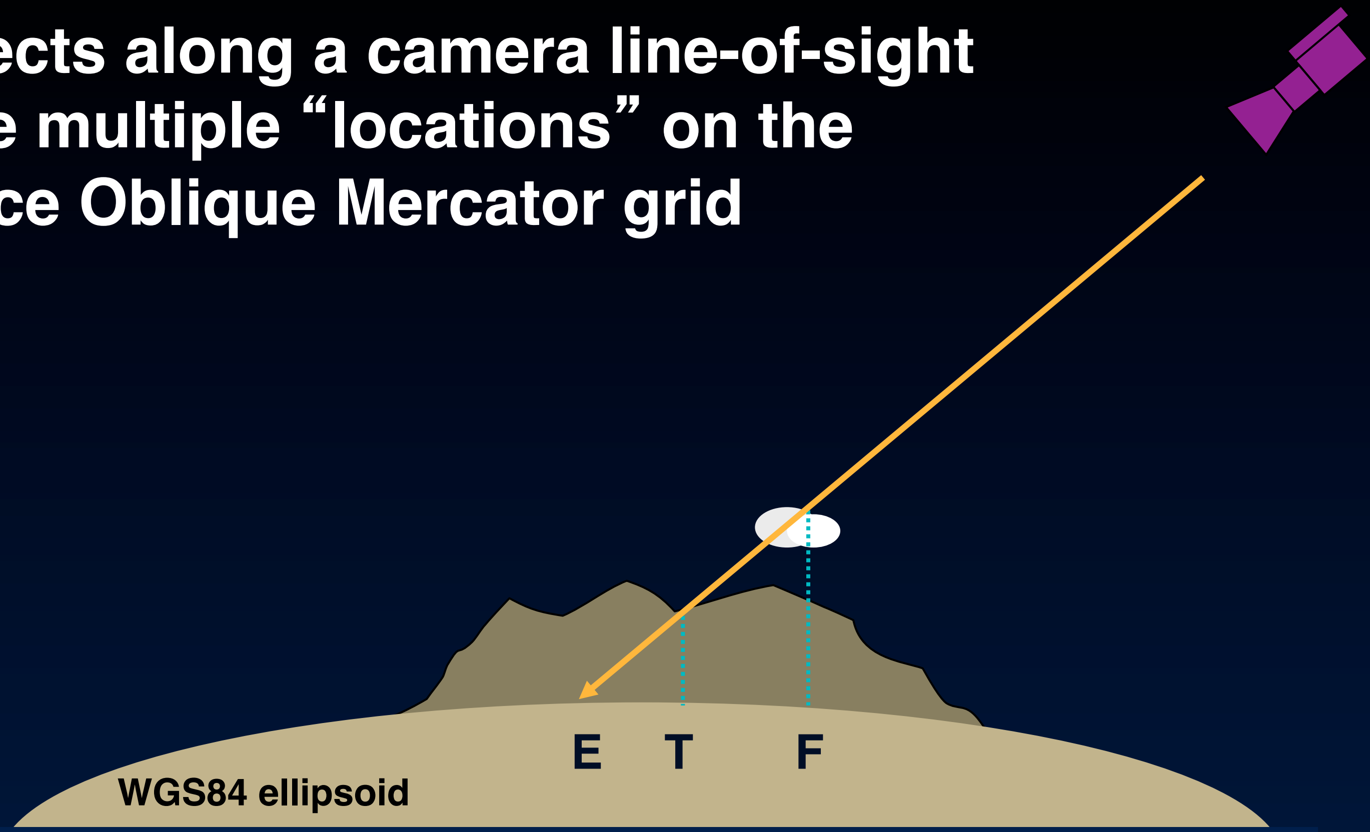

E = ellipsoid-projected location
T = terrain-projected location
F = feature-projected location

Camera-to-camera co-registration requires establishing a reference altitude

"Ellipsoid projection" is to the WGS84 ellipsoid

- performed during Level 1 processing
- used as input to stereoscopic processing

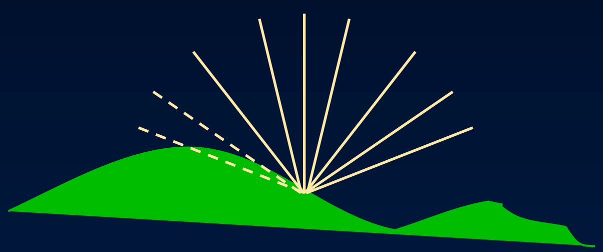

"Terrain projection " is to a digital elevation model

- performed during Level 1 processing
- used as input to aerosol/surface processing
- some views may be obscured

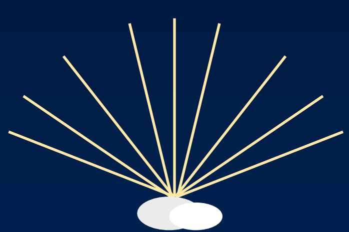

"Feature projection" uses stereoscopically derived cloud heights

- performed during Level 2 processing
- used as input to albedo and cloud classifiers processing

MISR data product generation

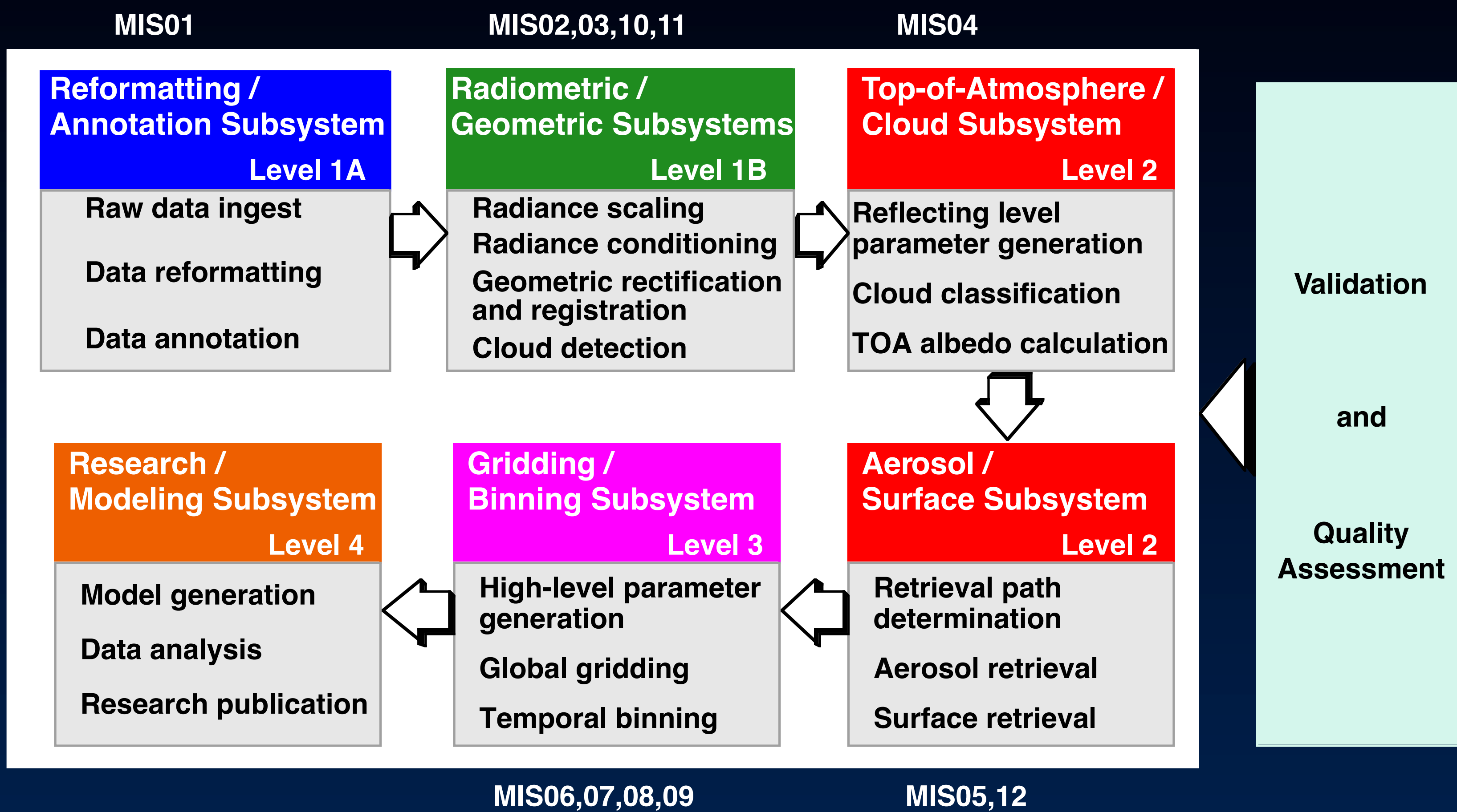

Level 1 Standard Products

Level 1 standard products

- Level 1A reformatted, annotated product
- Level 1B1 radiometric product
- Level 1B2 georectified radiance product, in two flavors:
  - ellipsoid
  - terrain (blocks containing land only)
- Level 1B2 browse (JPEG)
- Level 1B2 geometric parameters
- Level 1B2 radiometric camera-by-camera cloud mask

Space Oblique Mercator is used as the projection to minimize resampling distortions

Level 1 processing operates on each camera individually

A data "granule" is an entire pole-to-pole swath

L1B2 Georectified Radiance Product (MIS03)

Georectified (Earth-projected) radiance data

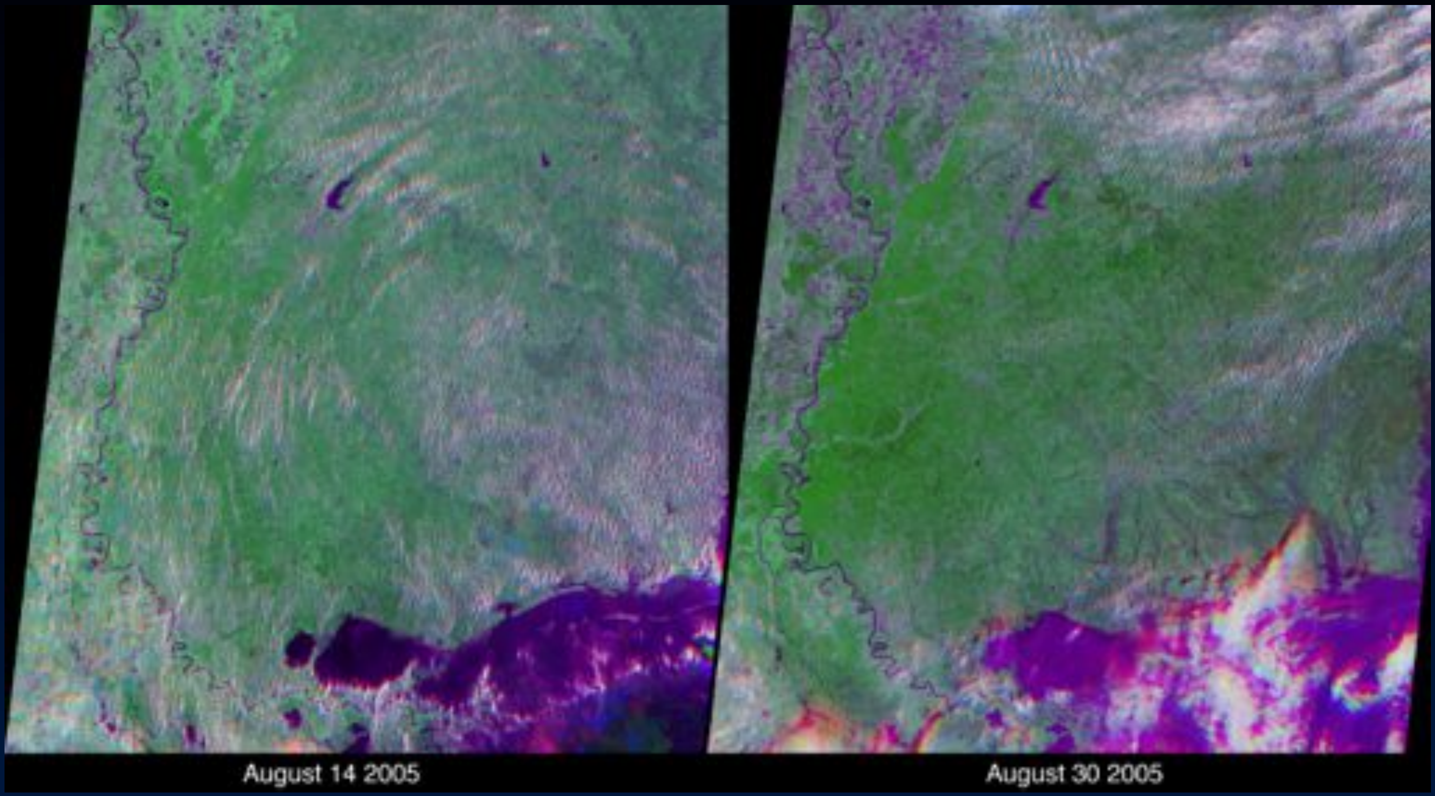

Multi-spectral, multi-angle composites of Mississippi and Louisiana before and after Hurricane Katrina
Blue: 46° forward red Green: Nadir NIR Red: 46° backward red

CONTENTS

- Space-Oblique Mercator map-projected calibrated radiances and radiometric data quality indicators (RDQI)
- Scale factors to convert radiances to top-of-atmosphere BRF’s

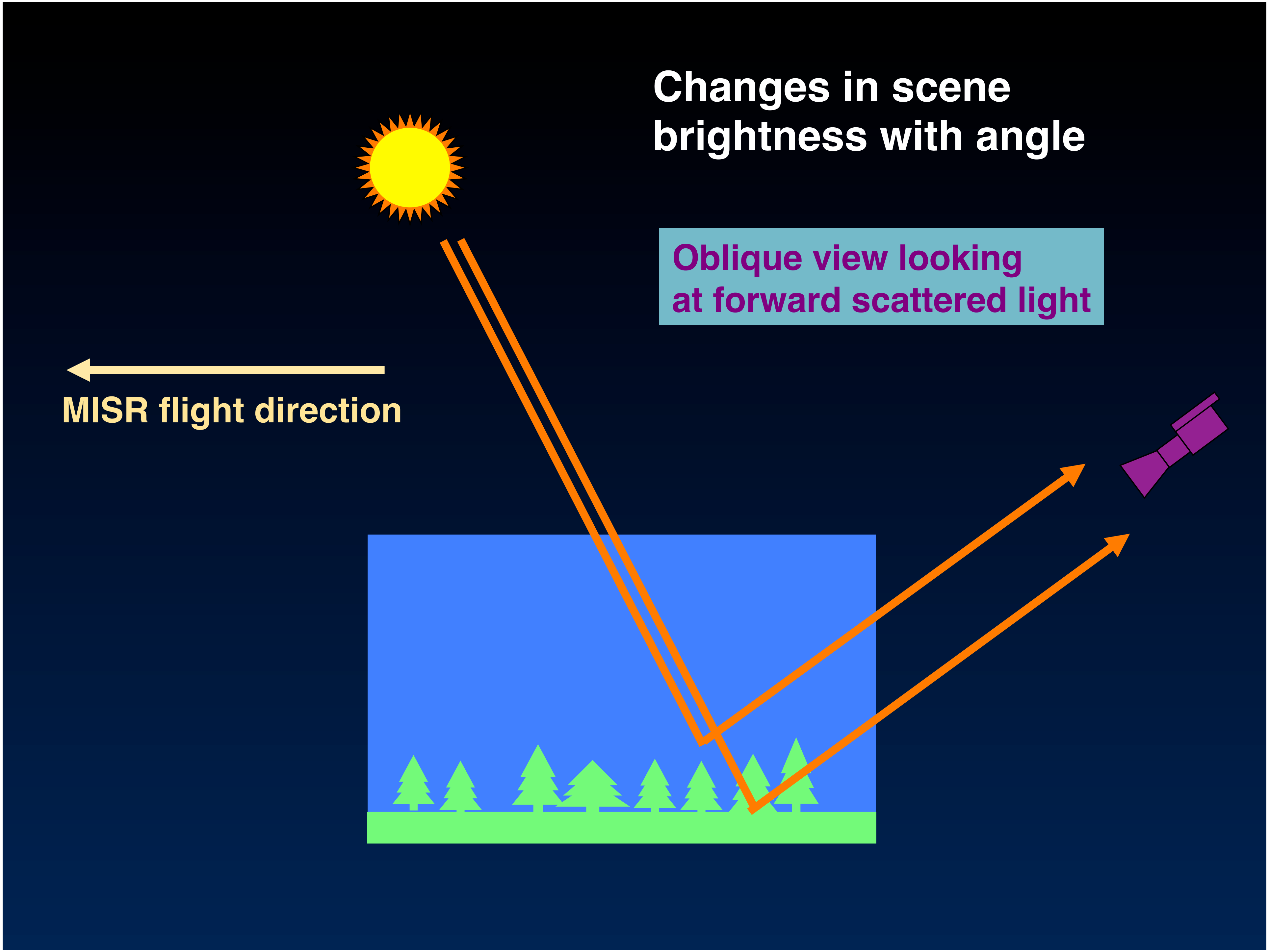
Changes in scene brightness with angle
Oblique view looking at forward scattered light
MISR flight direction

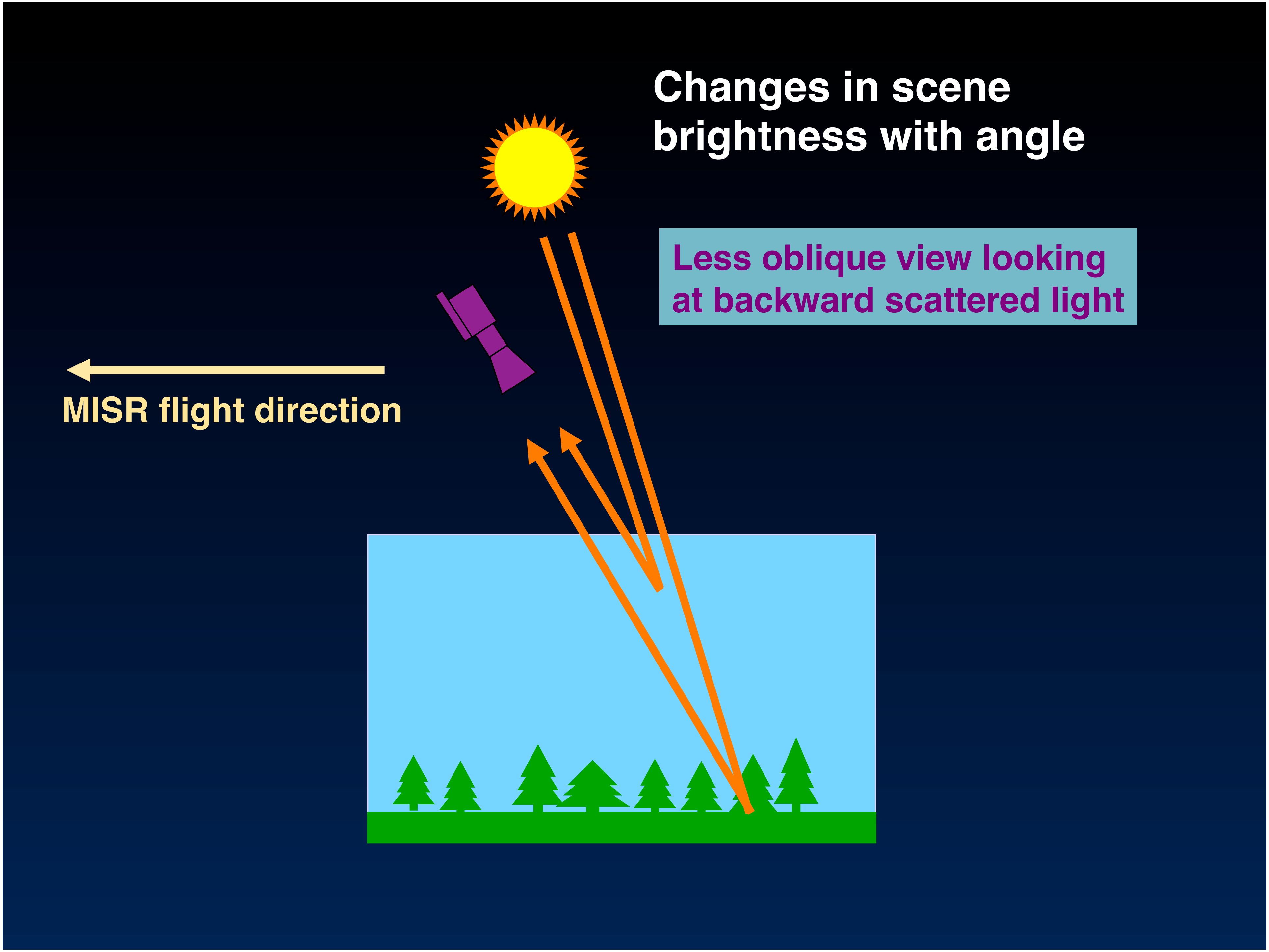
Changes in scene
brightness with angle
Less oblique view looking
at backward scattered light
MISR flight direction

Multiangle magic—making the invisible appear

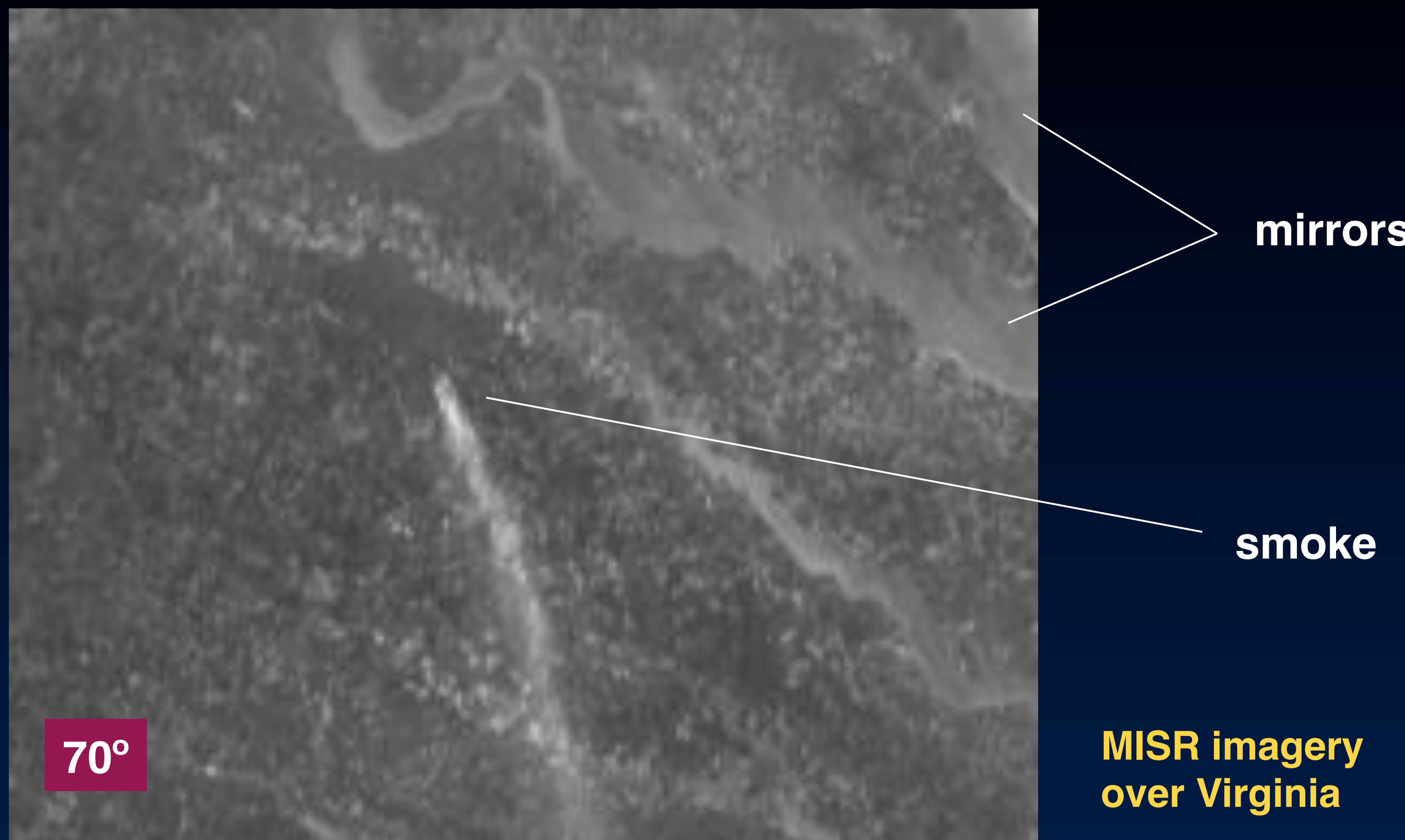

MISR imagery
over Virginia

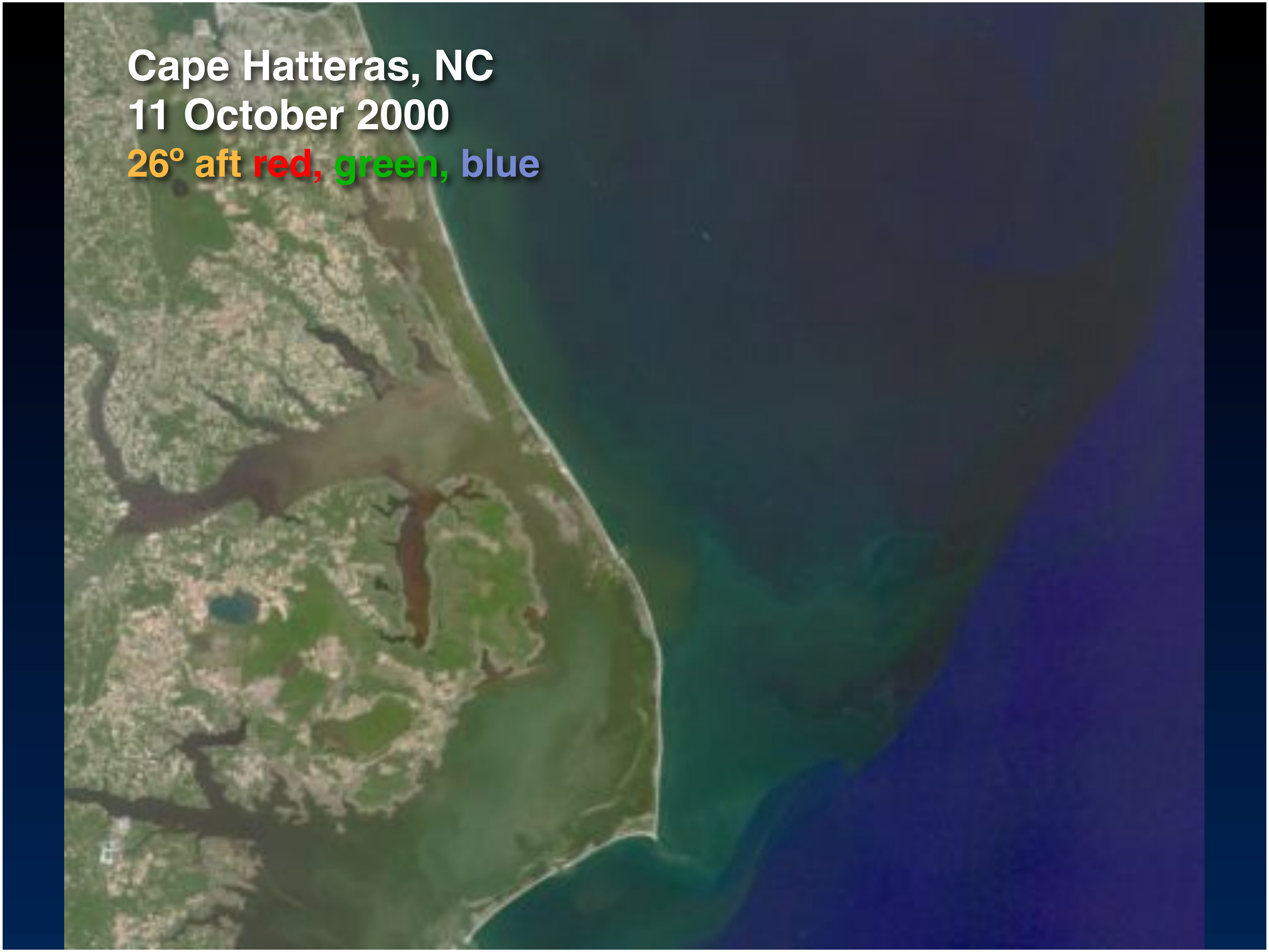
Cape Hatteras, NC
11 October 2000
26º aft red, green, blue

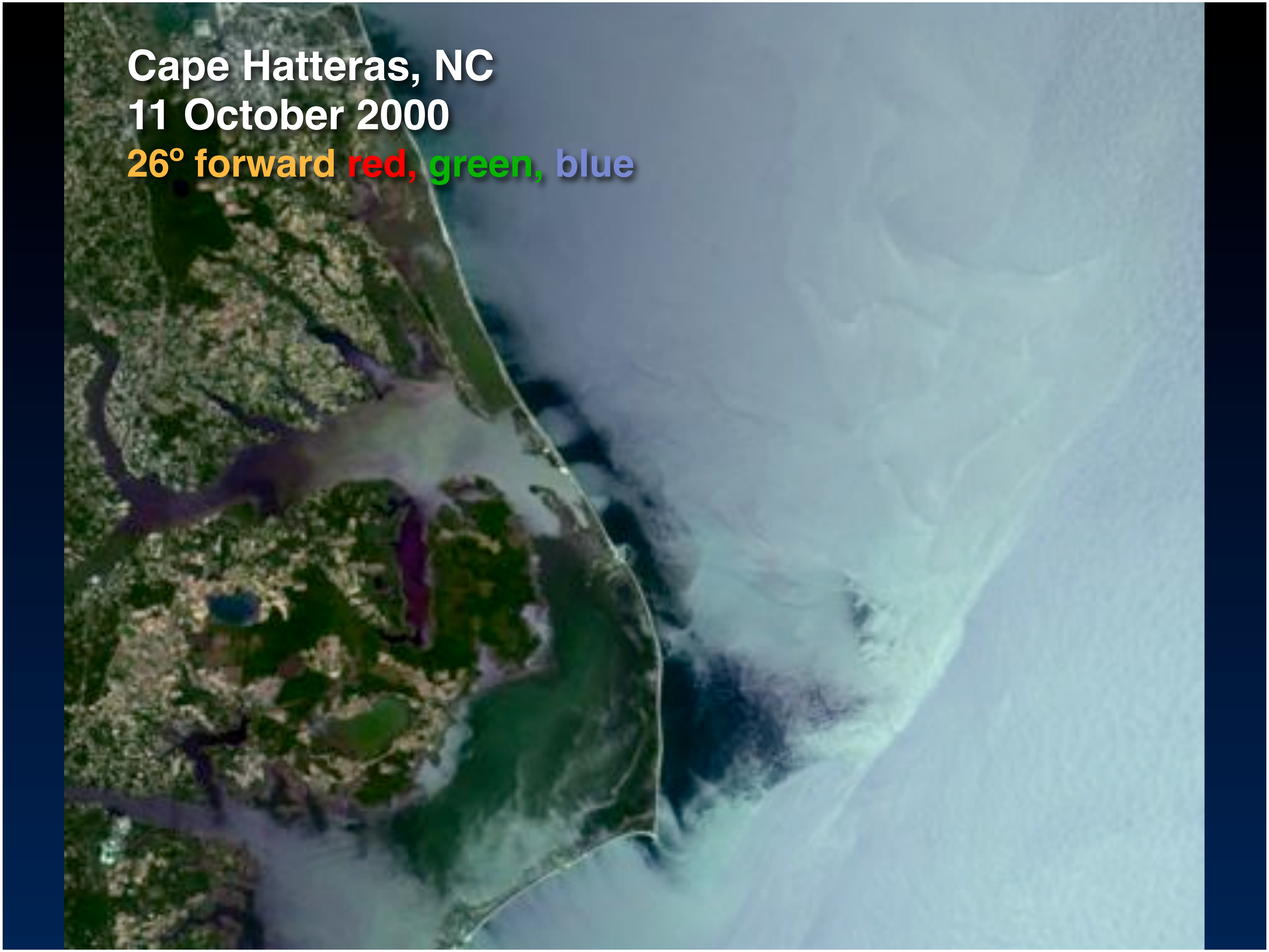
Cape Hatteras, NC
11 October 2000
26° forward red, green, blue

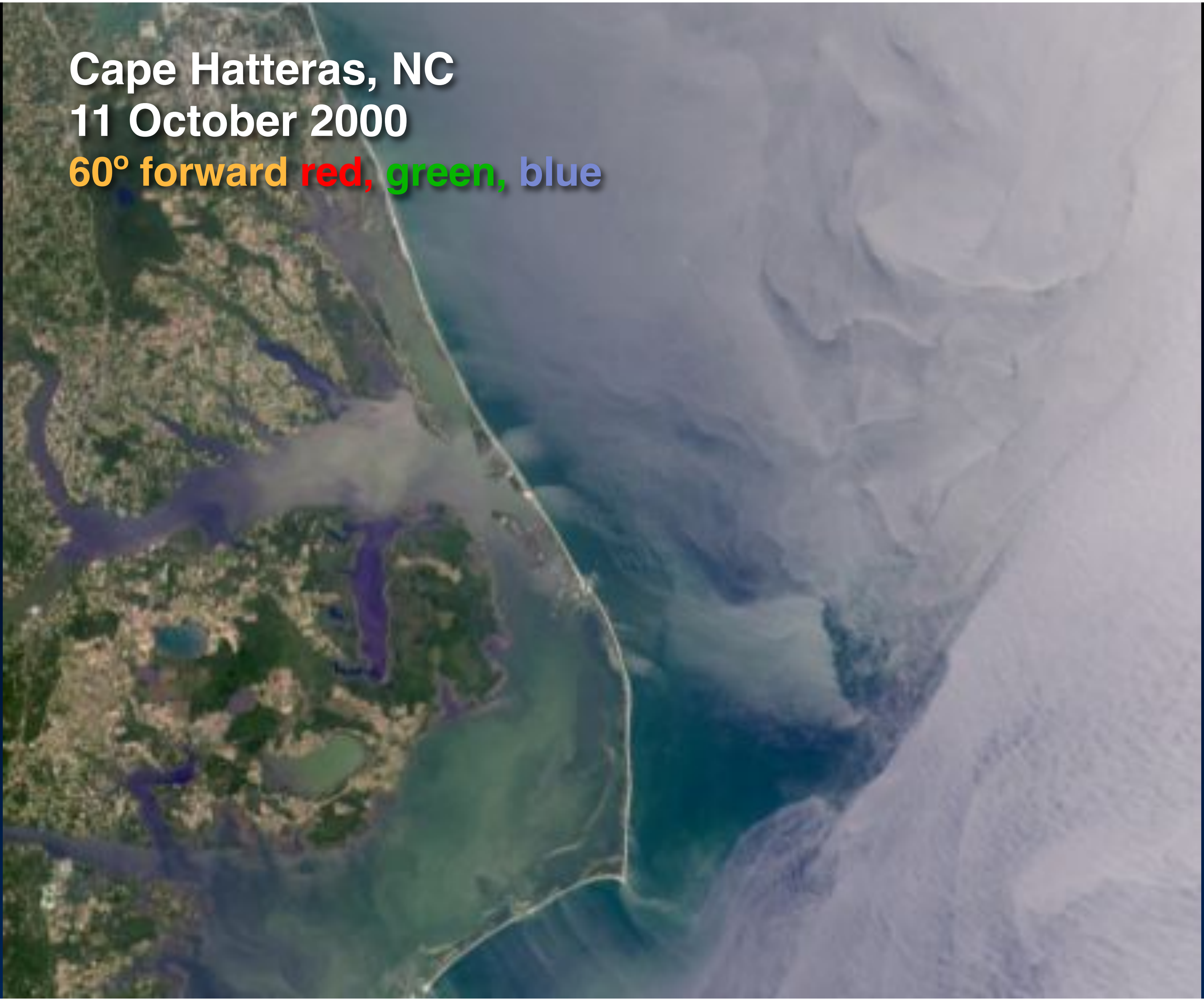
Cape Hatteras, NC
11 October 2000
60º forward red, green, blue

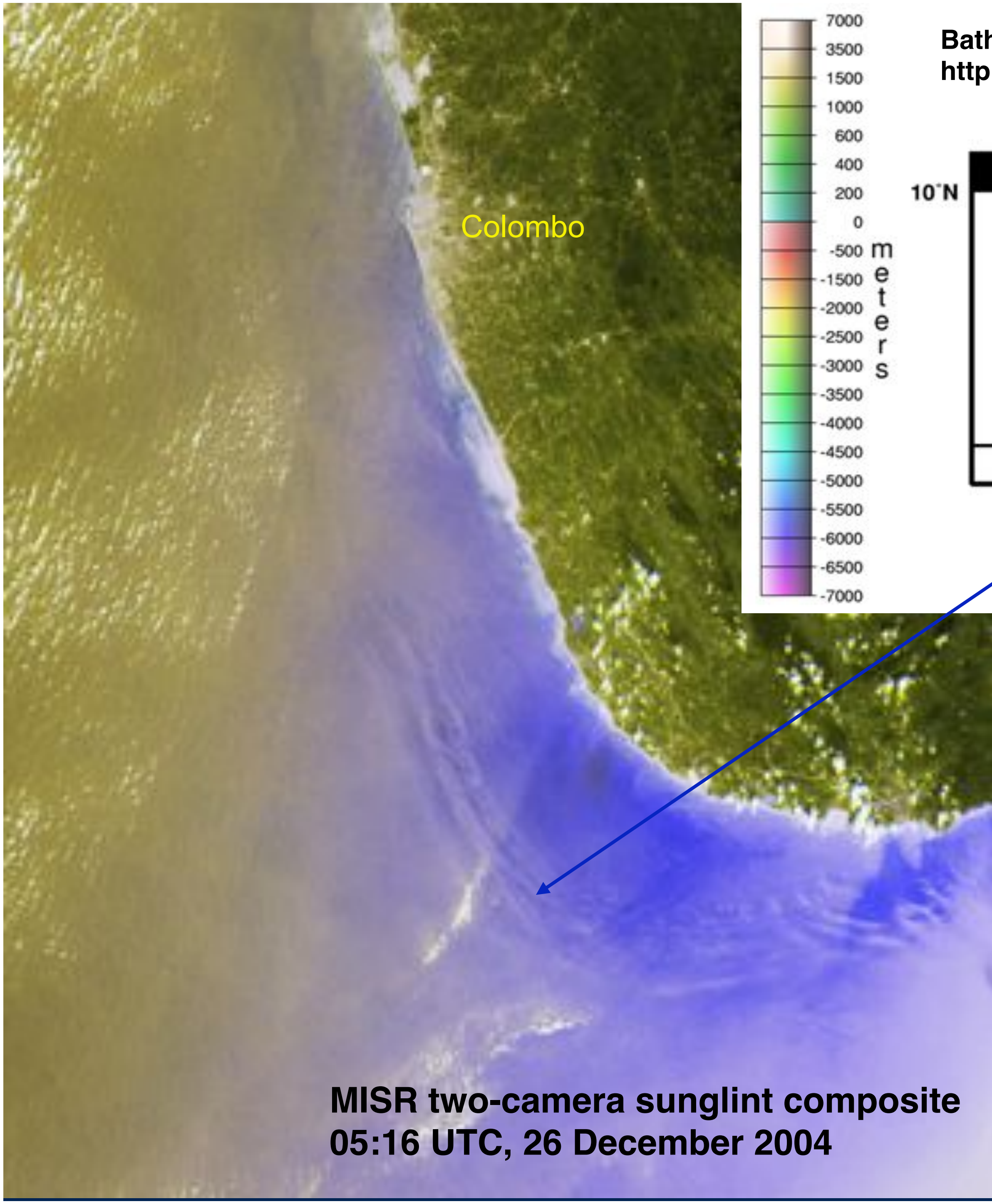

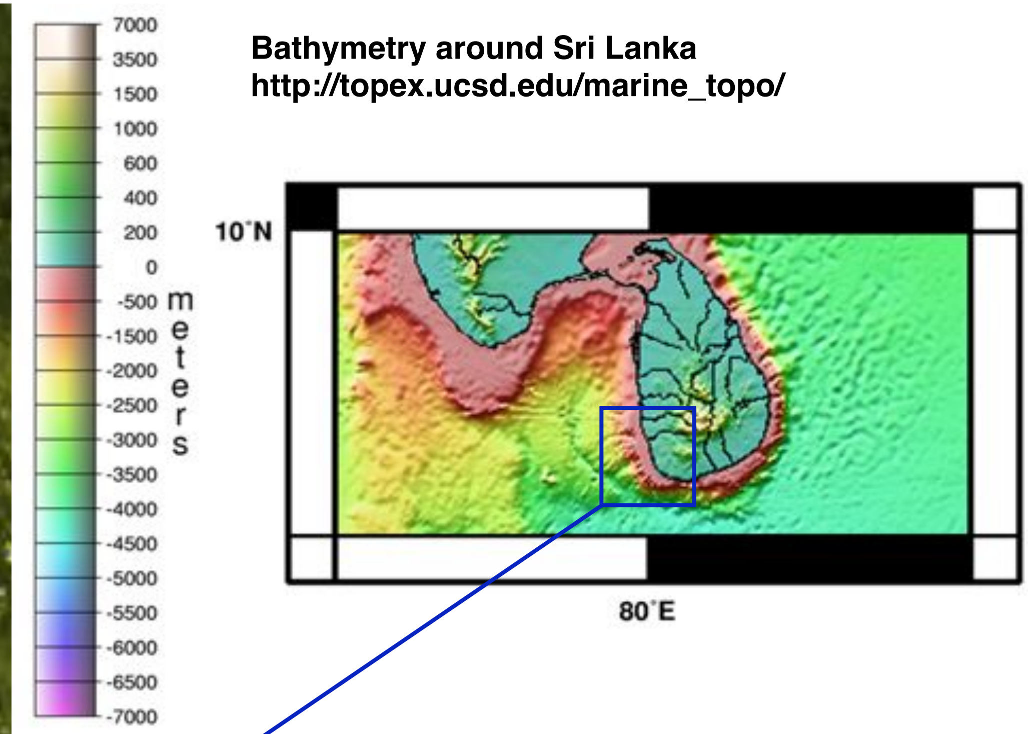

Tsunami-induced waves 30-40 km off SW Sri Lanka coast

Wave pattern is not seen on other dates

Wave location is coincident with dropoff in continental shelf

Waves are slow-moving

M. Garay et al., in preparation

Inclusion of sunglint in coupled aerosol/ocean retrieval approach

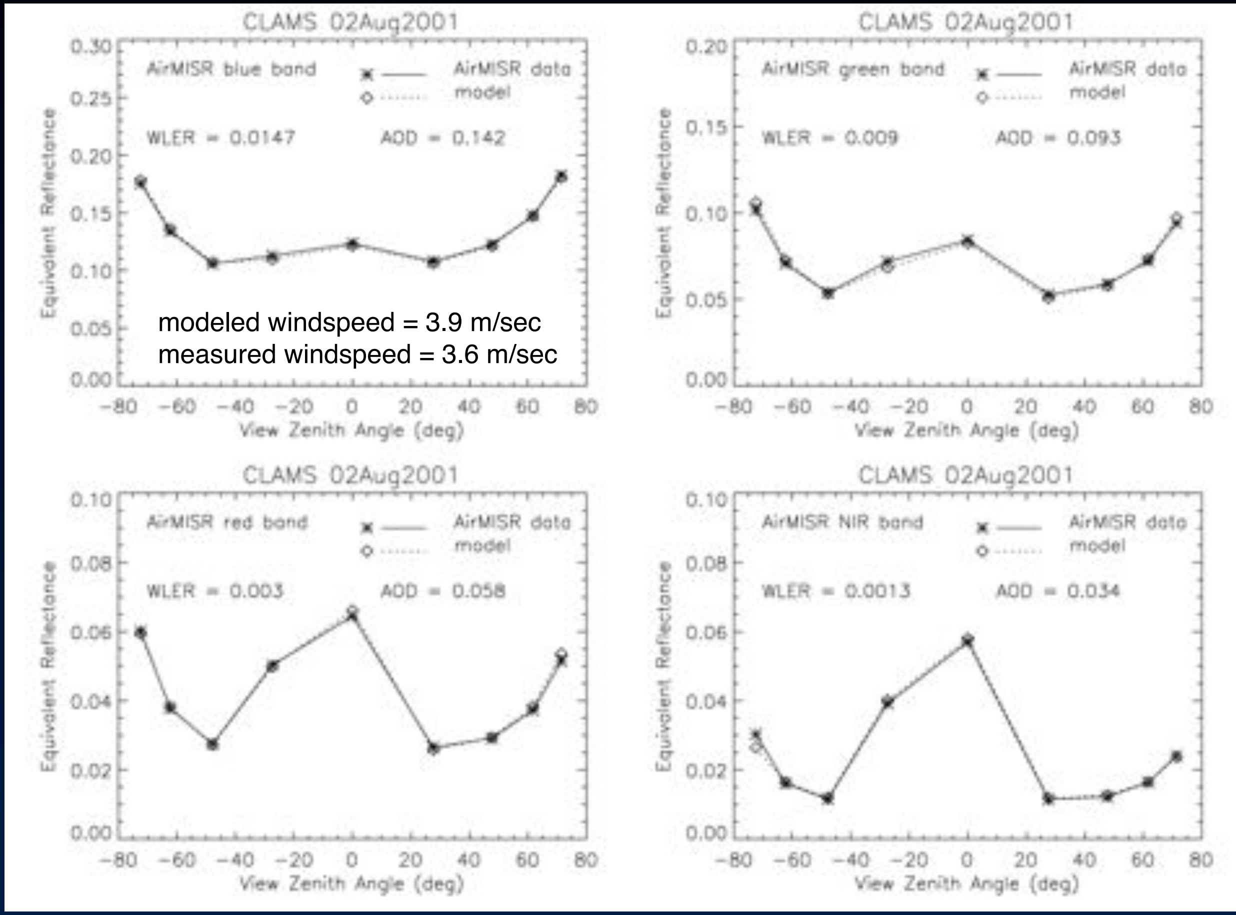

AirMISR data over the Chesapeake Lighthouse, 2 August 2001

Sunglint is wind-speed dependent and has a progressively greater influence on over-water radiances as wavelength increases.

Multiangle observations distinguish sunglint effects from aerosol path radiance.

Simultaneous retrieval of wind speed is possible.

Using multiangle sunglint to determine ocean surface wind speed

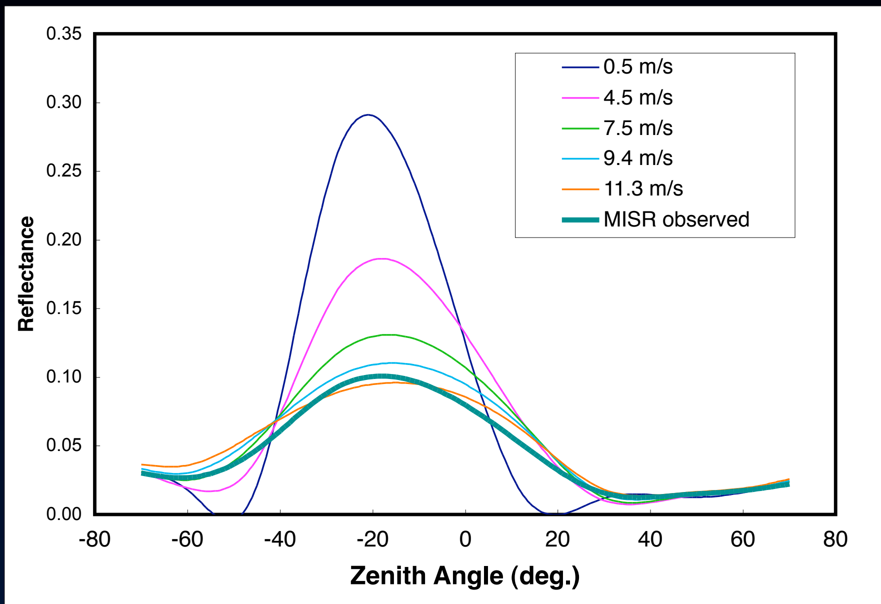

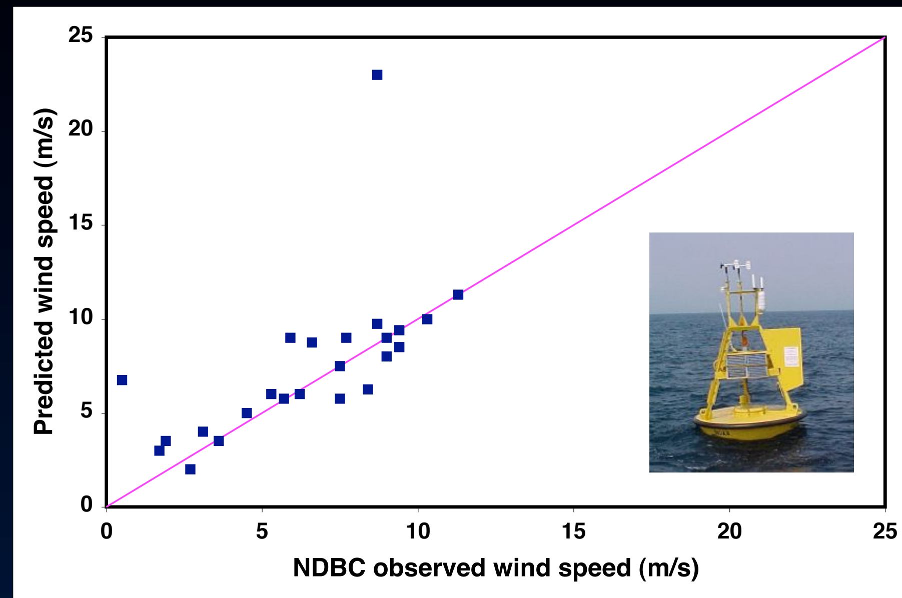

Spline fits to MISR observations vs. angle and to an ocean surface model (Tsang et al., with Cox-Munk coefficients to provide wind speed)

NOAA's National Data Buoy Center (NDBC) measures the wind speed and direction, 5 meters above the surface.

13 buoys (8 near California and 5 near Hawaii) are currently included.

RMS error = 3 m/s (all points)
RMS error = 1 m/s (without outliers)

E. Gonzales, D. Fox, in preparation

Visualizing surface texture

multi-spectral compositing

Hudson and James Bays
24 February 2000

nadir blue band	nadir green band	nadir red band

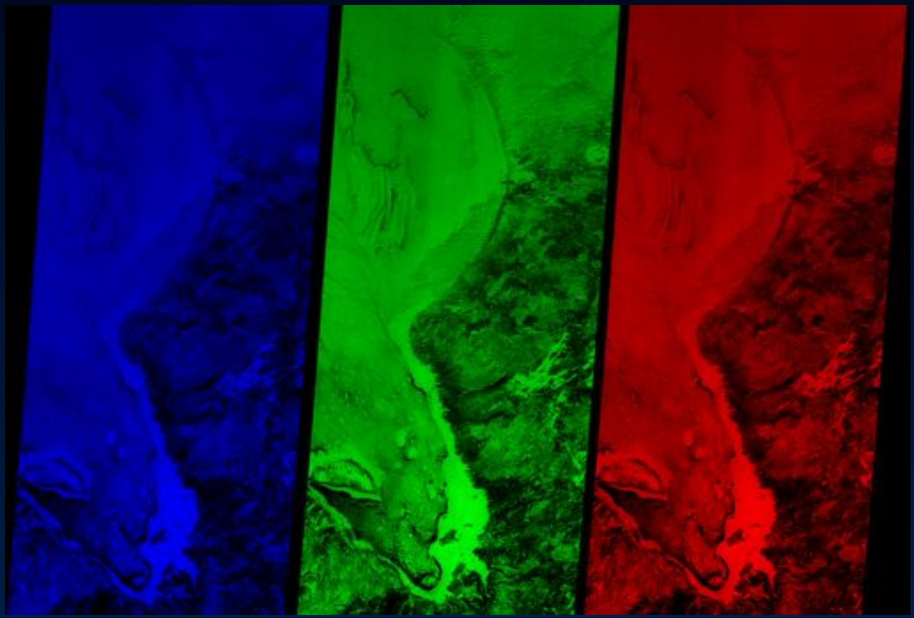

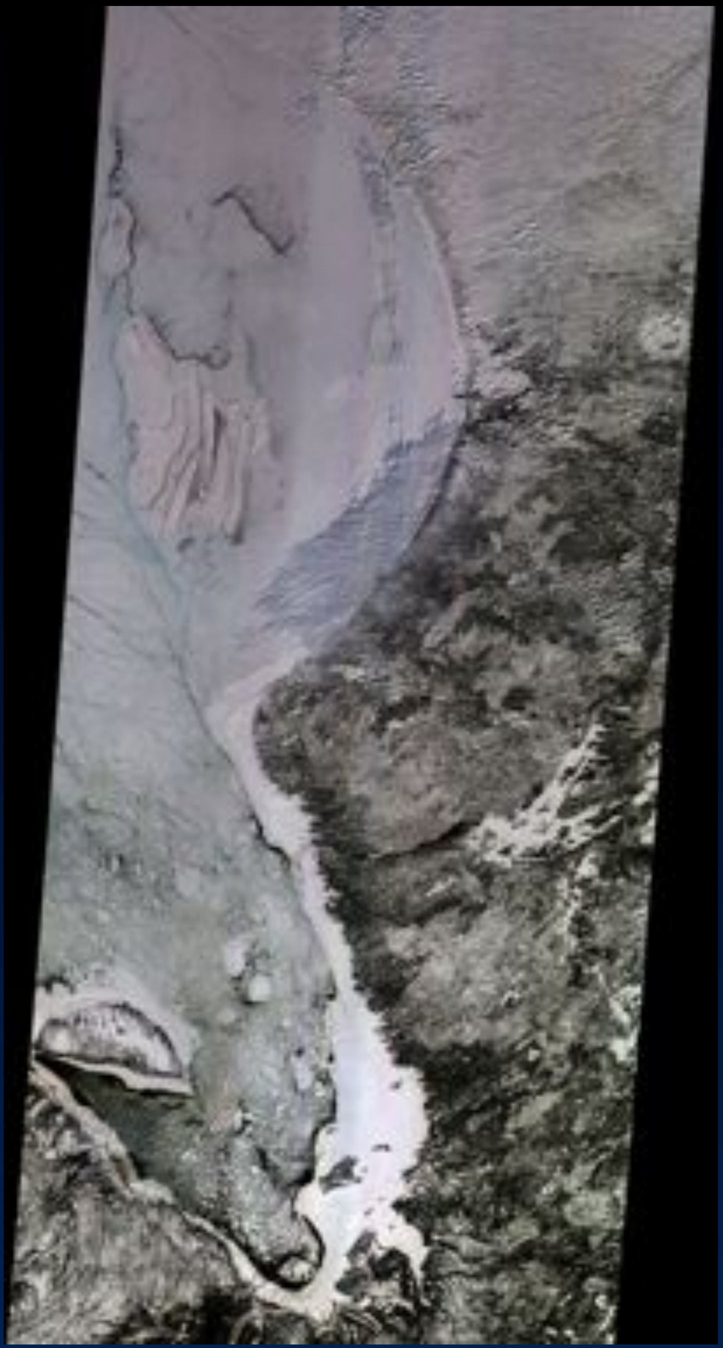

Visualizing surface texture

multi-angle compositing

Hudson and James Bays
24 February 2000

70° forward red band | nadir red band | 70° backward red band

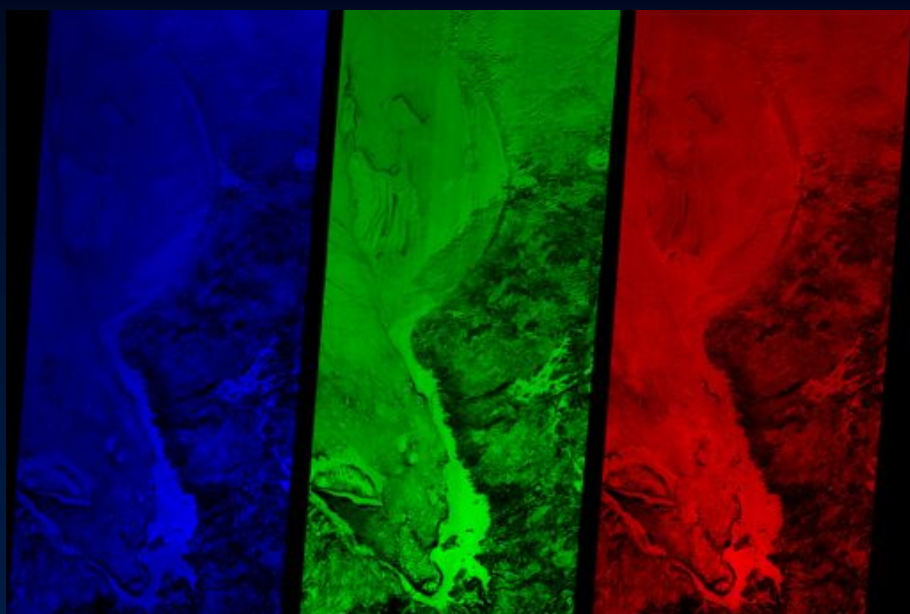

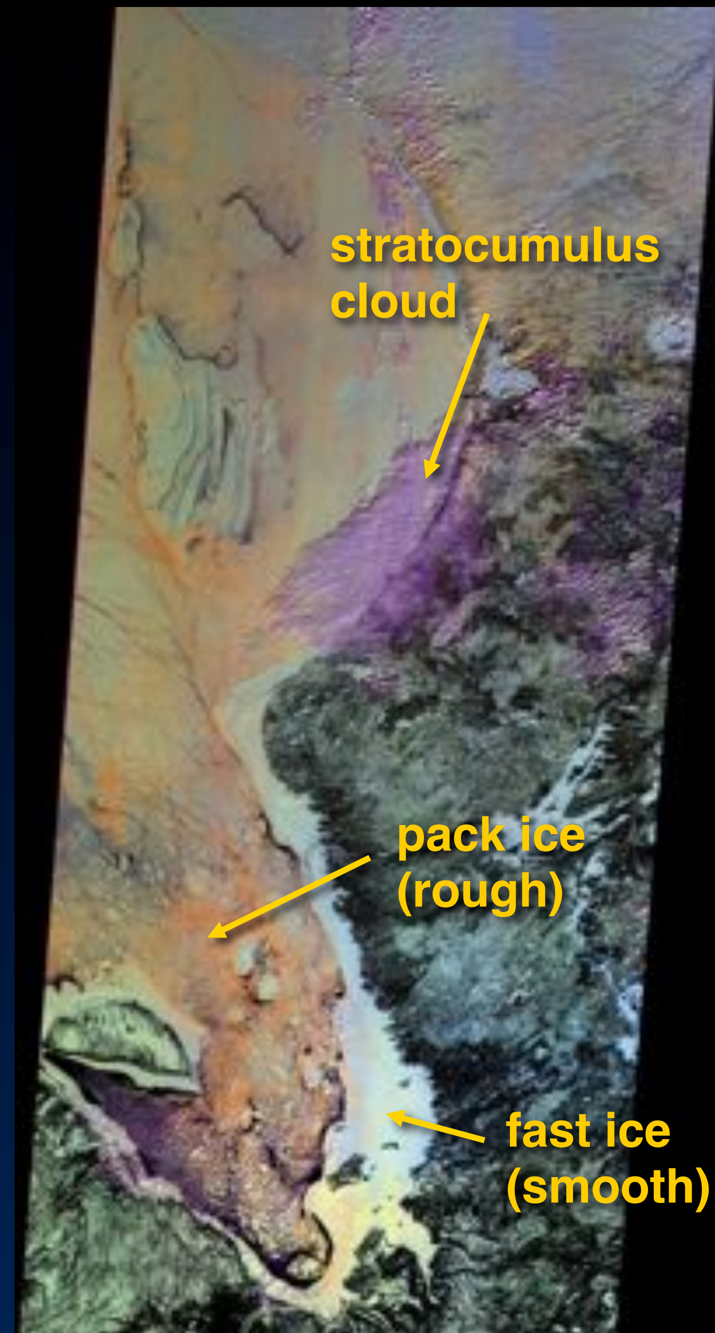

Cloud and ice bidirectional reflectances

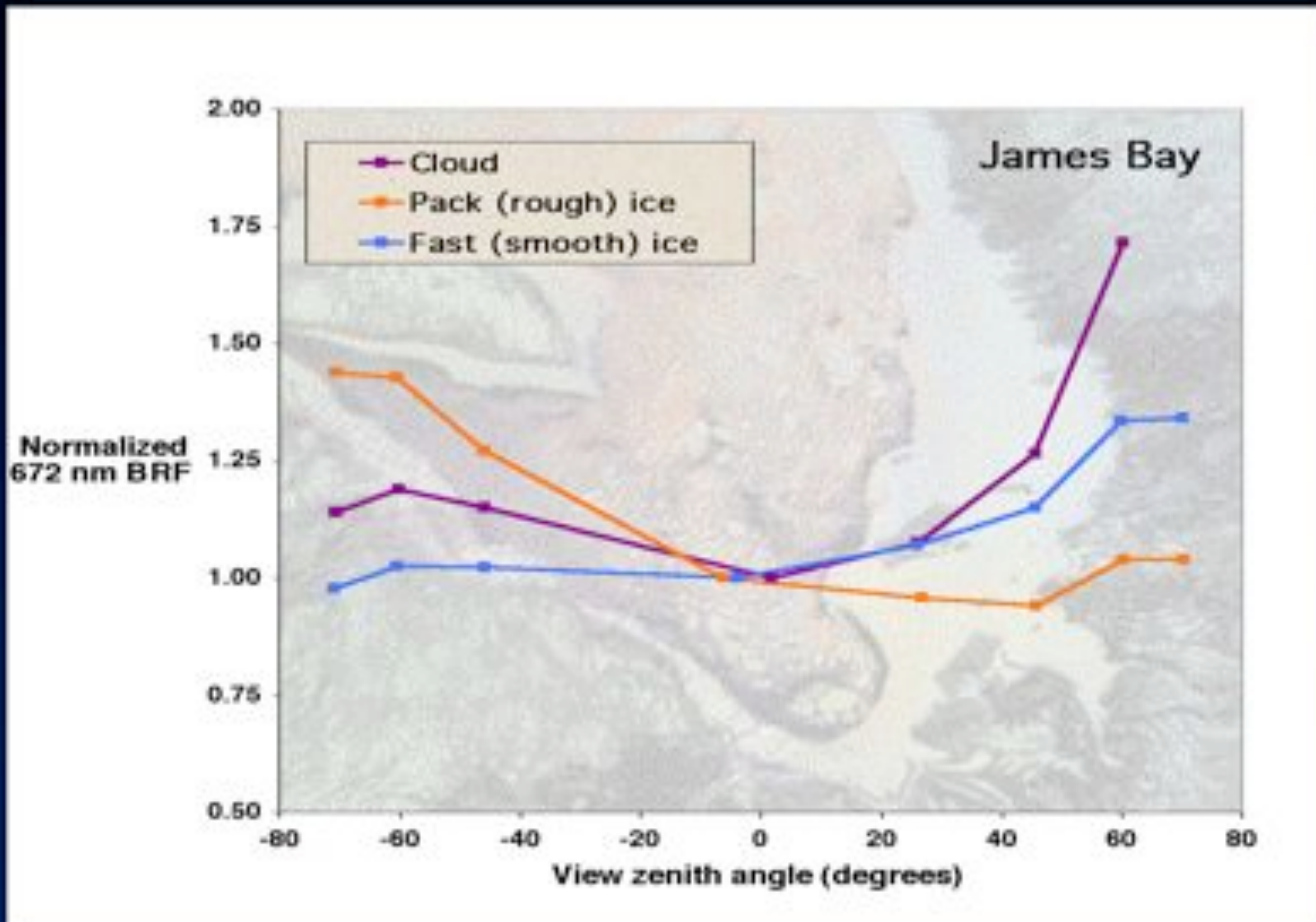

Changes in ice sheet surface roughness

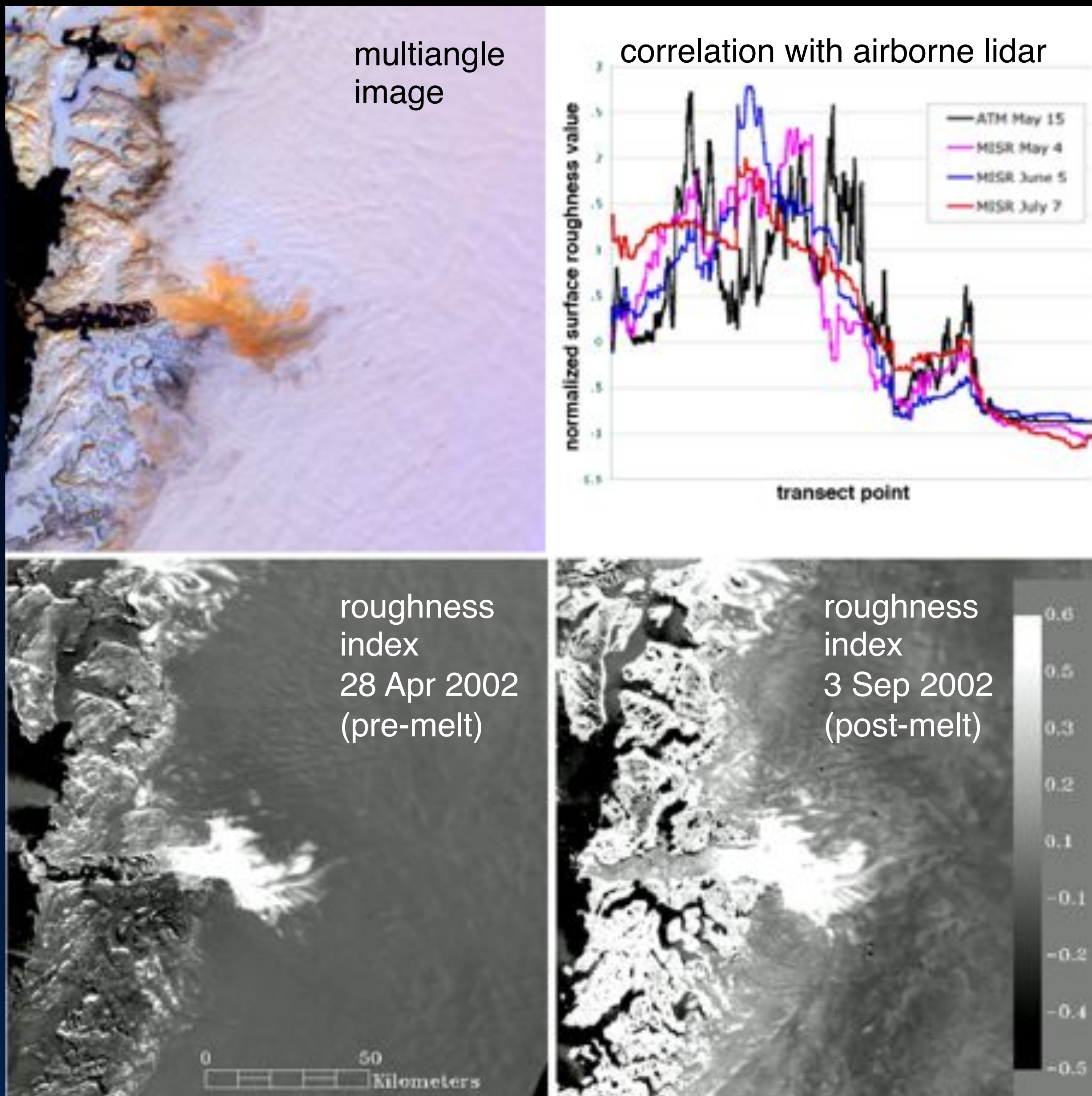

Surface morphology is influenced by ice accumulation, ablation, and melt.

Spatial and temporal changes in ice sheet roughness are revealed in MISR data.

Jakobshavn glacier, Greenland

A. Nolin et al. (2002), TGARS

Mapping changes in ice sheet rifts

Amery Ice Shelf “Loose Tooth”

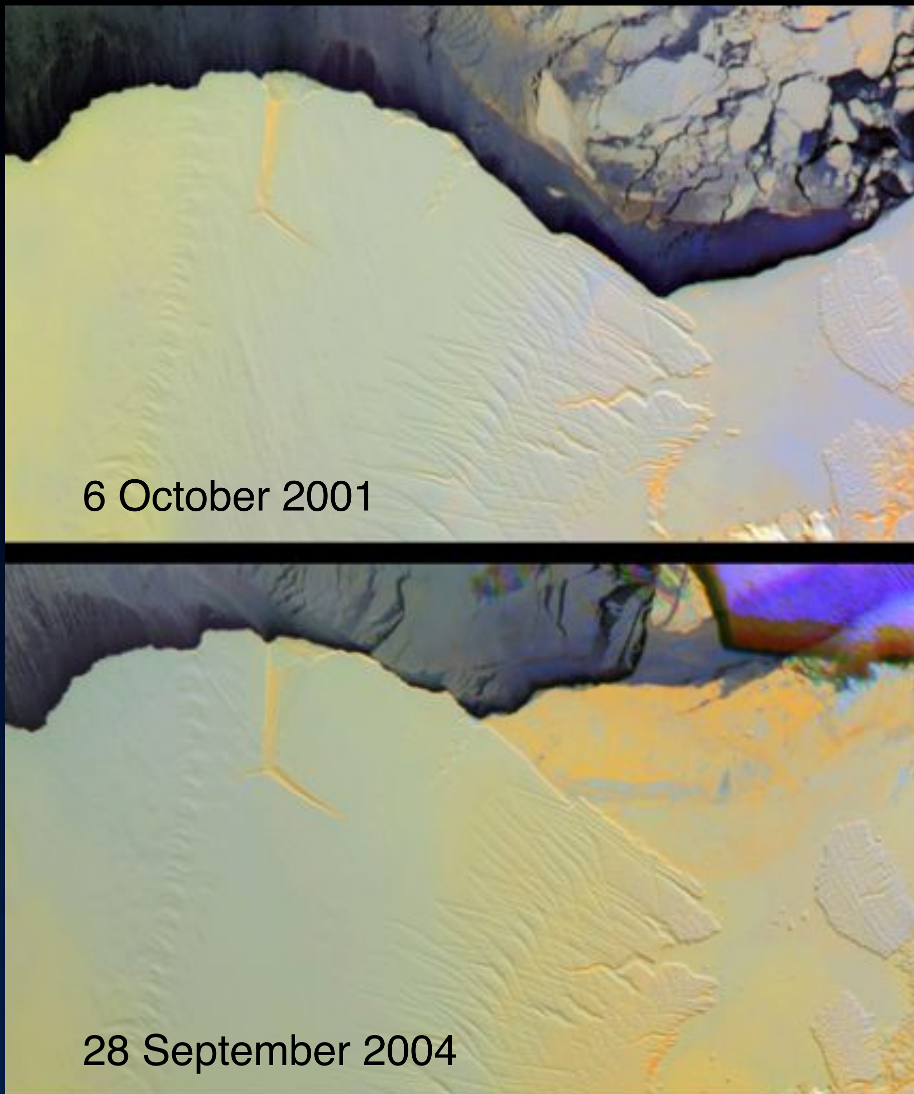

Multiangle red-band composites

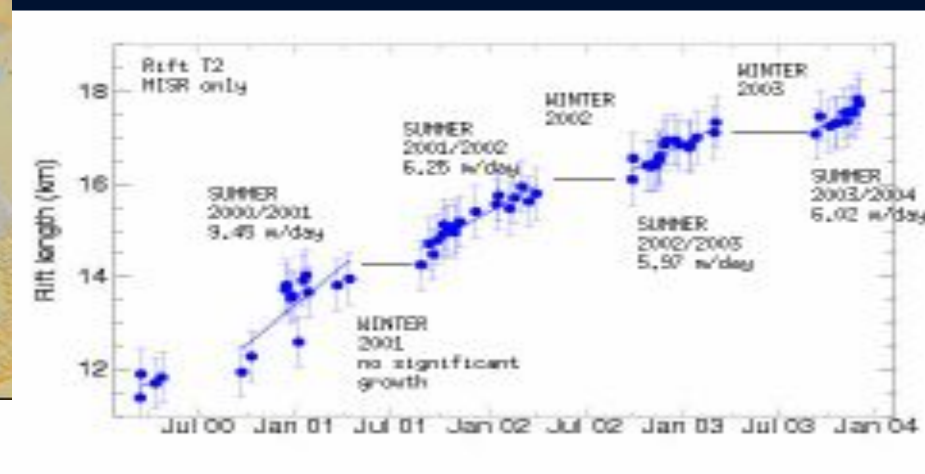

H.A. Fricker et al. (2005), GRL

Distinguishing sea ice types

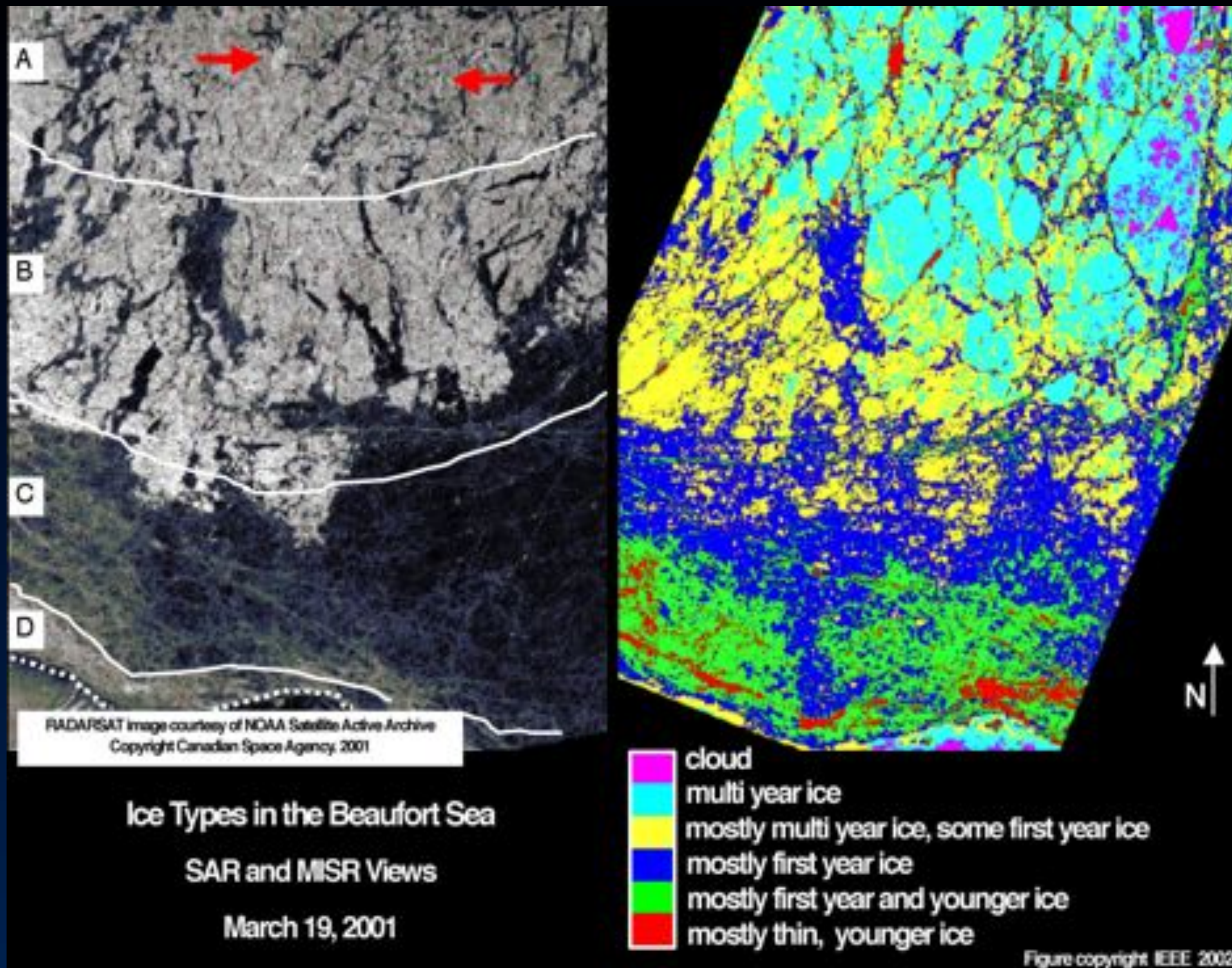

A. Nolin et al. (2002), TGARS

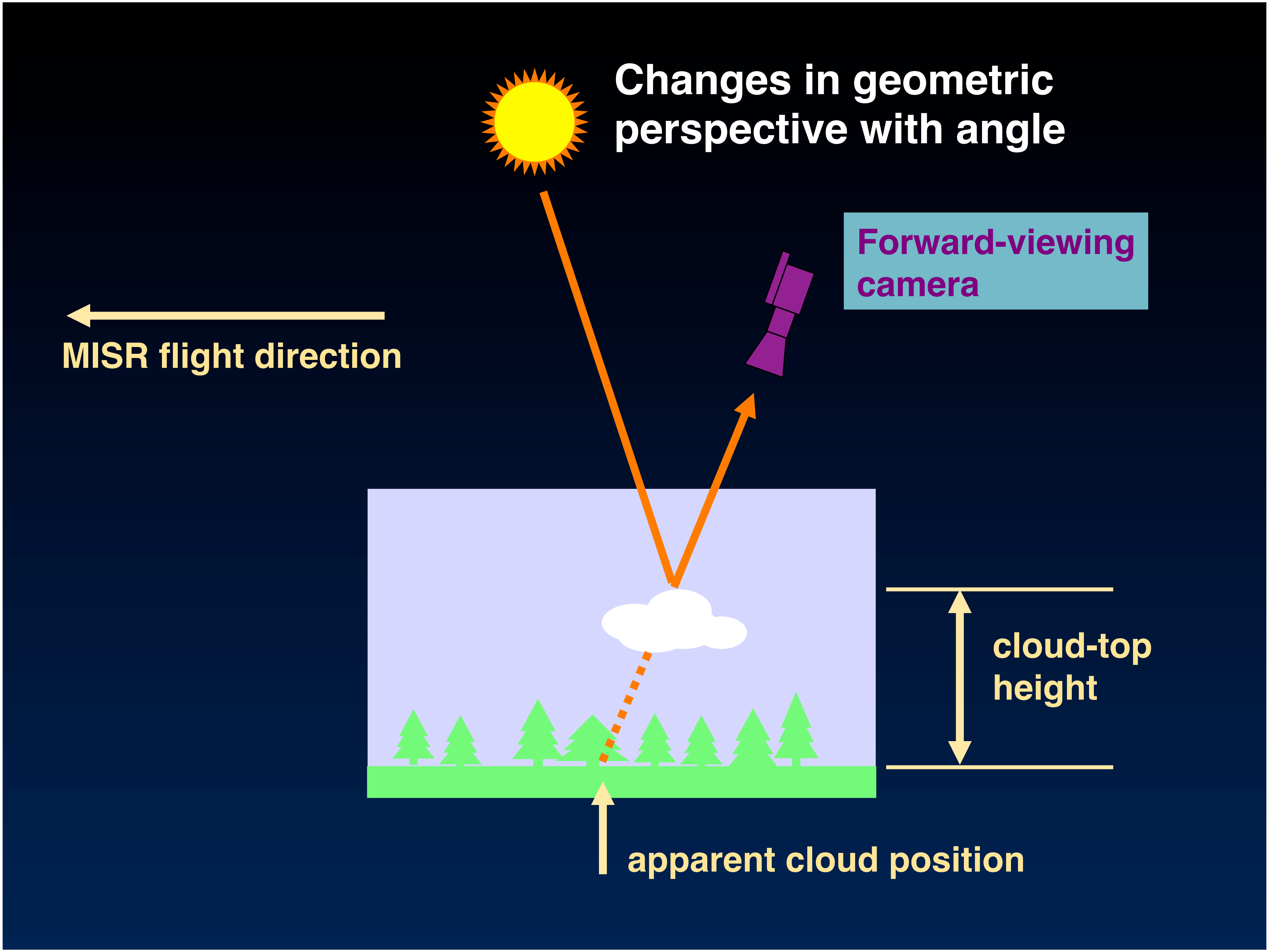
Changes in geometric perspective with angle
Forward-viewing camera
MISR flight direction
cloud-top height
apparent cloud position

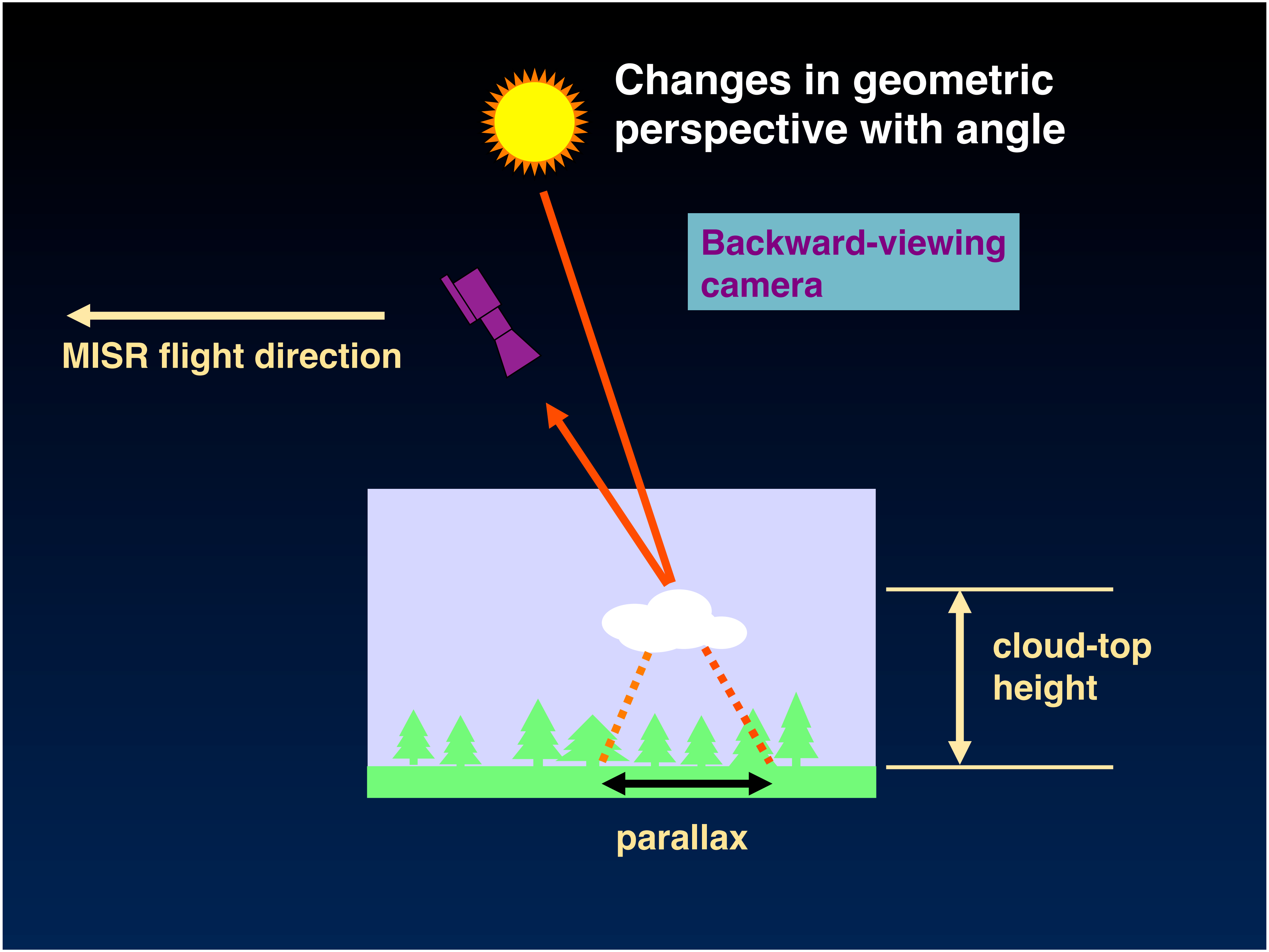
Changes in geometric perspective with angle
Backward-viewing camera
MISR flight direction
cloud-top height
parallax

Georgian Bay, Ontario, 6 March 2000

Nadir (An)

70° forward (Df)

Georgian Bay, Ontario, 6 March 2000

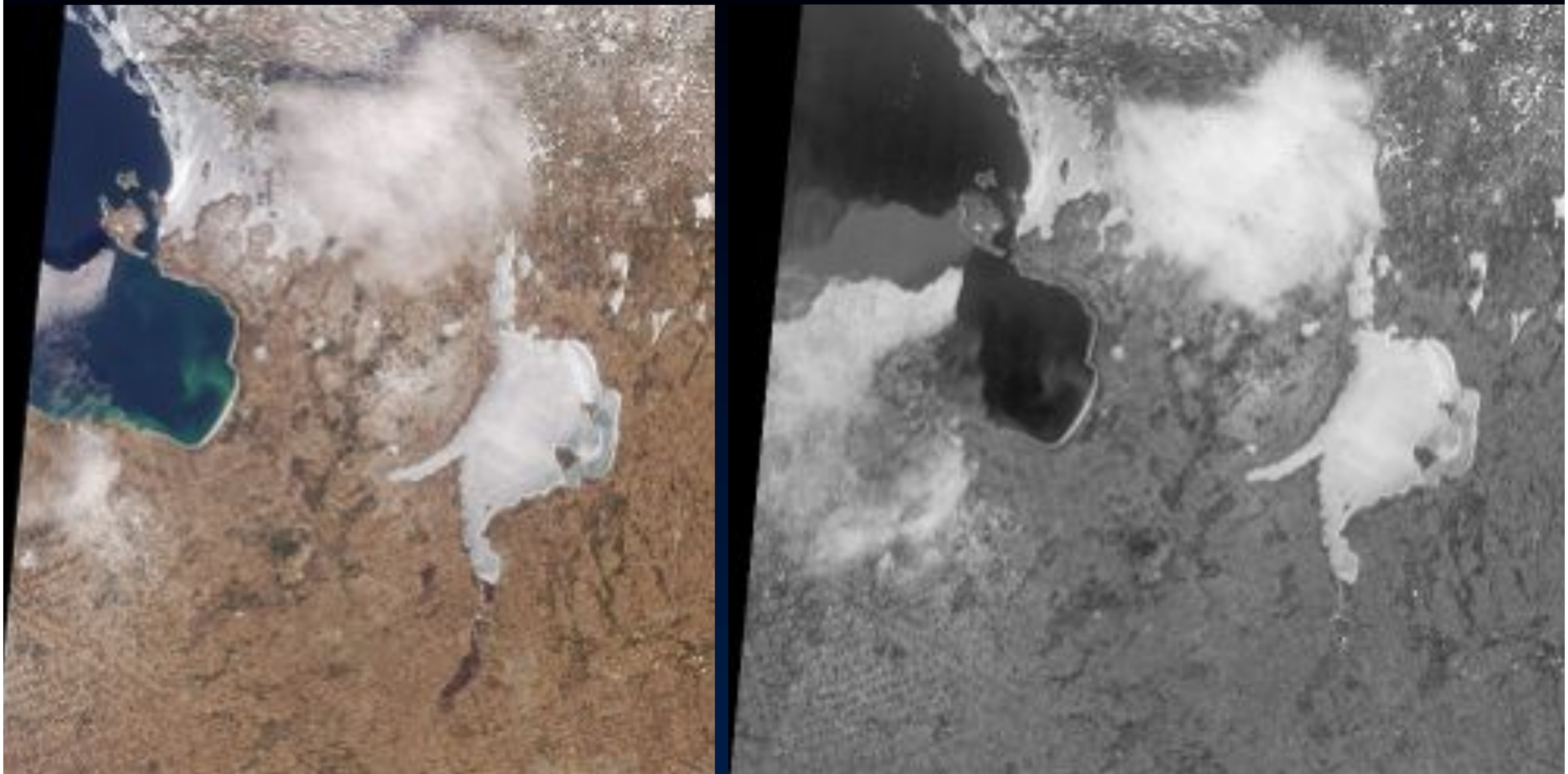

Nadir (An) **60° forward (Cf)**

Georgian Bay, Ontario, 6 March 2000

Nadir (An)

46º forward (Bf)

Georgian Bay, Ontario, 6 March 2000

Nadir (An)

26° forward (Af)

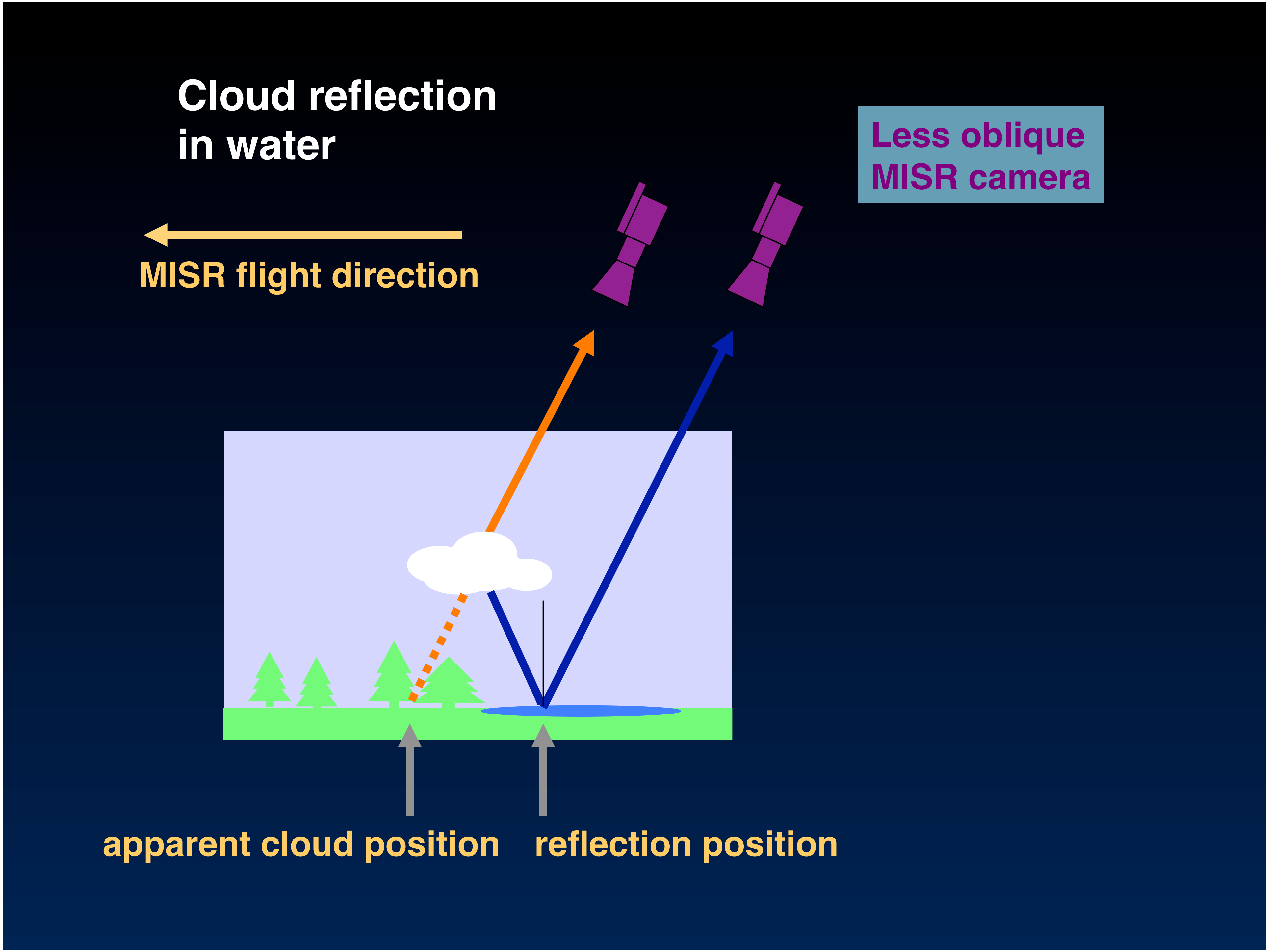
Cloud reflection
in water
Less oblique
MISR camera
MISR flight direction
apparent cloud position
reflection position

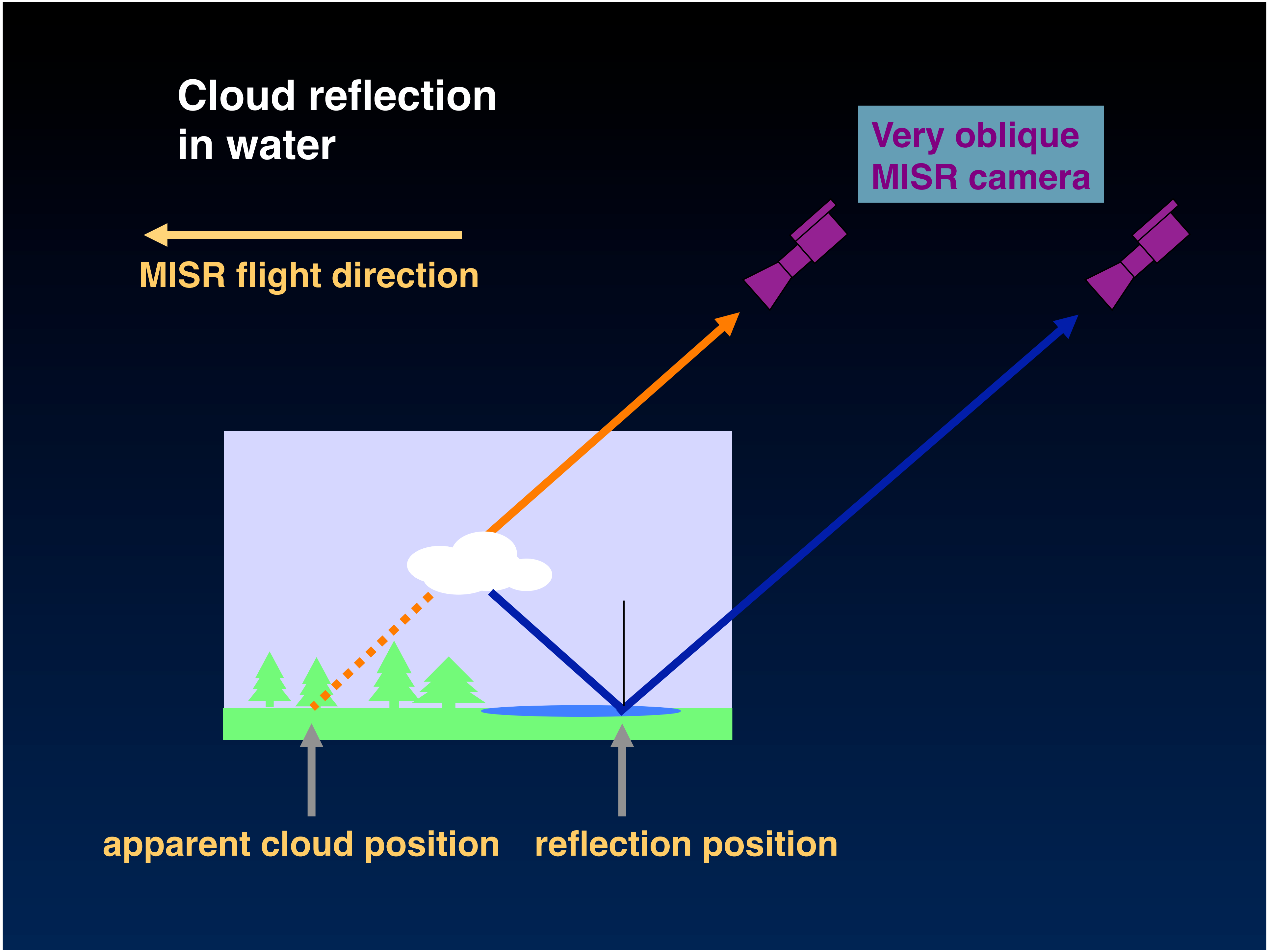
Cloud reflection
in water
Very oblique
MISR camera
MISR flight direction
apparent cloud position
reflection position

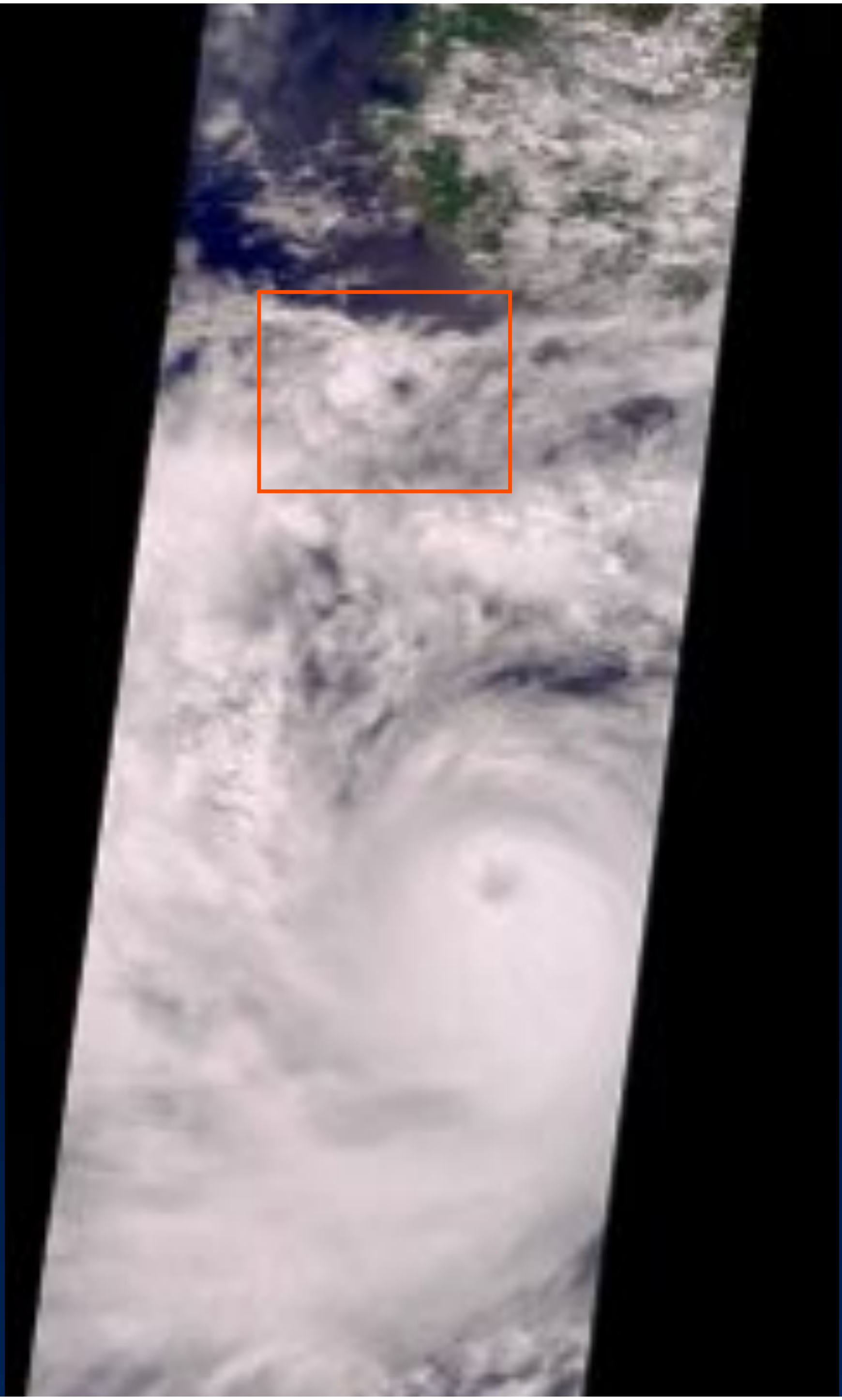

Hurricane Carlotta

21 June 2000

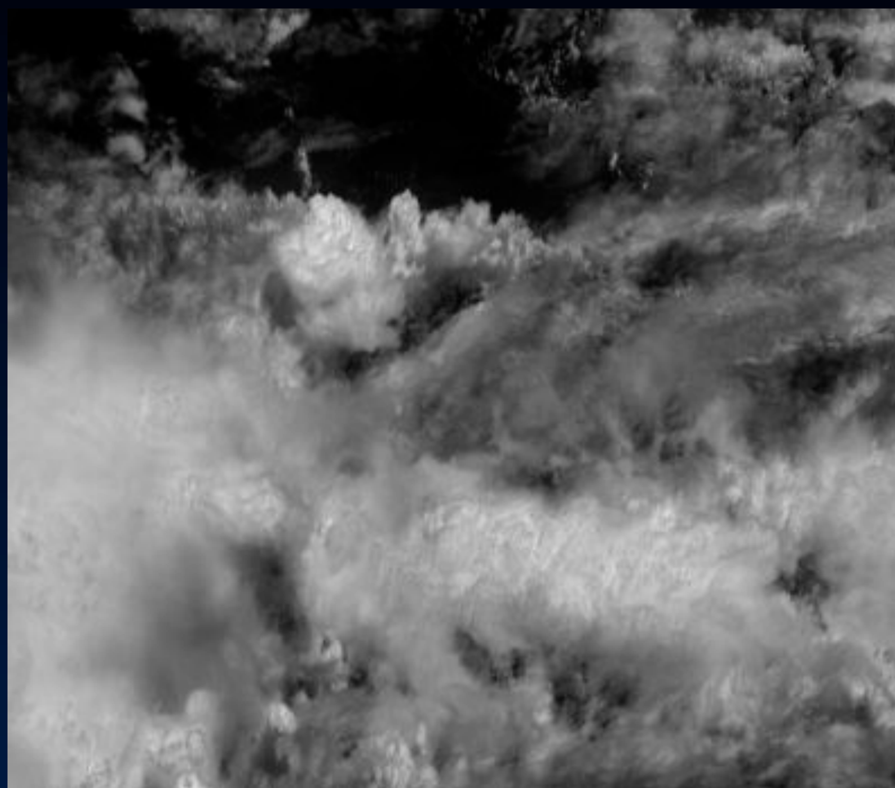

50 km

Multi-angle “fly-over” of Hurricane Carlotta thunderclouds

19 August 2000

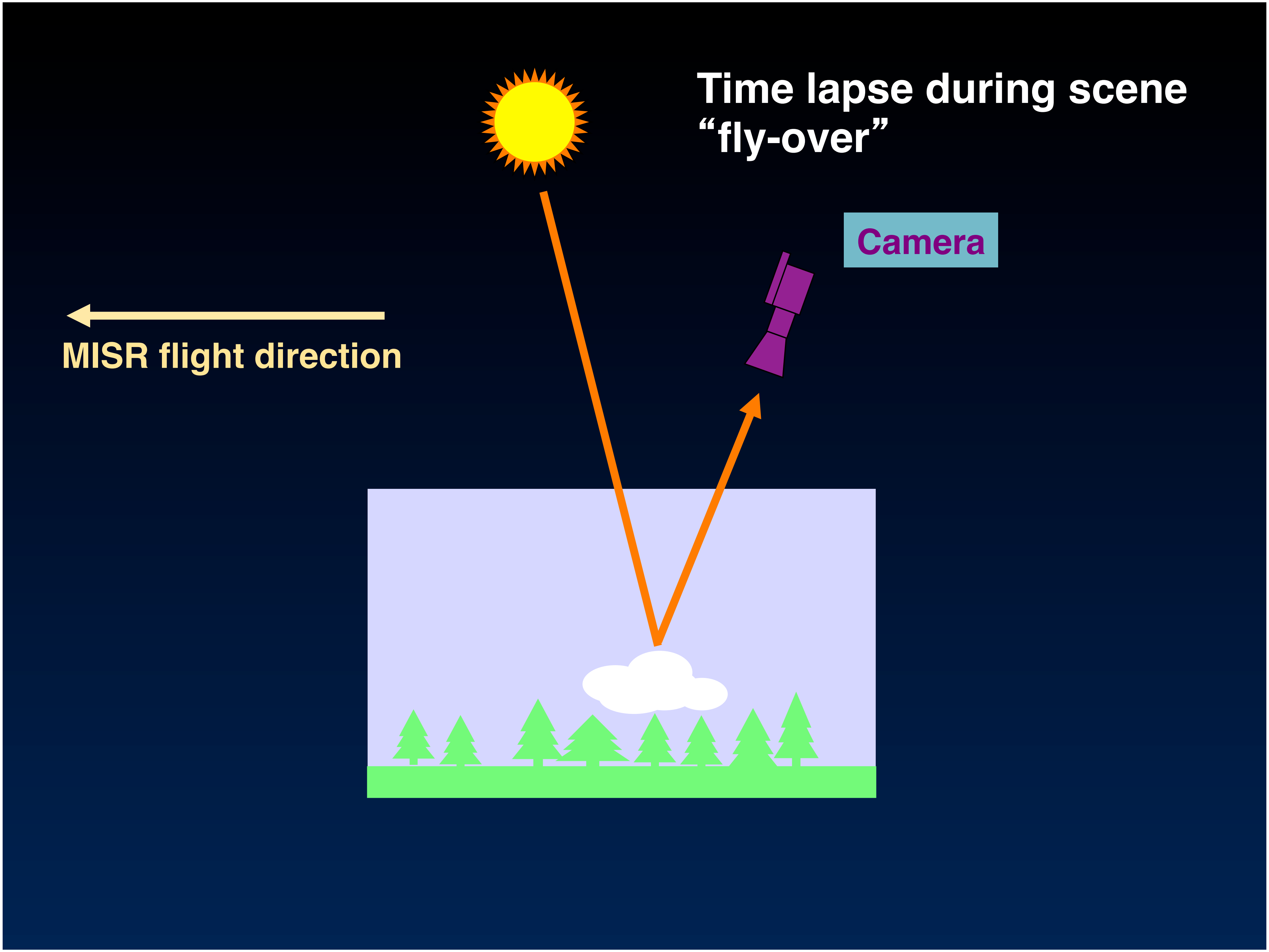
Time lapse during scene
"fly-over"
Camera
MISR flight direction

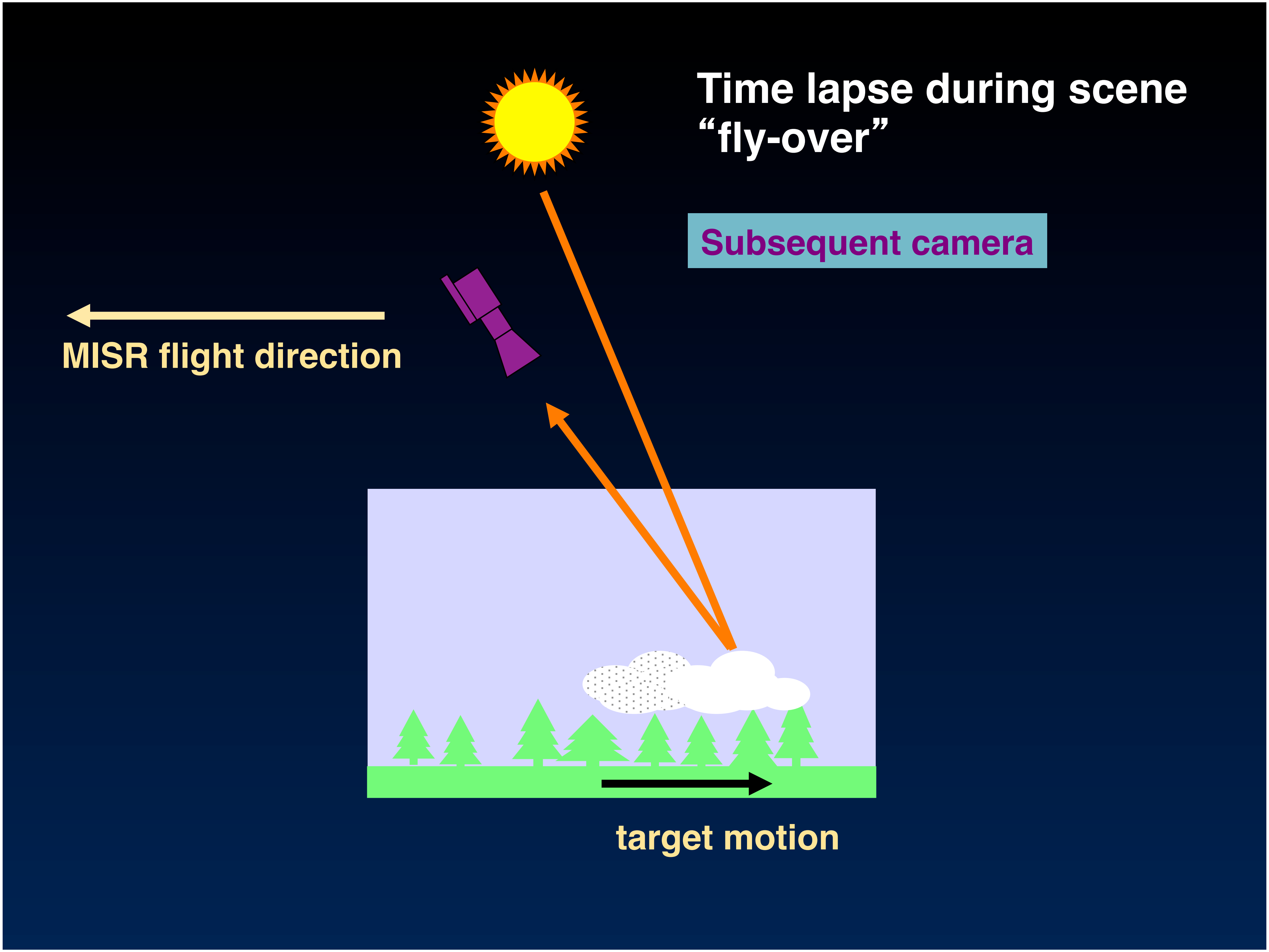
Time lapse during scene
"fly-over"
Subsequent camera
MISR flight direction
target motion

Von Karman vortex street near Jan Mayen Island

6 June 2001

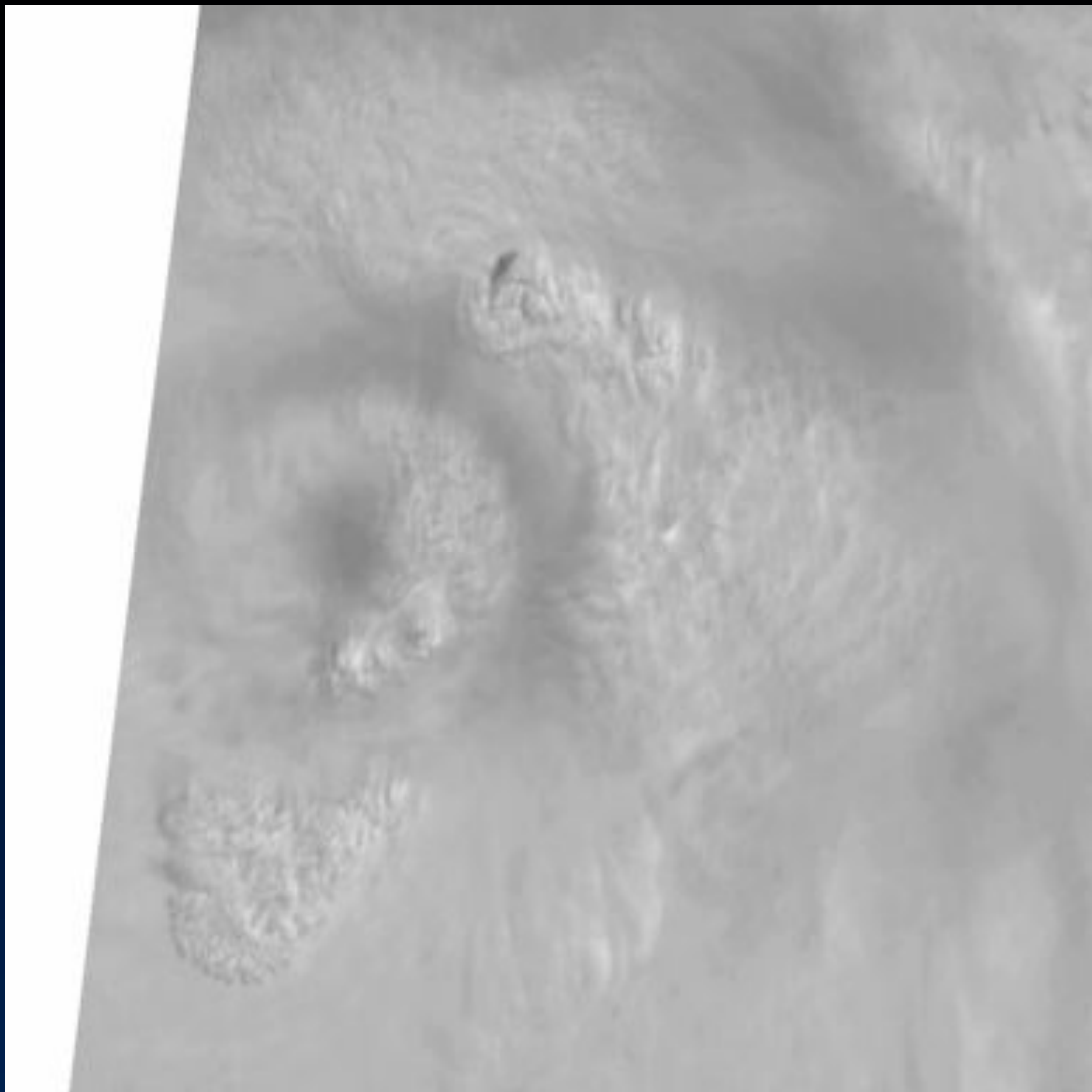

The Eye of Hurricane Katrina

Multiangle time-lapse

27 August 2005


Indian coast
Godavari River Delta
Approx. 16.4ºN, 81.8ºE
26 December 2004
86 km
49 km
MISR 60º fwd - 70º aft
05:11 - 05:17 UTC
cloud motion is due to parallax
resulting from their height above the surface;
tsunami waves are at sea level and
show actual motion
10 km

L1B2 Geometric Parameters (MIS03)

Provided on 17.6-km centers

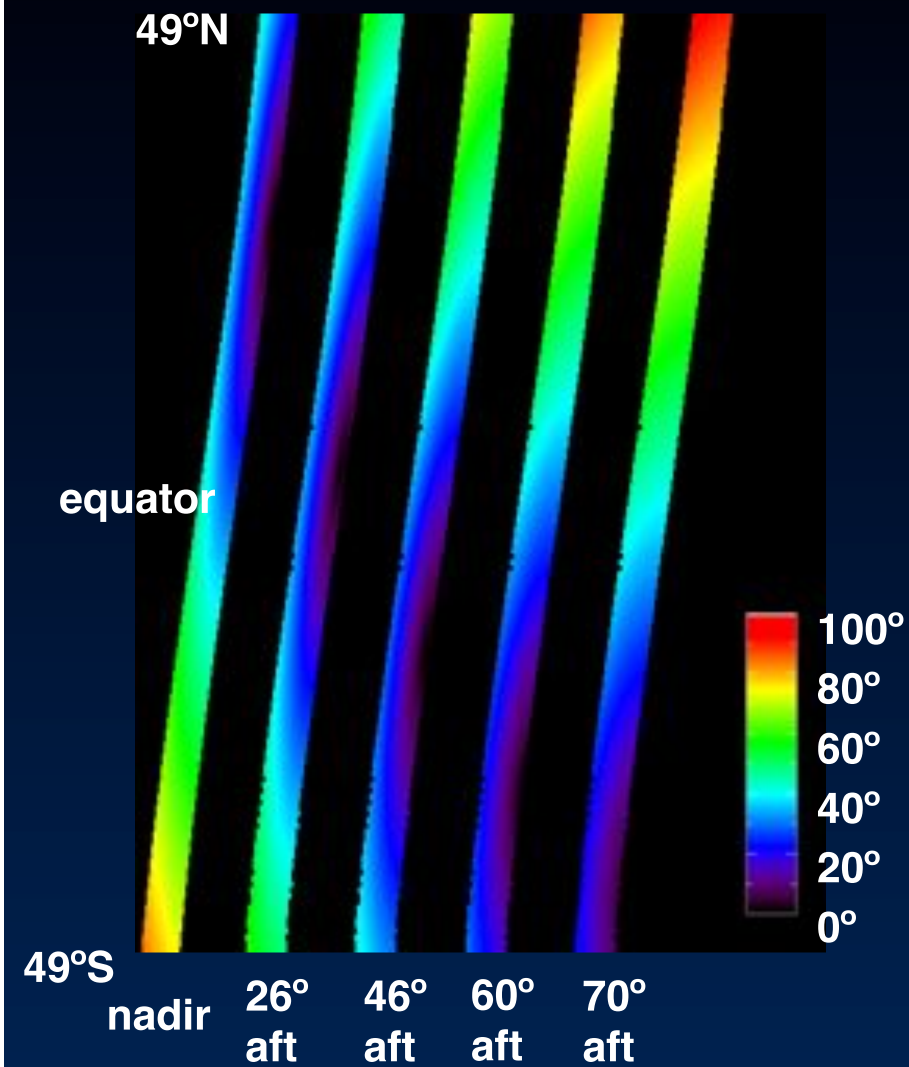

Example of glitter angle July 3

CONTENTS

- View zenith and azimuth angles per camera; azimuths measured relative to local north
- Solar zenith and azimuth angles correspond to midpoint viewing time of only those cameras which observed the point
- Scatter and glitter angles also included in product

L1B2 Radiometric Camera-by-camera Cloud Mask (MIS03)

Radiometric threshold-based cloud mask

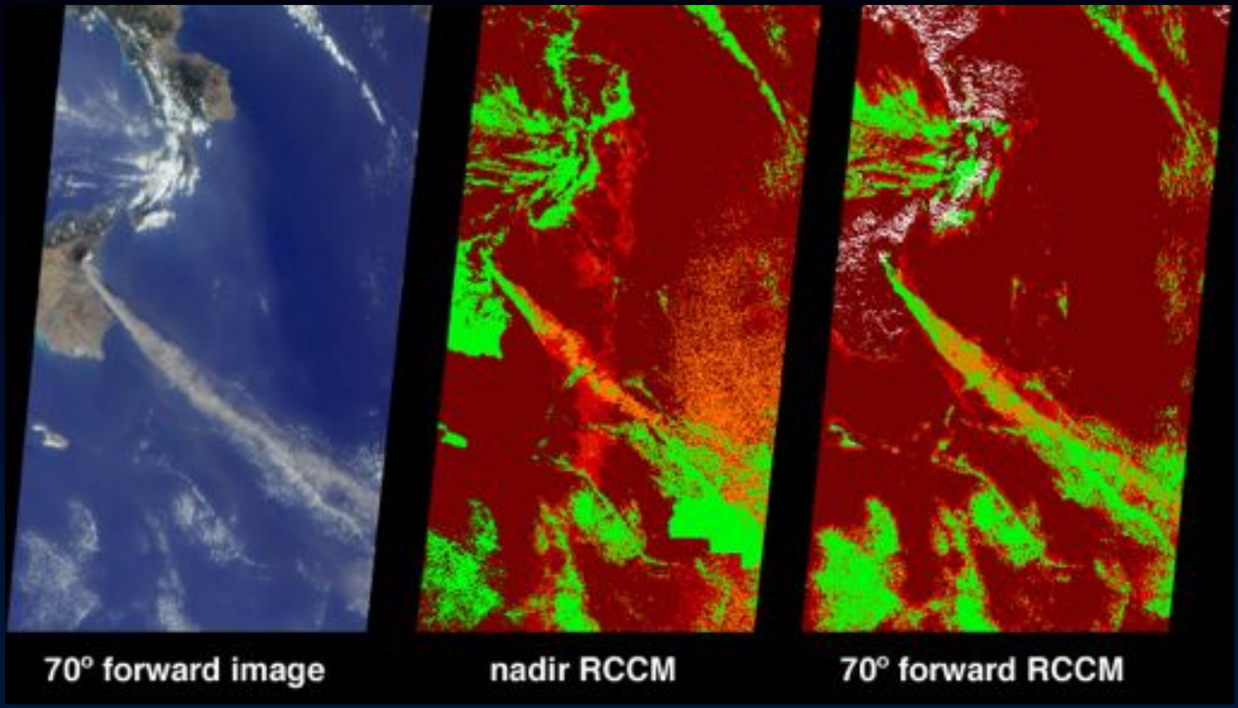

Mt. Etna eruption,
22 July 2001

- No retrieval
- High confidence clear
- Low confidence clear
- Low confidence cloud
- High confidence cloud

Level 2 Standard Products

Level 2 standard products

- Level 2TC stereo
- Level 2TC cloud classifiers
- Level 2TC top-of-atmosphere albedo
- Level 2AS aerosol
- Level 2AS land surface

Level 2 processing uses multiple cameras simultaneously

- Angular radiance signatures
- Geometric parallax
- Time lapse

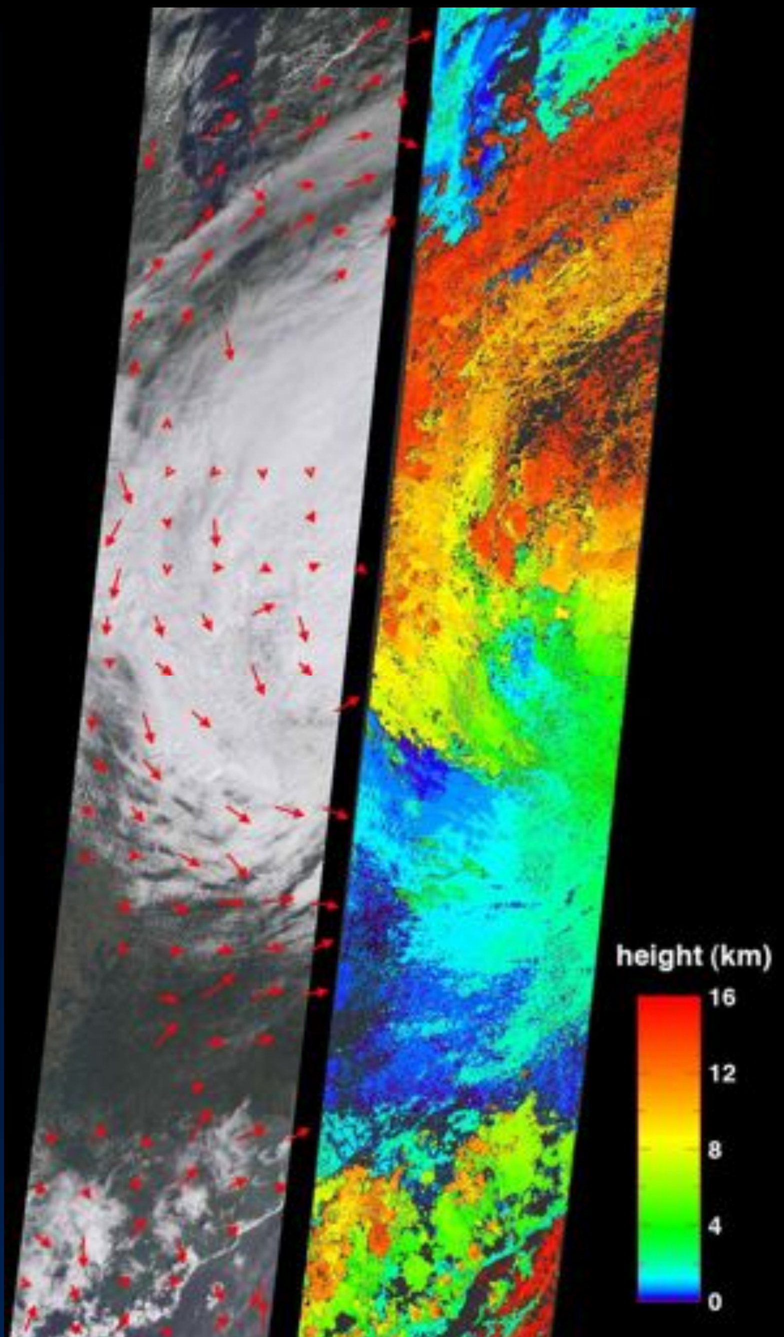

L2 TOA/Cloud Stereo Product (MIS04)

Retrieved cloud heights and cloud-tracked winds

HEIGHT ATTRIBUTES

- 1.1-km resolution
- Purely geometric retrievals of height
- Independent of temperature profiles and cloud emissivity
- Independent of radiometric calibration
- Accuracy 500 -1000 m

WIND ATTRIBUTES

- 70.4-km resolution
- Uses stereo triplets
- Accuracy 1-3 m/s with 300 m height resolution

Hurricane Katrina
30 August 2005

Measuring aerosol plume injection heights

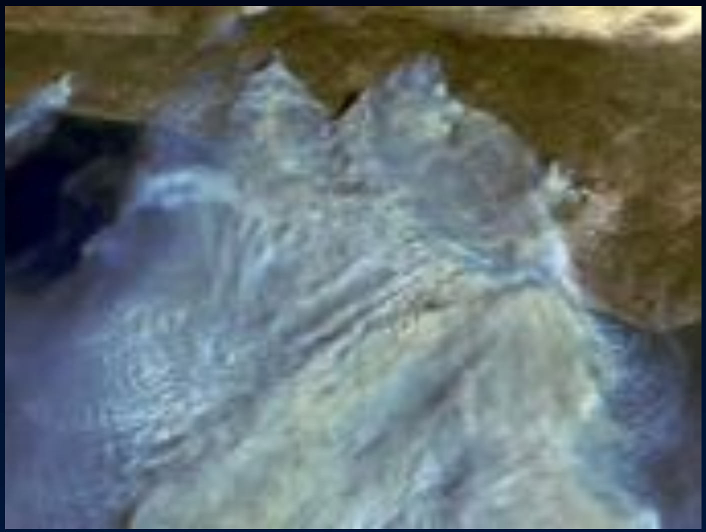

California Cedar Fire, October 2003

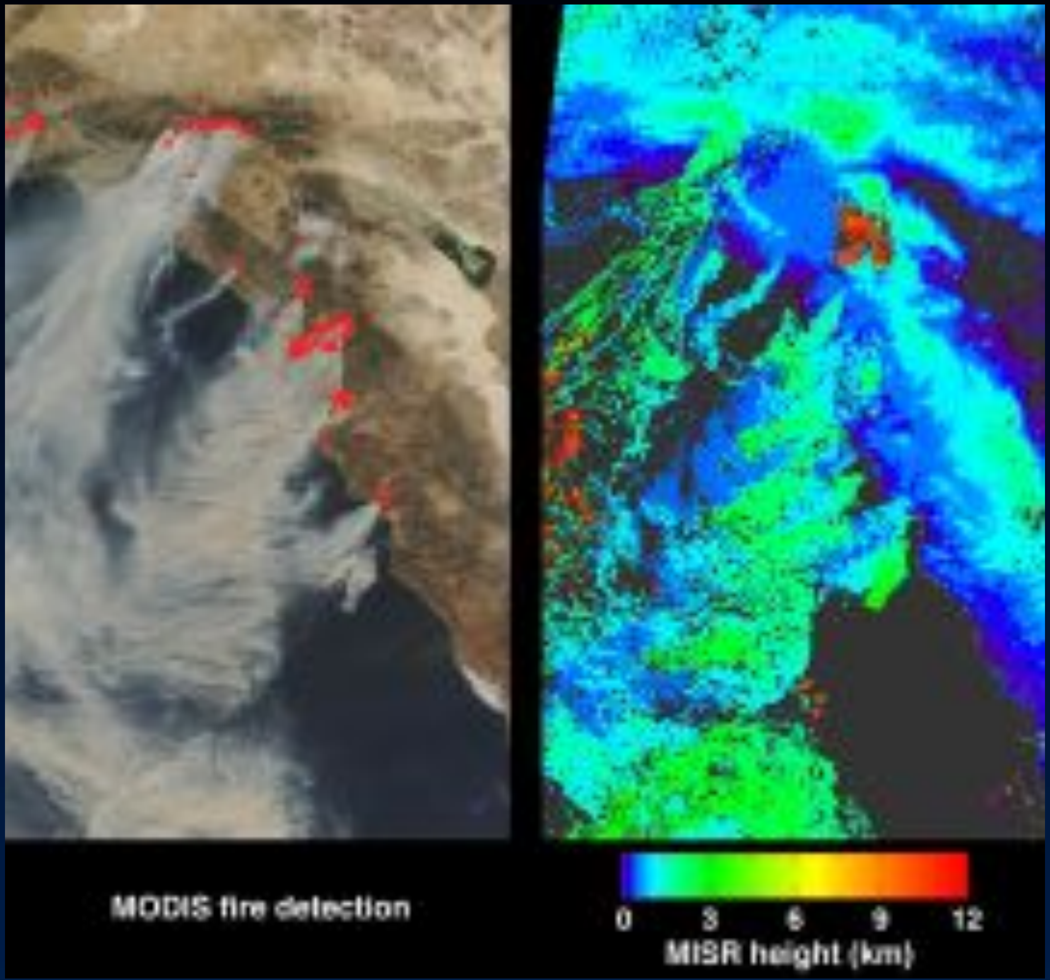

MISR: Stereo retrieves plume-top heights, oblique views enhance plume sensitivity
MODIS: Thermal channels pinpoints fire locations

Data mining for automated smoke plume detection and height retrieval

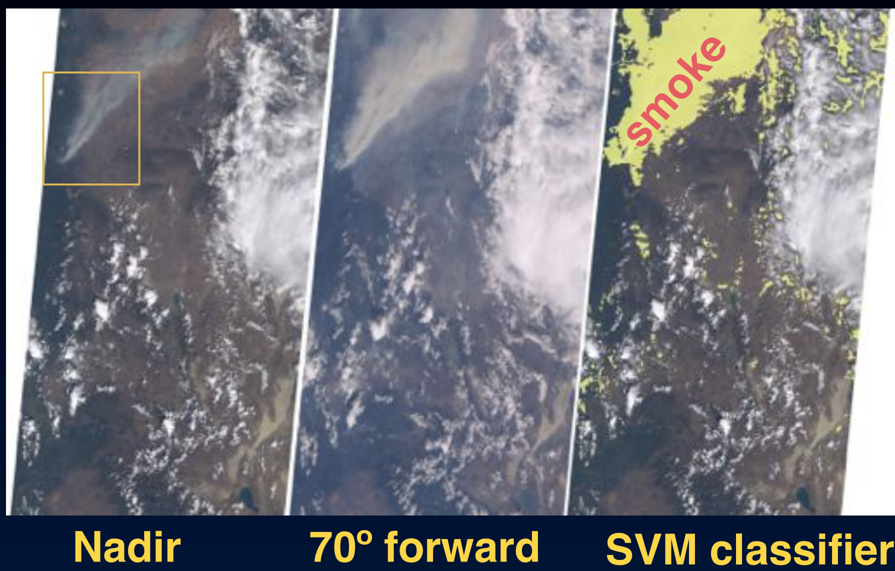

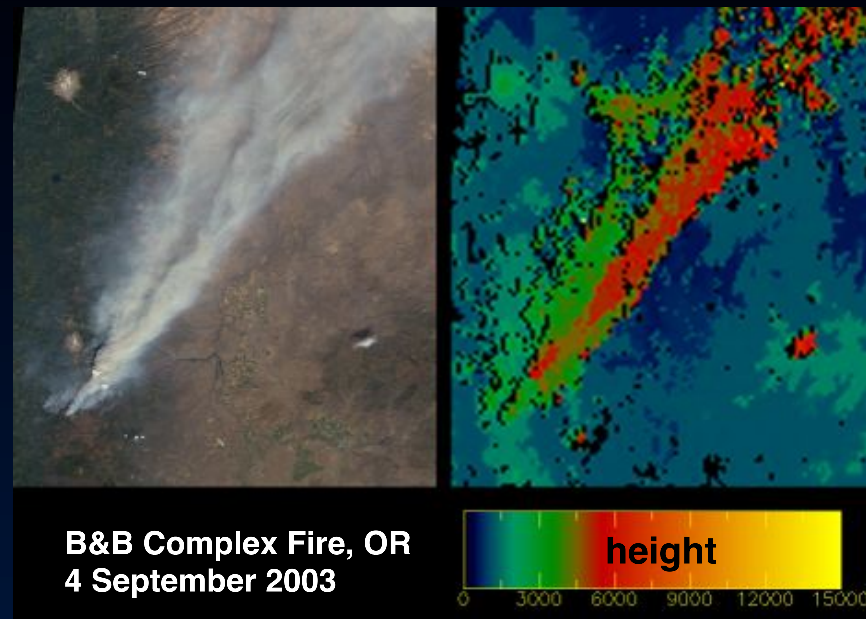

Automated smoke detection → **Injection height measurement** → **Plume height database for transport model initialization**

M. Garay, D. Mazzoni (2005), AMS annual meeting

L2 TOA/Cloud Albedo Product (MIS04)

Cloud-top-projected TOA albedo and bidirectional reflectance

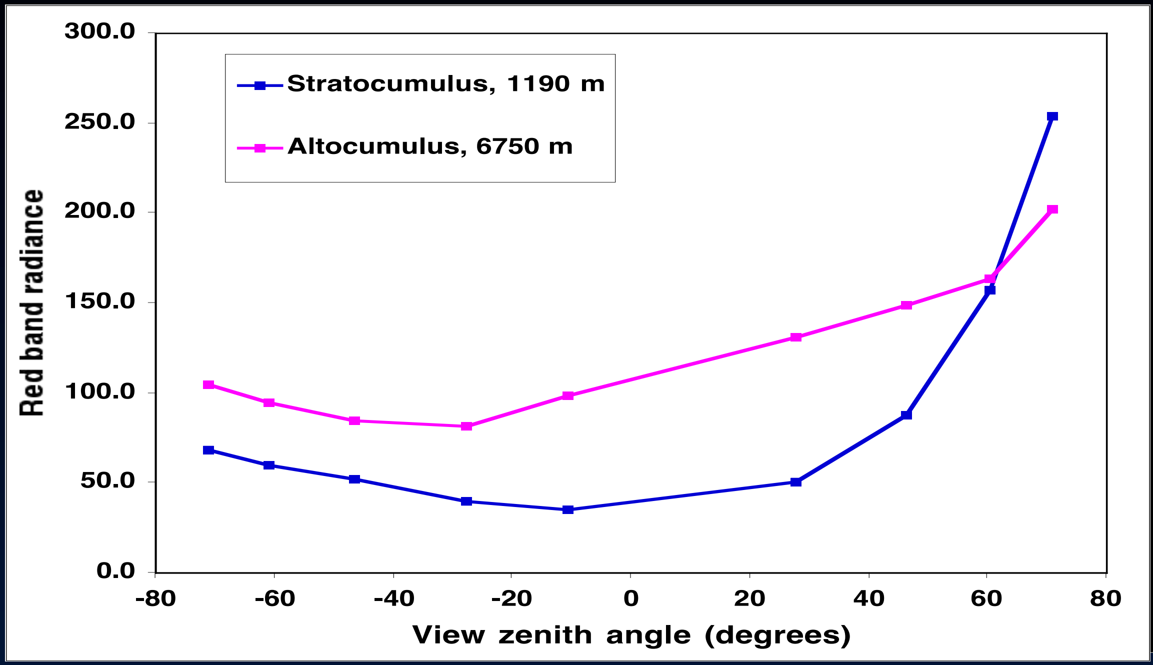

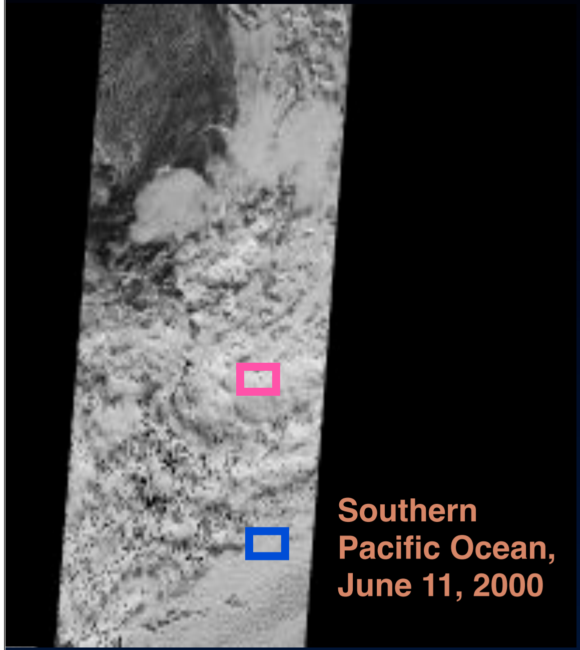

CONTENTS

- Contains “feature-referenced” top-of-atmosphere bidirectional reflectances
- Includes TOA albedos at fine (2.2. km) resolution for scene classification, and coarse (35.2 km resolution) for mesoscale radiation budget
- Regressions against CERES being used to facilitate narrow-to-broadband conversion

Is the Earth getting brighter?

Measurements of Earthshine on the Moon from Big Bear suggest an increase in Earth's albedo (Pallé et al., Science 2004) by about 4%

CERES Terra data show opposite trend (decrease of 2%), and about one-half of the CERES trend appears due to darkening of the optics due to UV exposure

What does MISR say?

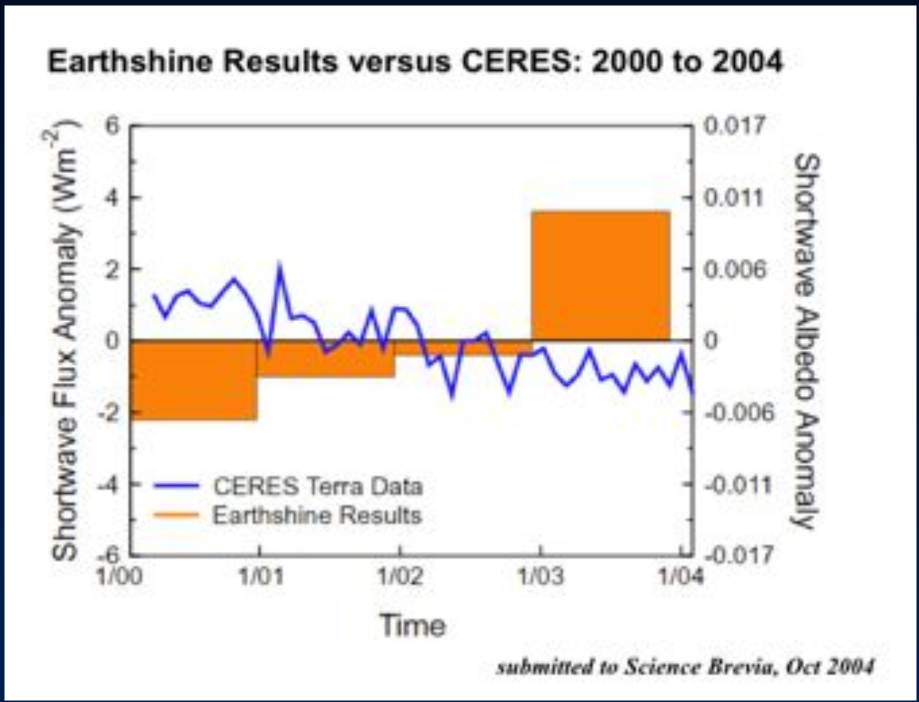

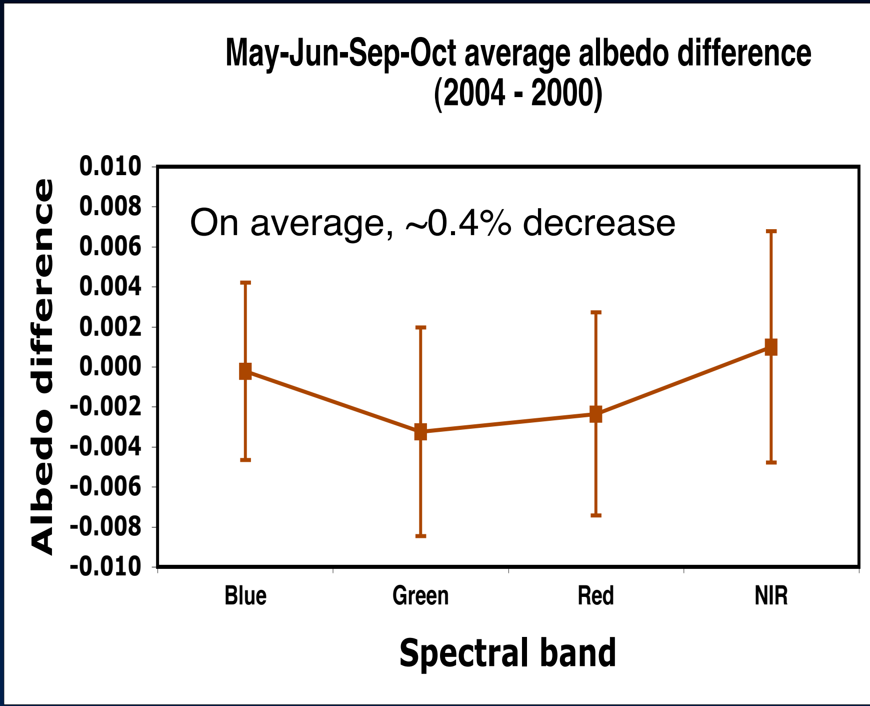

B. Wielicki et al. (2005), Science; R. Davies

Multiangle tests of cloud homogeneity

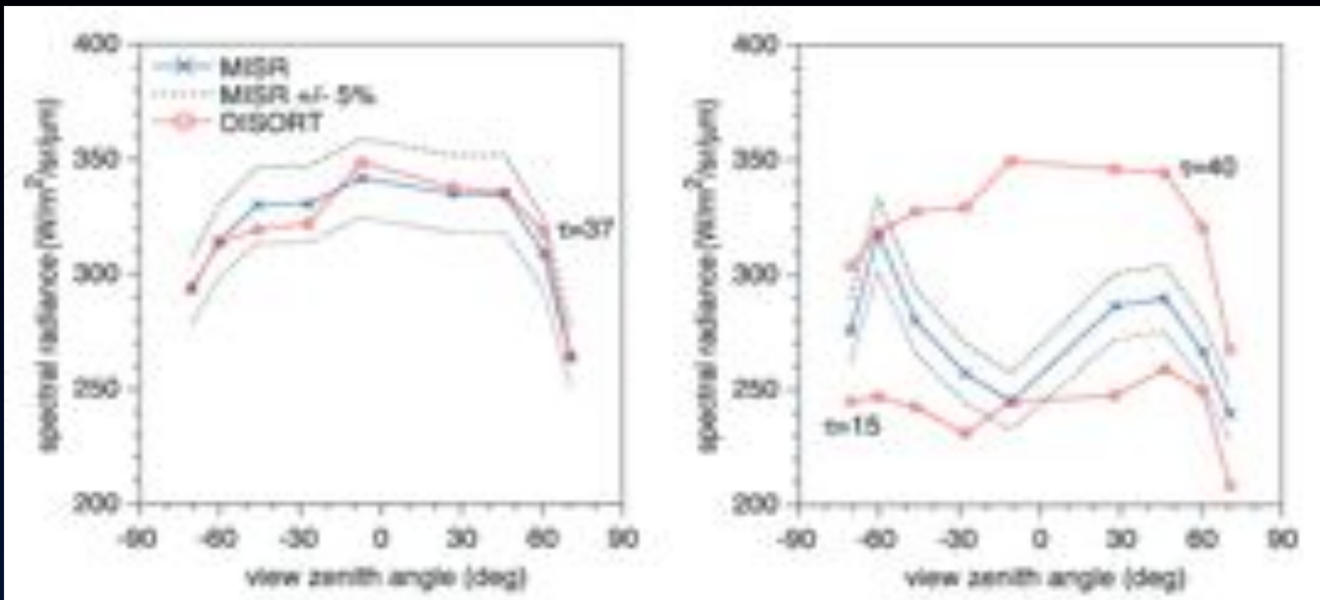

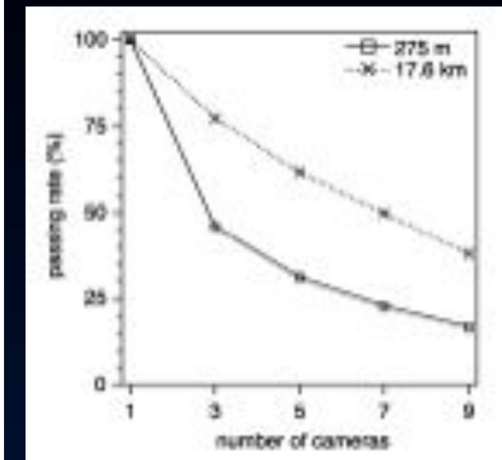

1-D theory fits
MISR observations

1-D theory does not fit
MISR observations

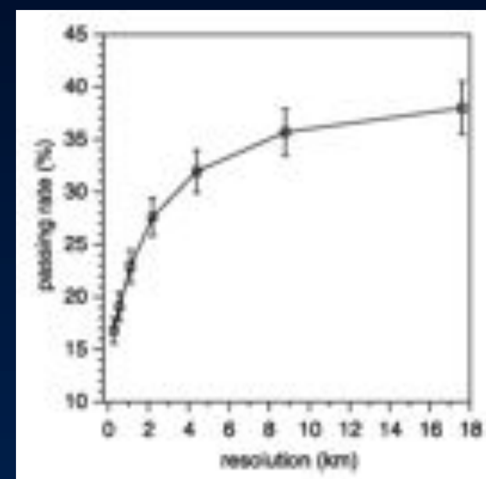

Multiangle data provides a physical consistency check on MODIS 1-D cloud retrieval assumption

Cloud morphology, not just cloud microphysics, plays a major role in determining TOA bidirectional reflectance

A. Horvath, R. Davies (2004), GRL

3-D reconstruction of convective clouds

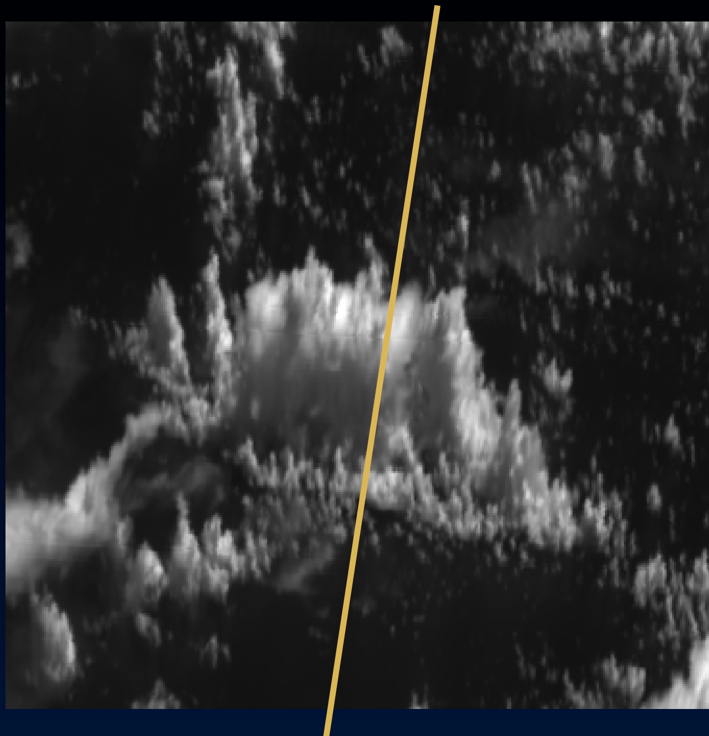

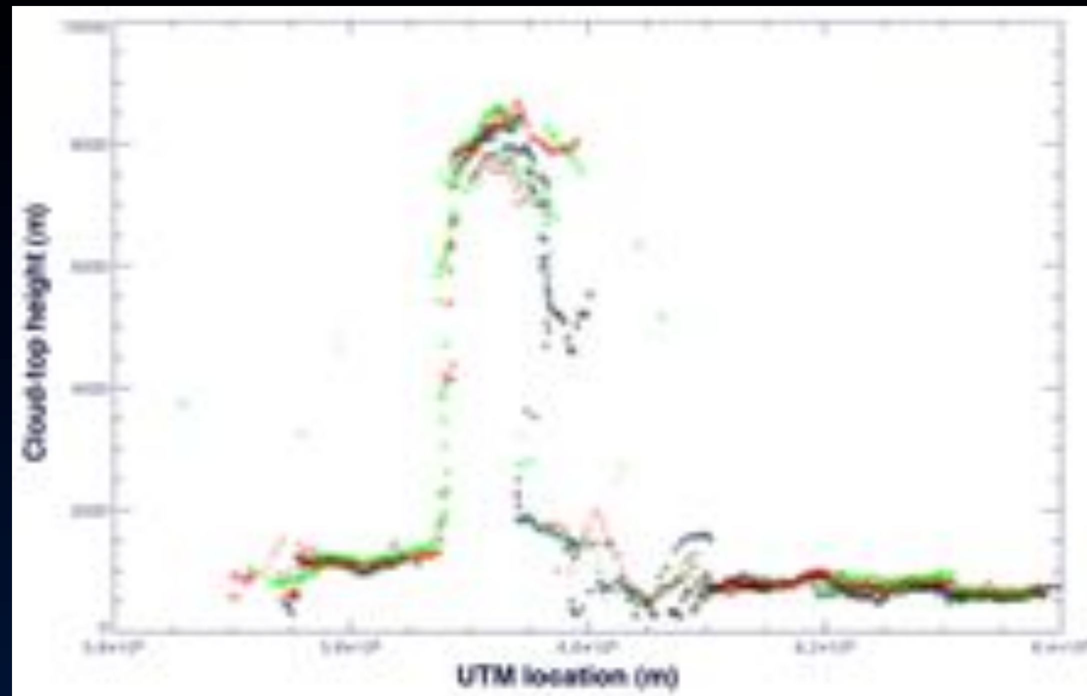

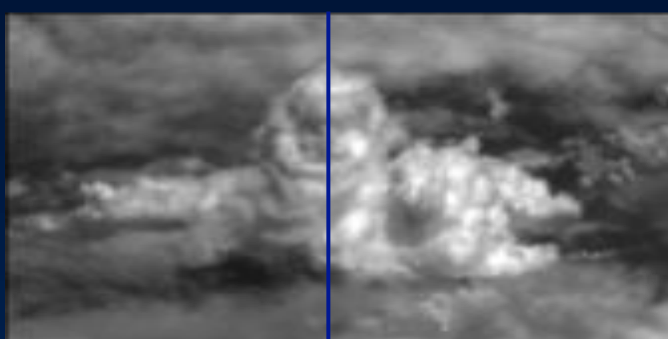

MISR 60° aft image

	nadir only	nadir+60°
cloud vertical extent	no information	10.5±0.8 km
extinction coefficient	no information	8–22 km^{-1} (higher at base)
cloud optical depth	> 60	150±30

G. Seiz, R. Davies et al., in preparation

L2 TOA/Cloud Classifiers Product (MIS04)

Angular signature cloud mask and height-binned cloud fractions

ATTRIBUTES

- Angular signature readily distinguishes clouds and low-lying polar fogs from snow and ice

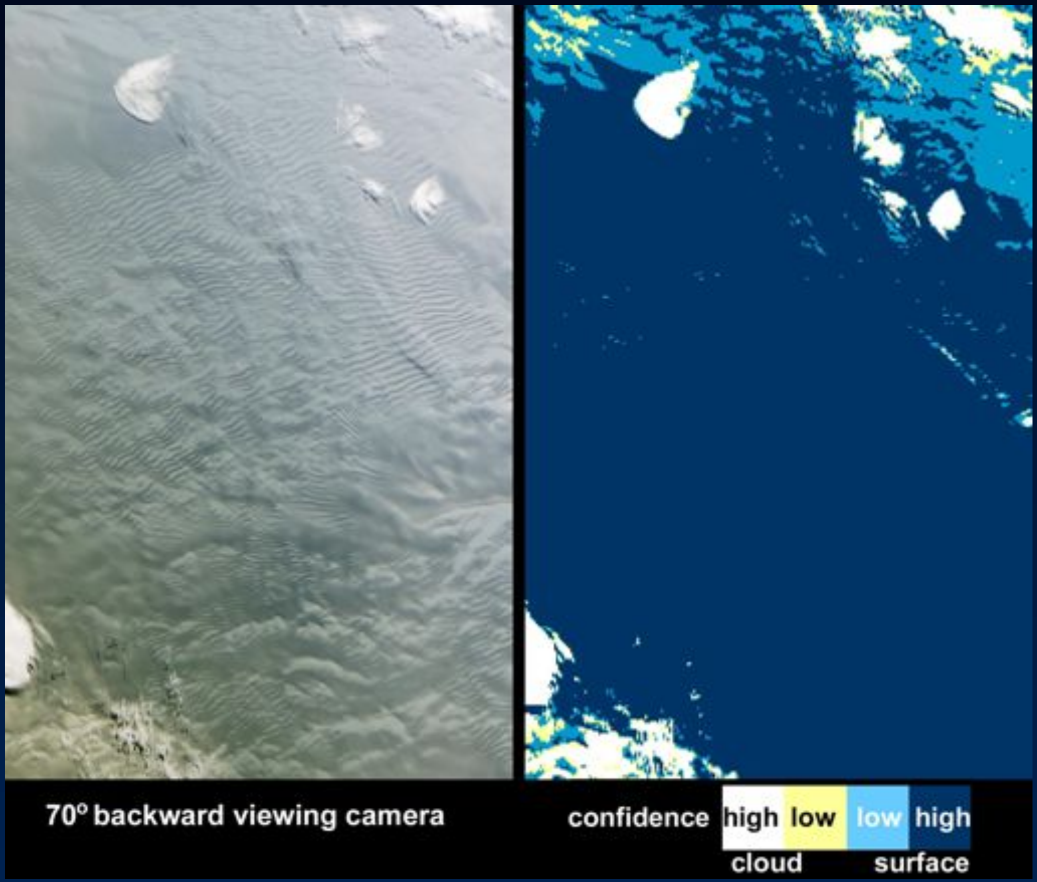

Megadunes in East Antarctica
Angular Signature Cloud Mask
16 December 2004

L2 Aerosol/Surface Product (MIS05)

Aerosol parameters

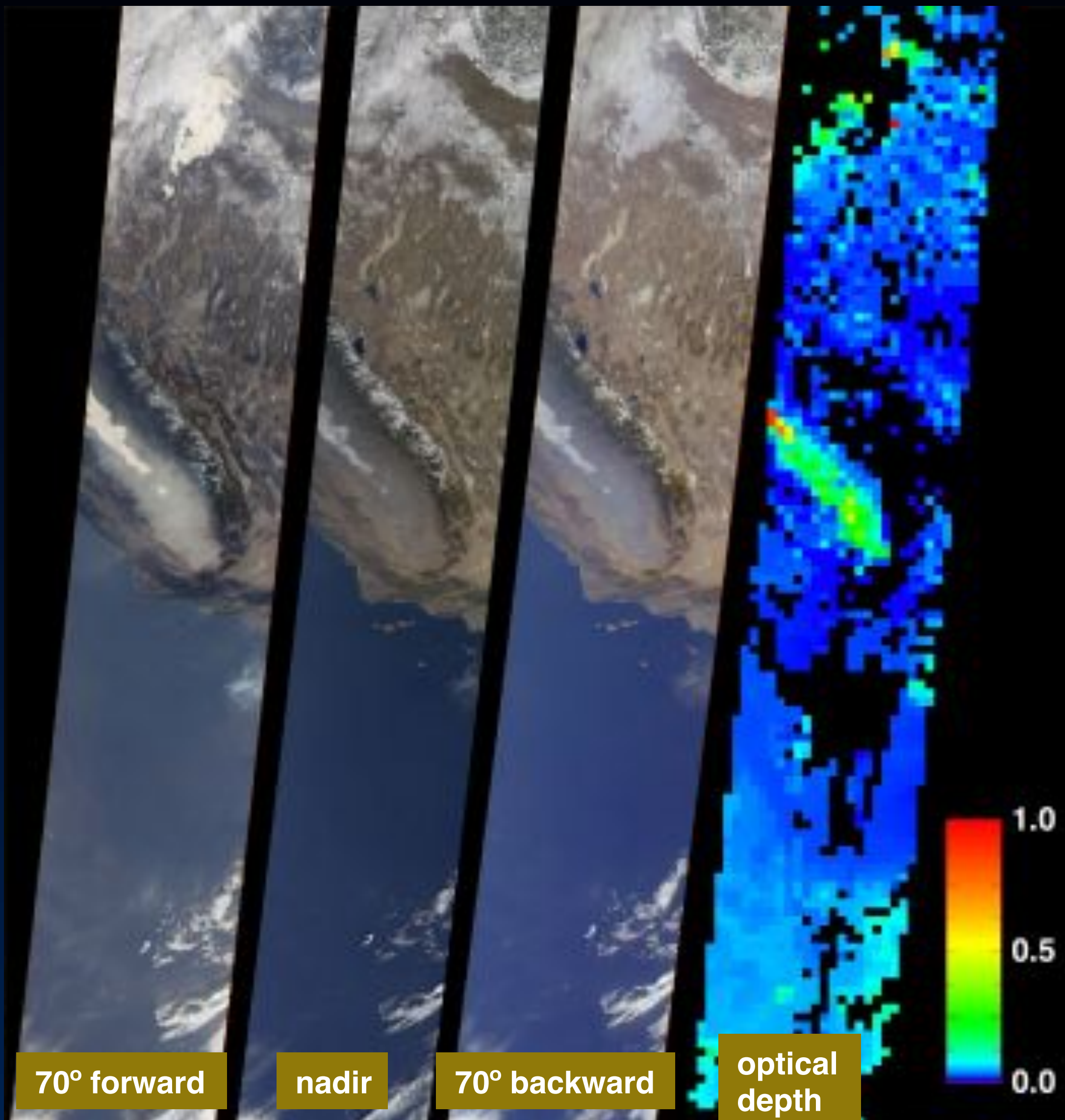

J. Martonchik et al. (2002), TGARS

ATTRIBUTES

- Different algorithms used over land and water
- Validation and quality assessment of aerosol optical depth performed
- Validation of aerosol particle properties under way

  --Angstrom exponent
  --Size binned fractions
  --Single-scattering albedo
  --Sphericity

Southern California and Southwestern Nevada
January 3, 2001

Retrieval of aerosol optical depth over a wide range of surface types

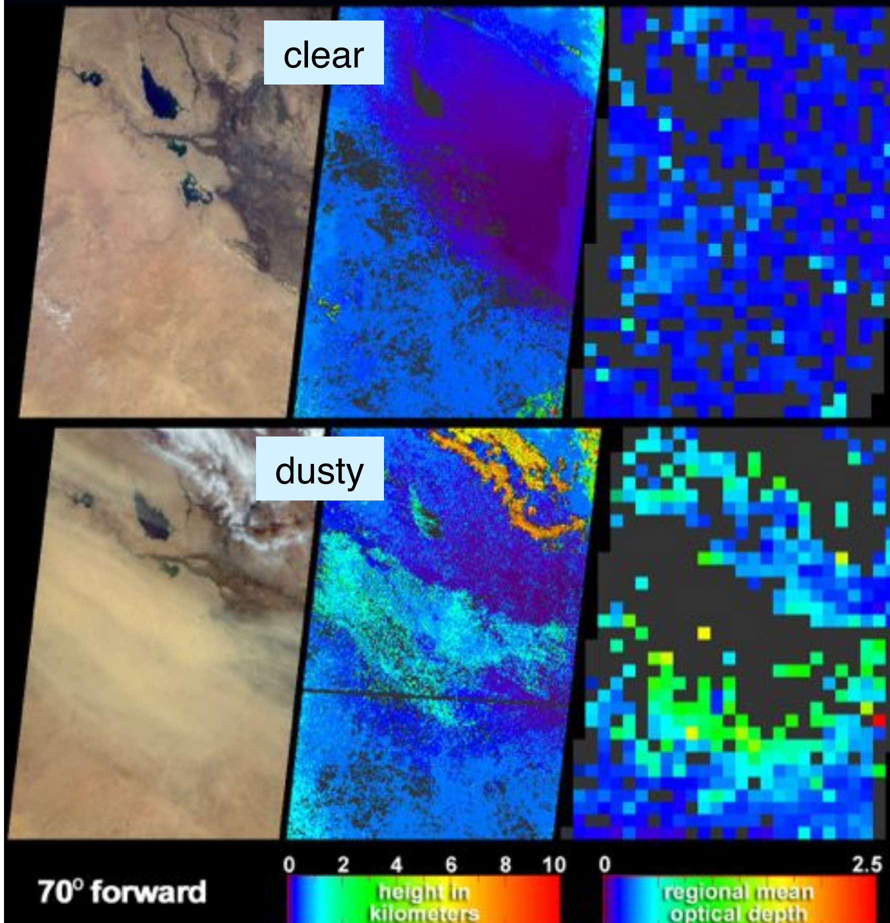

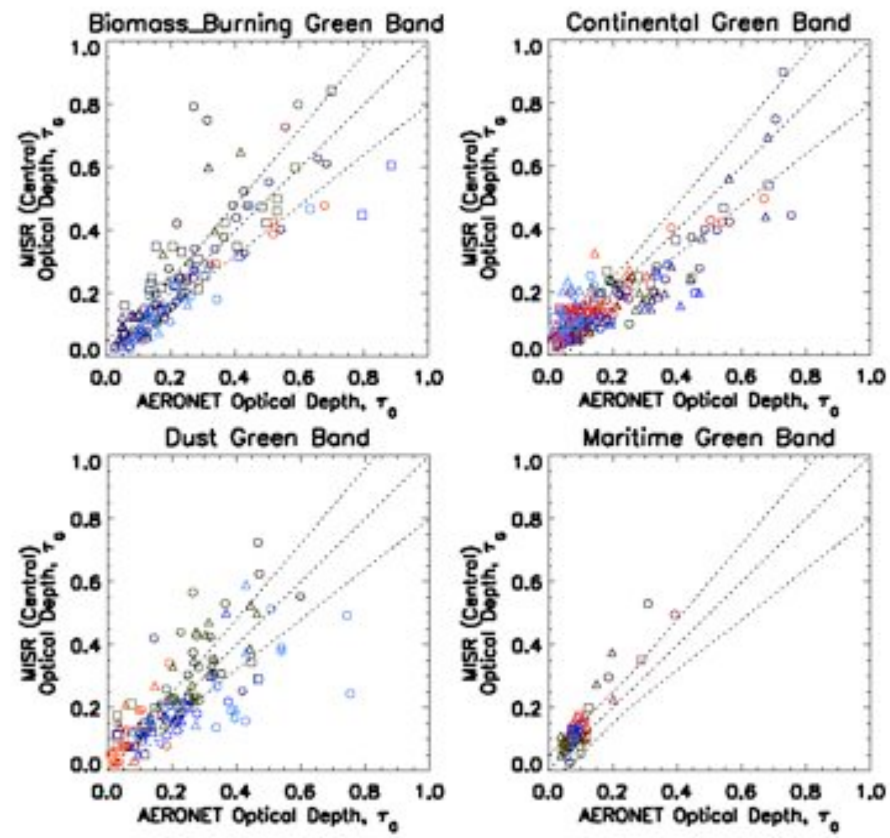

Iraq and Saudi Arabia, April 2004 (top) and May 2004 (bottom)

Global optical depth comparisons With AERONET

A vast pool of tiny particles over India

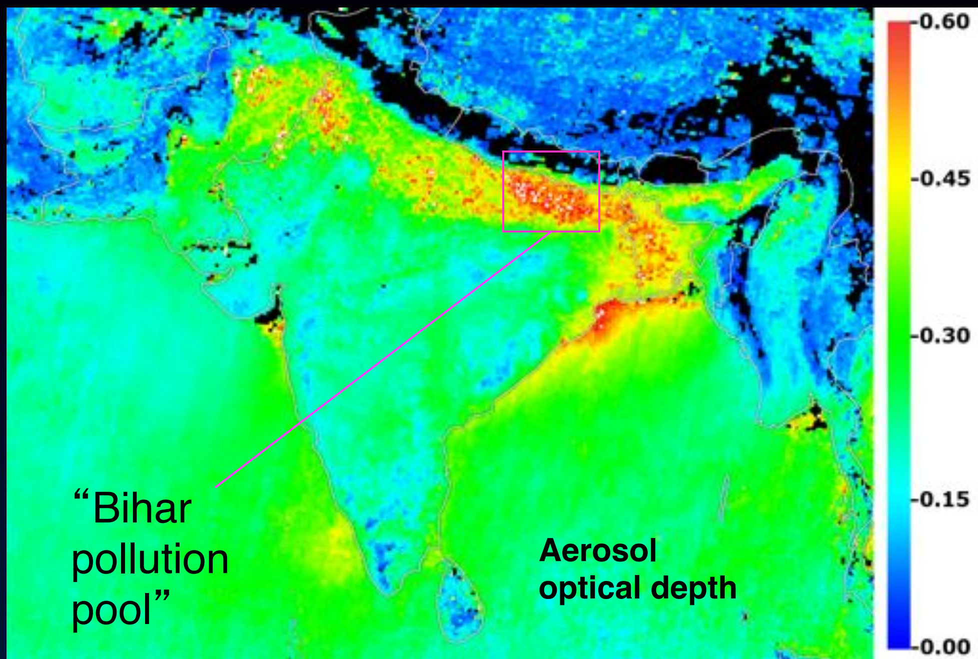

Winter aerosol climatology
derived from 4 years of MISR data

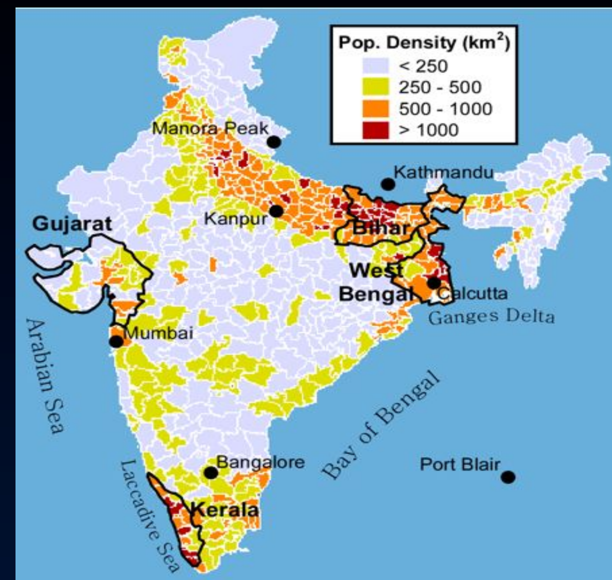

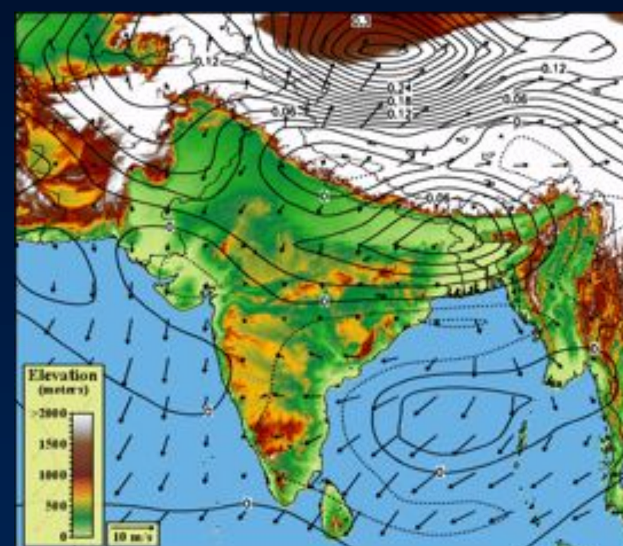

Topography and
winds

L. Di Girolamo et al. (2004), GRL

MISR sensitivity to aerosol particle properties

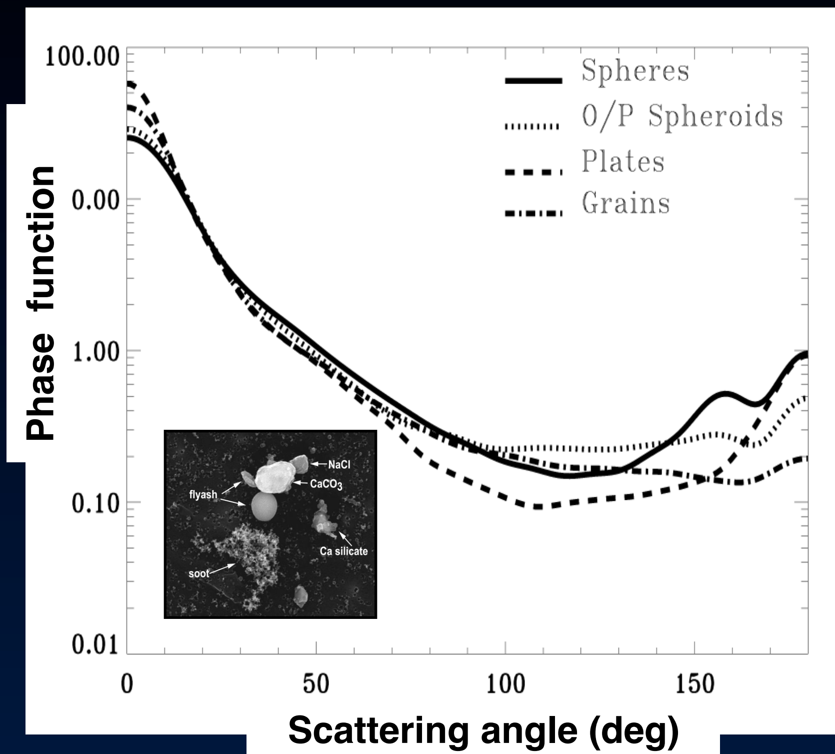

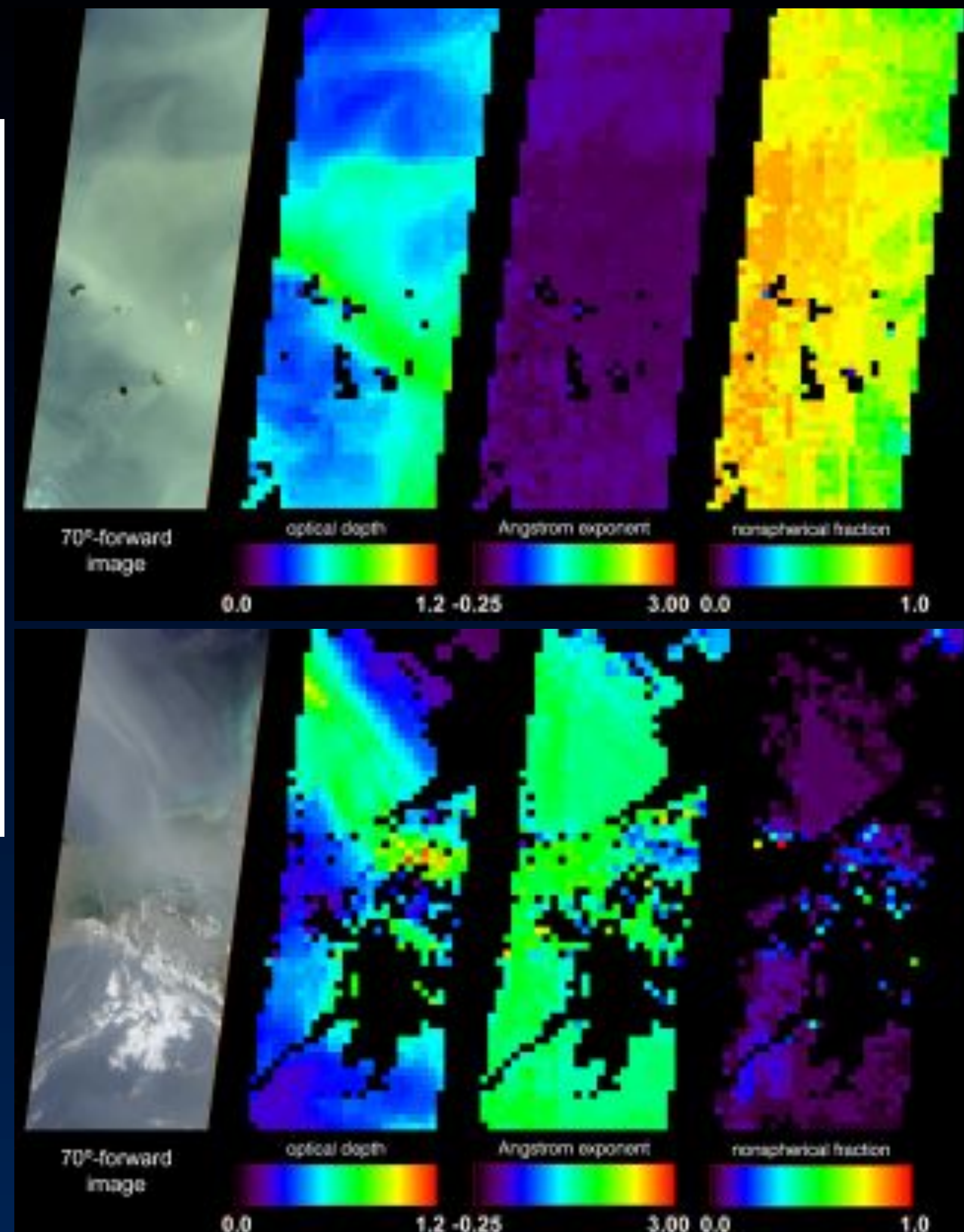

O. Kalashnikova et al. (2005), JGR

Mapping particulate air pollution

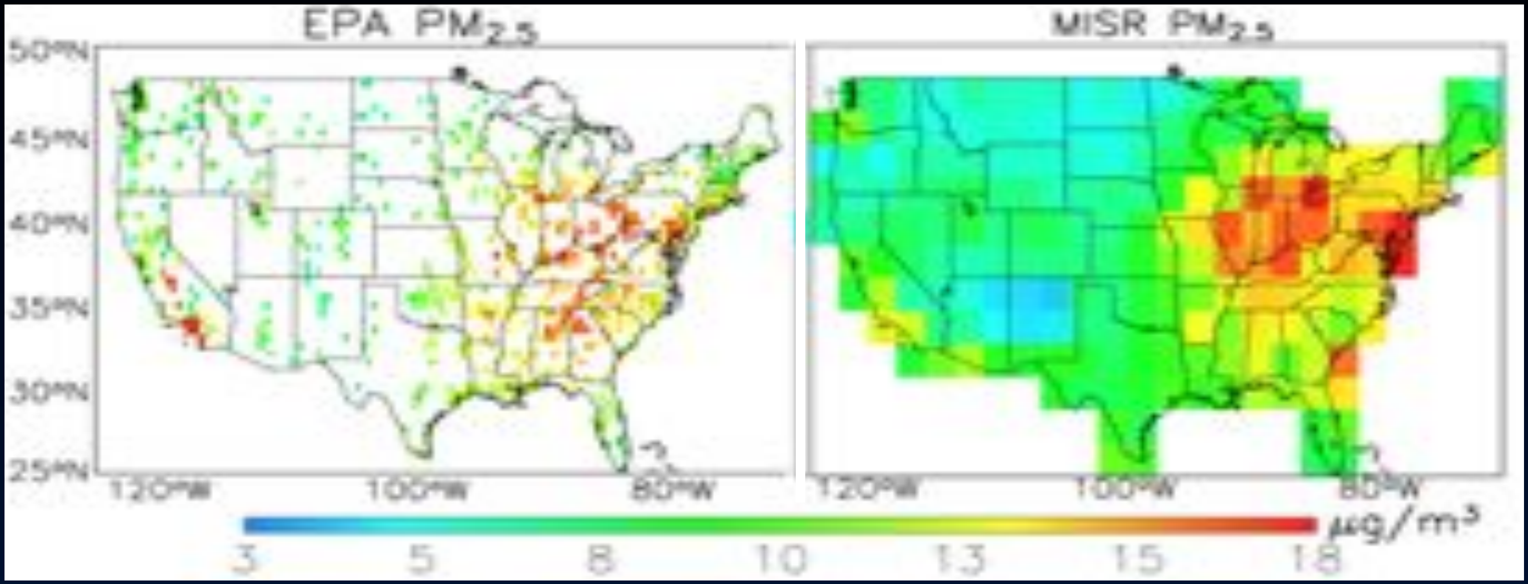

MISR column optical depths are scaled to PM2.5 using a chemical transport model (GEOS-CHEM)

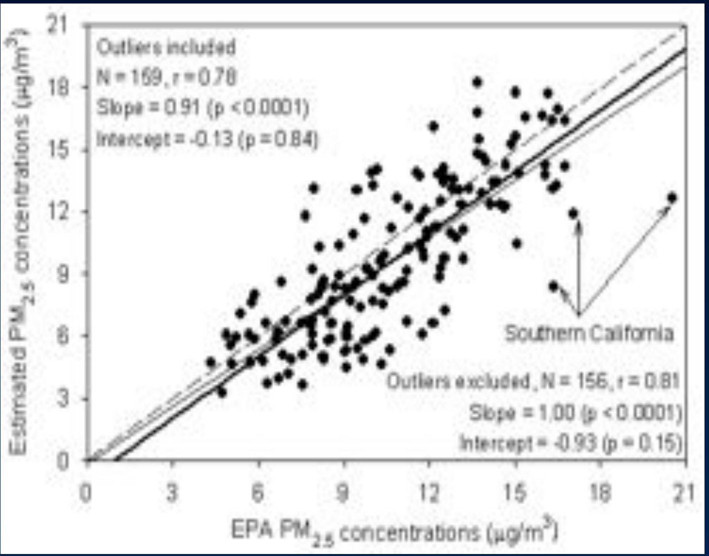

Y. Liu et al. (2005), JGR

L2 Aerosol/Surface Product (MIS05)

Surface parameters

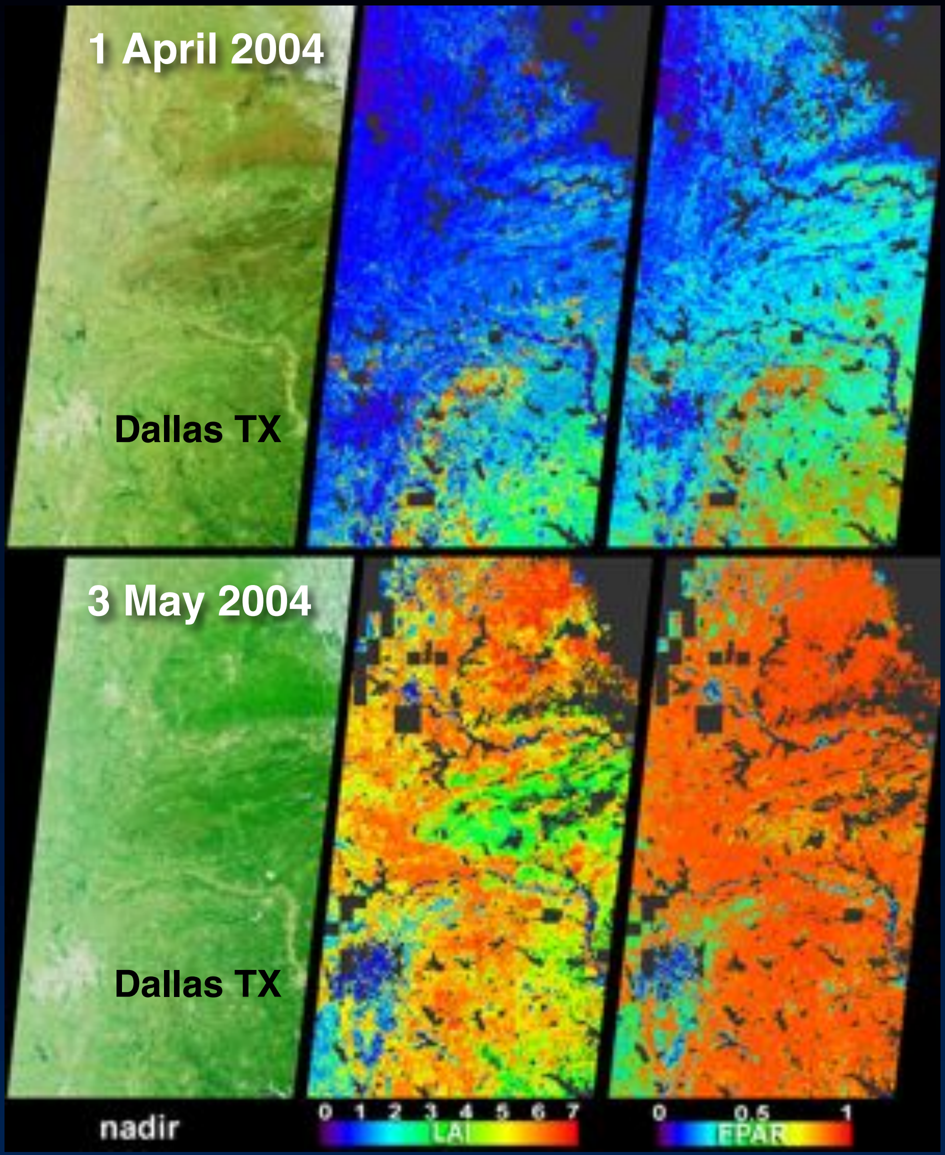

CONTENTS AND ATTRIBUTES

- Radiometric surface parameters (directional reflectances, albedos)

  Derived from single overpass-- no temporal compositing

  Atmospherically corrected

- Vegetation-related quantities (albedo-based surface NDVI, LAI, FPAR)

  LAI-FPAR retrievals are based on 3-D RT models

  Prescribed biome map is not required

Dependence of bidirectional reflectance on surface vegetation subpixel structure: parametric approach

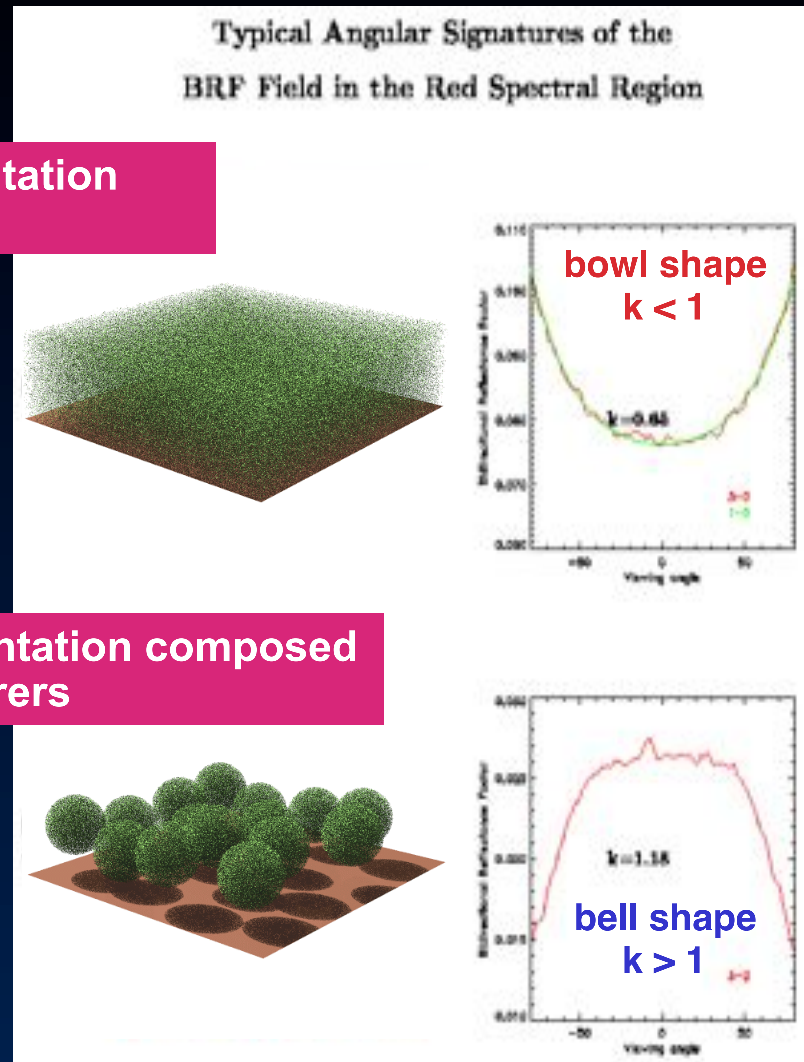

Structurally homogeneous canopy representation composed of finite-sized scatterers

Parametric models
(e.g., Rahman-Pinty-Verstraete function)
$BRF = BRF_0$ * Shape term * Asymmetry term
Shape term = $[\mu\mu_0(\mu+\mu_0)]^{k-1}$

Structurally heterogeneous canopy representation composed of clumped ensembles of finite-sized scatterers

Exponent k establishes whether BRF angular signature gets darker off-nadir (bell-shaped, $k > 1$) or brighter off-nadir (bowl-shaped, $k < 1$)

B. Pinty, N. Gobron, J-L. Widlowski, M. Verstraete

Bell and bowl-shaped BRFs

Manitoba and Saskatchewan, 17 April 2001

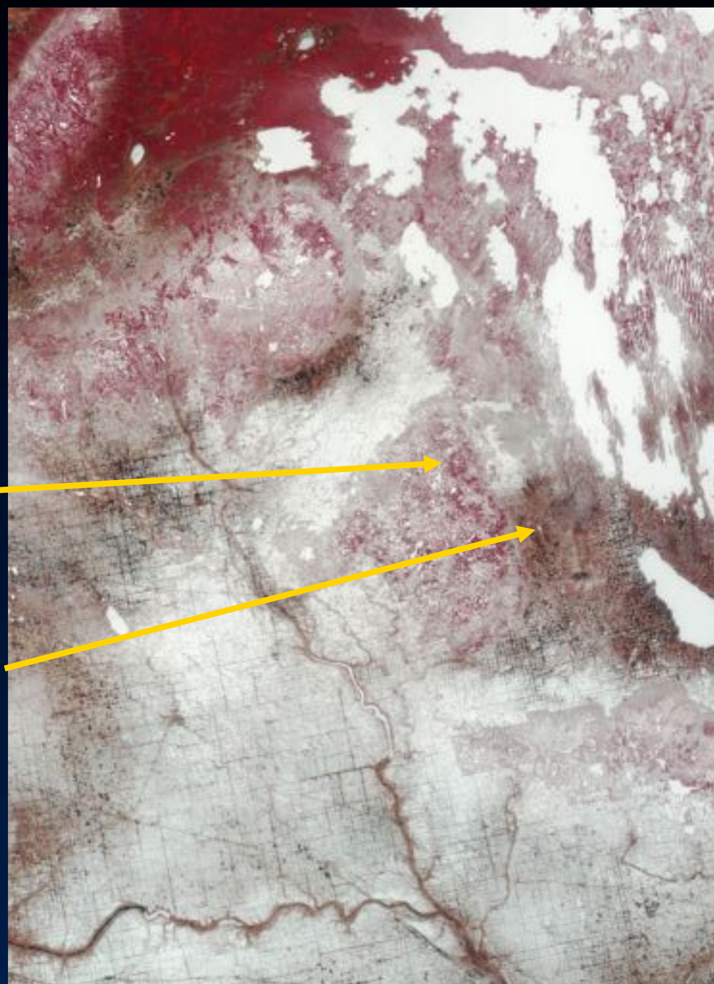

Nadir false-color composite:
RGB = near-IR, red, green

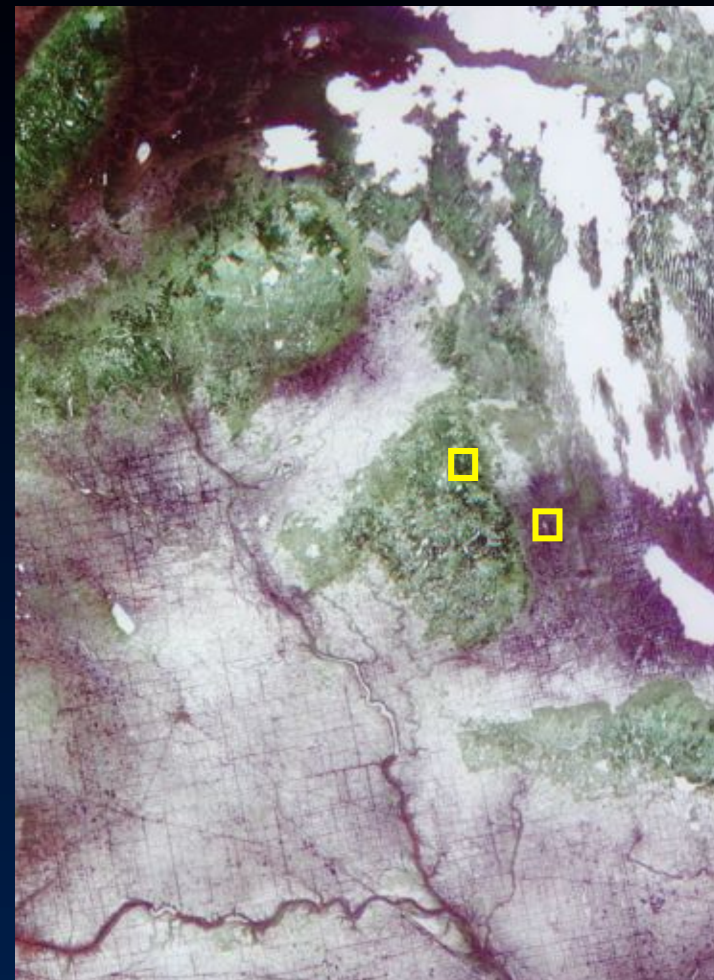

Multi-angle red band composite:
RGB = 60° backward, nadir, 60° forward

Bidirectional reflectances of surface vegetation as observed by MISR

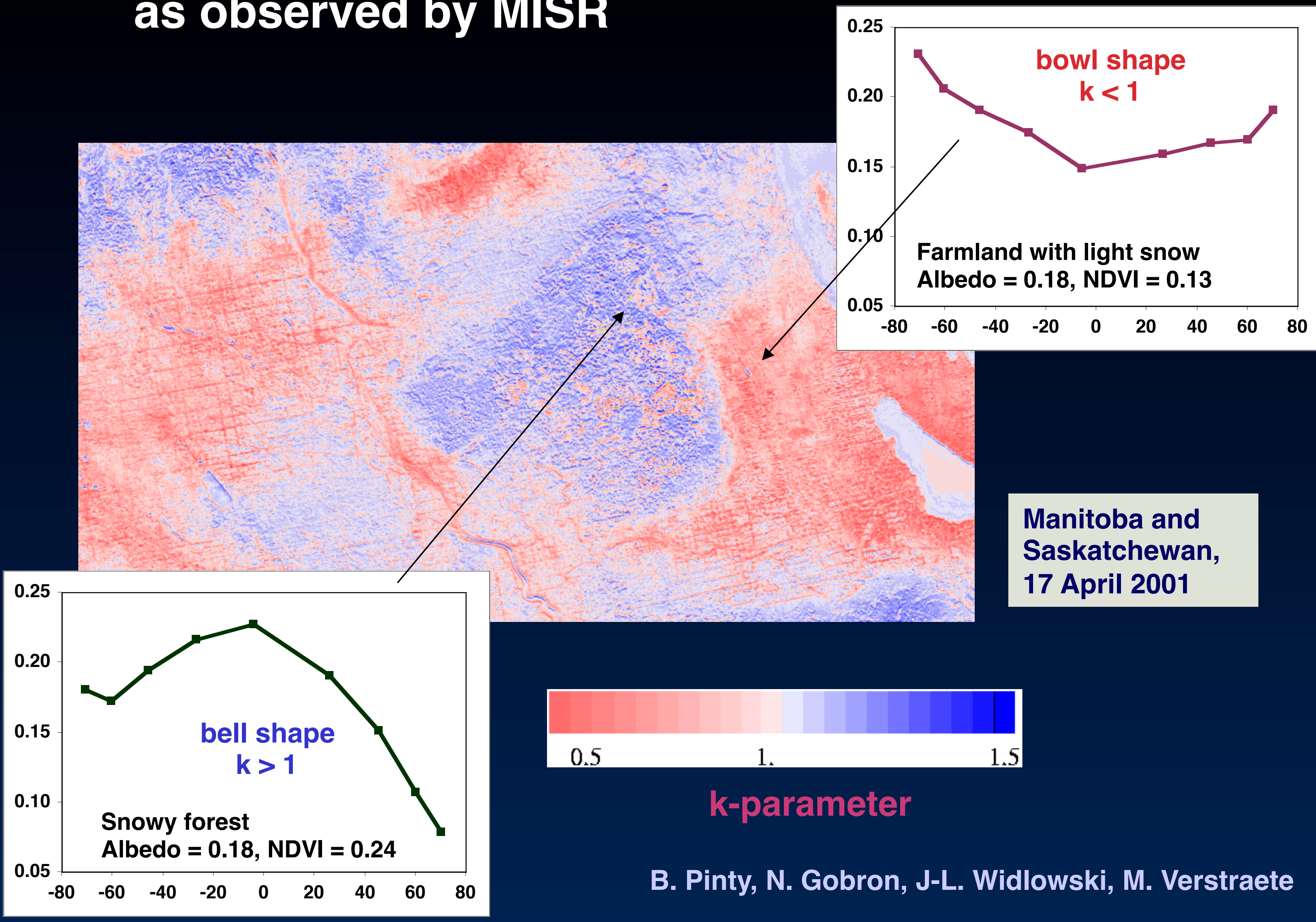

Manitoba and Saskatchewan, 17 April 2001

k-parameter

B. Pinty, N. Gobron, J-L. Widlowski, M. Verstraete

Mapping forest density over snow

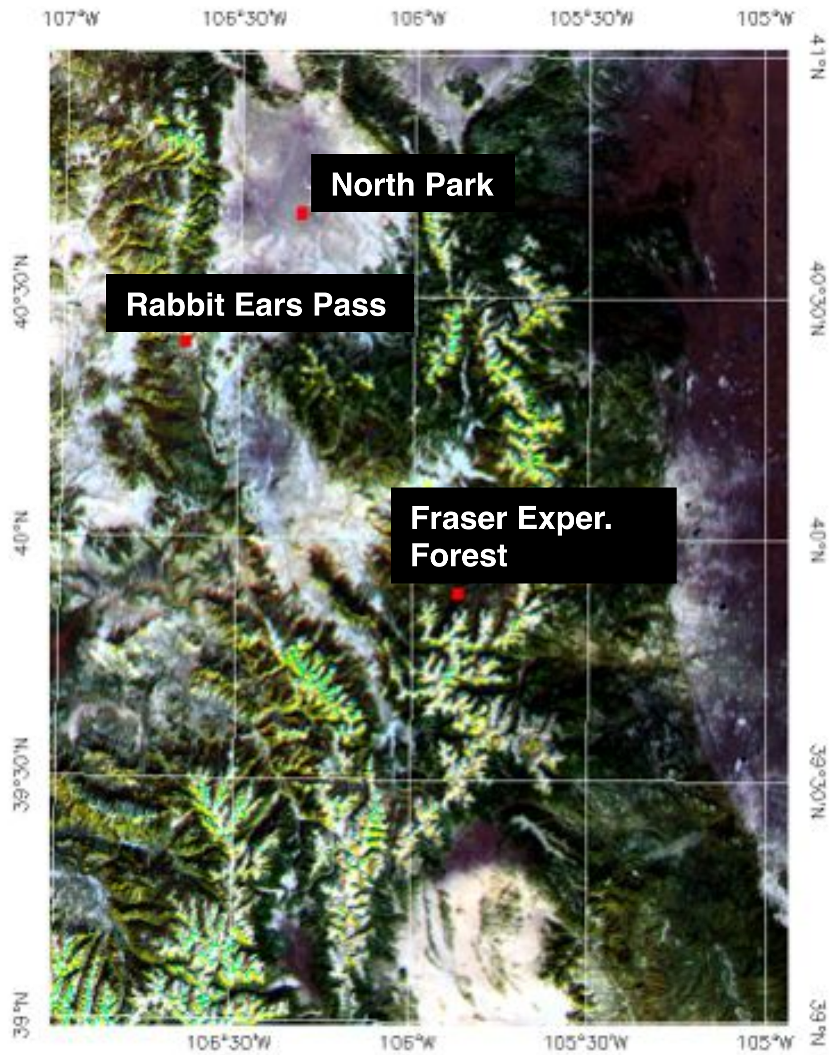

MISR multiangle composite

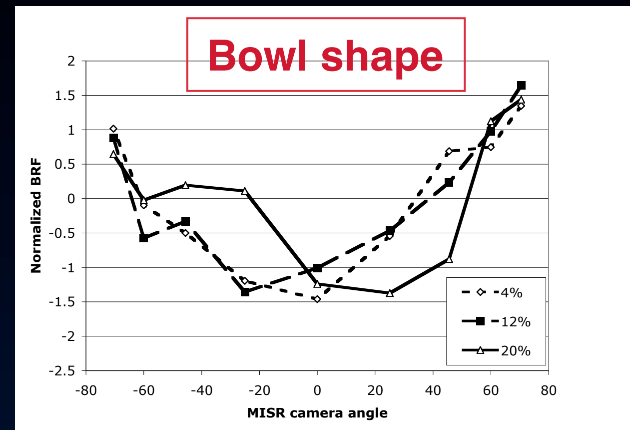

non-forested, low density

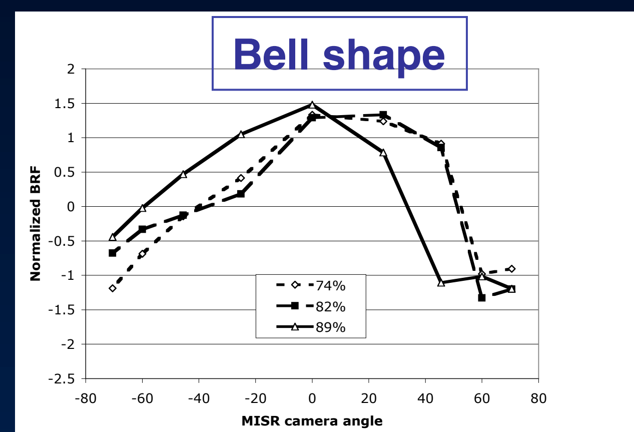

lodgepole pine, medium/high density

A. Nolin (2004), Hydrol. Proc.

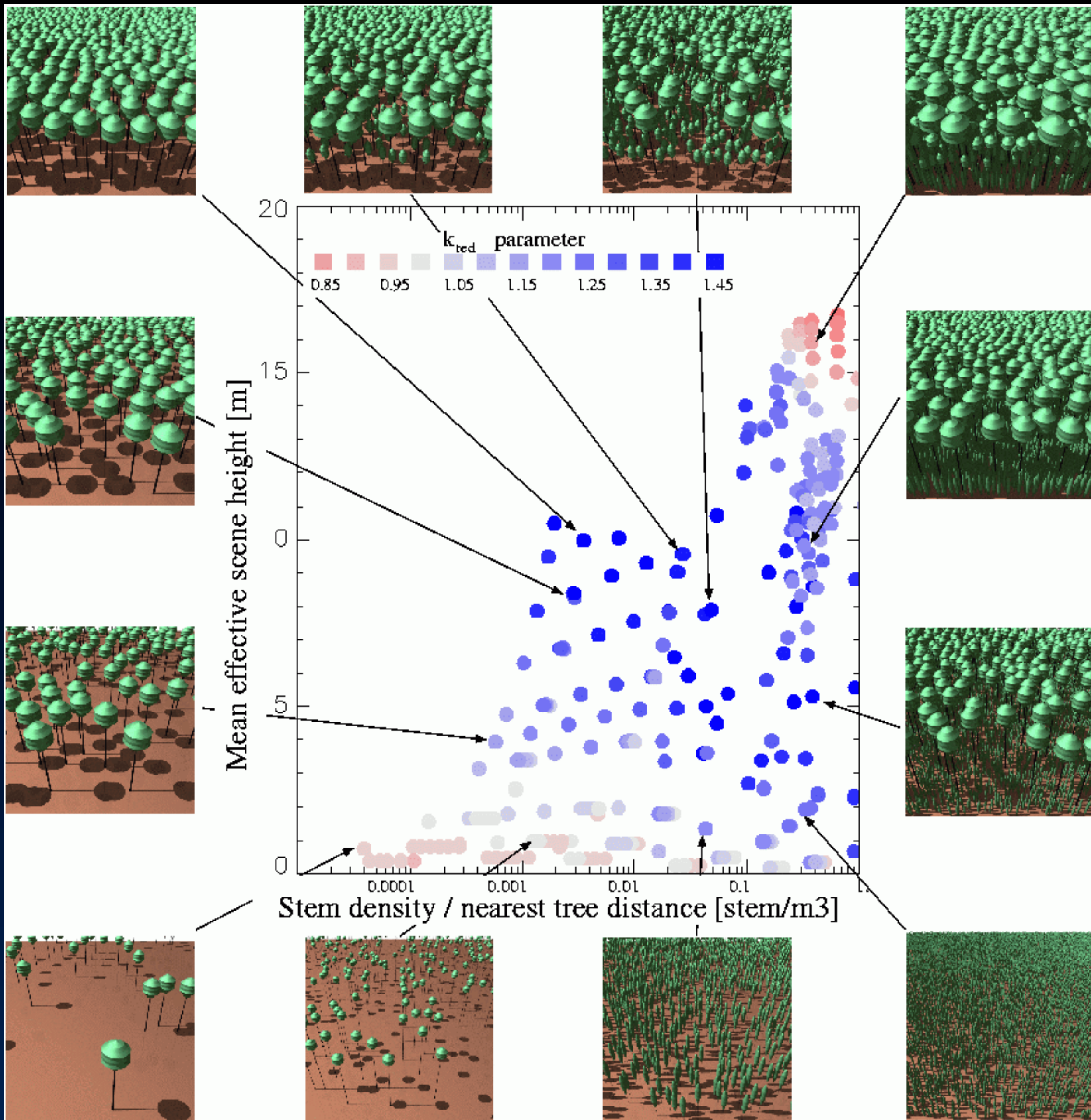

Relating bowl-shaped and bell-shaped BRFs to measures of canopy structure

Bell-shaped BRF:
Tree crowns of medium-high density against bright background

Bowl-shaped BRF:
Sparse vegetation and dense, closed canopies

J-L. Widlowski et al. (2004), Clim. Change

L3 Gridded Radiances (MIS06)

Means, variances, and covariances

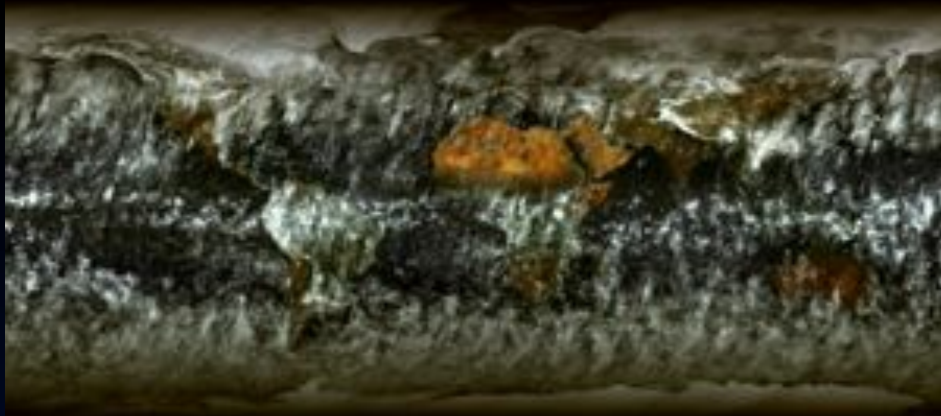

Nadir red, green, blue

Nadir near-infrared, red, green

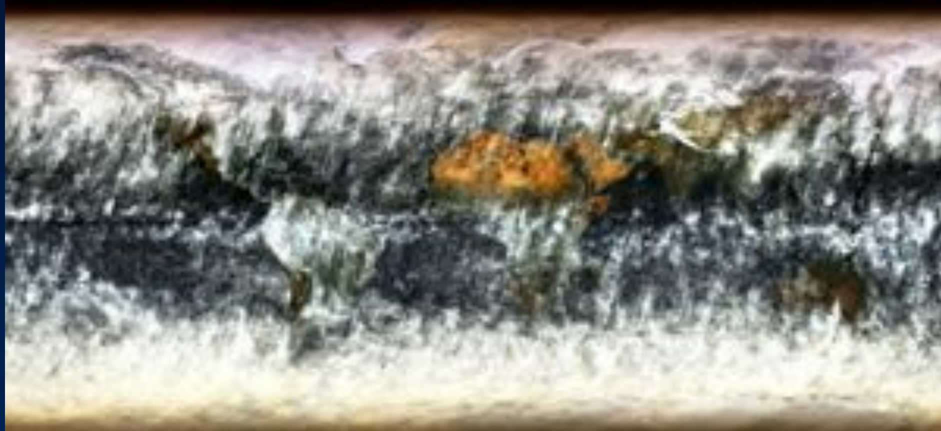

March 2002

70° forward: red, green, blue (N. hemisphere)
70° backward: red, green, blue (S. hemisphere)

L3 Gridded Aerosol (MIS08)

Global optical depths

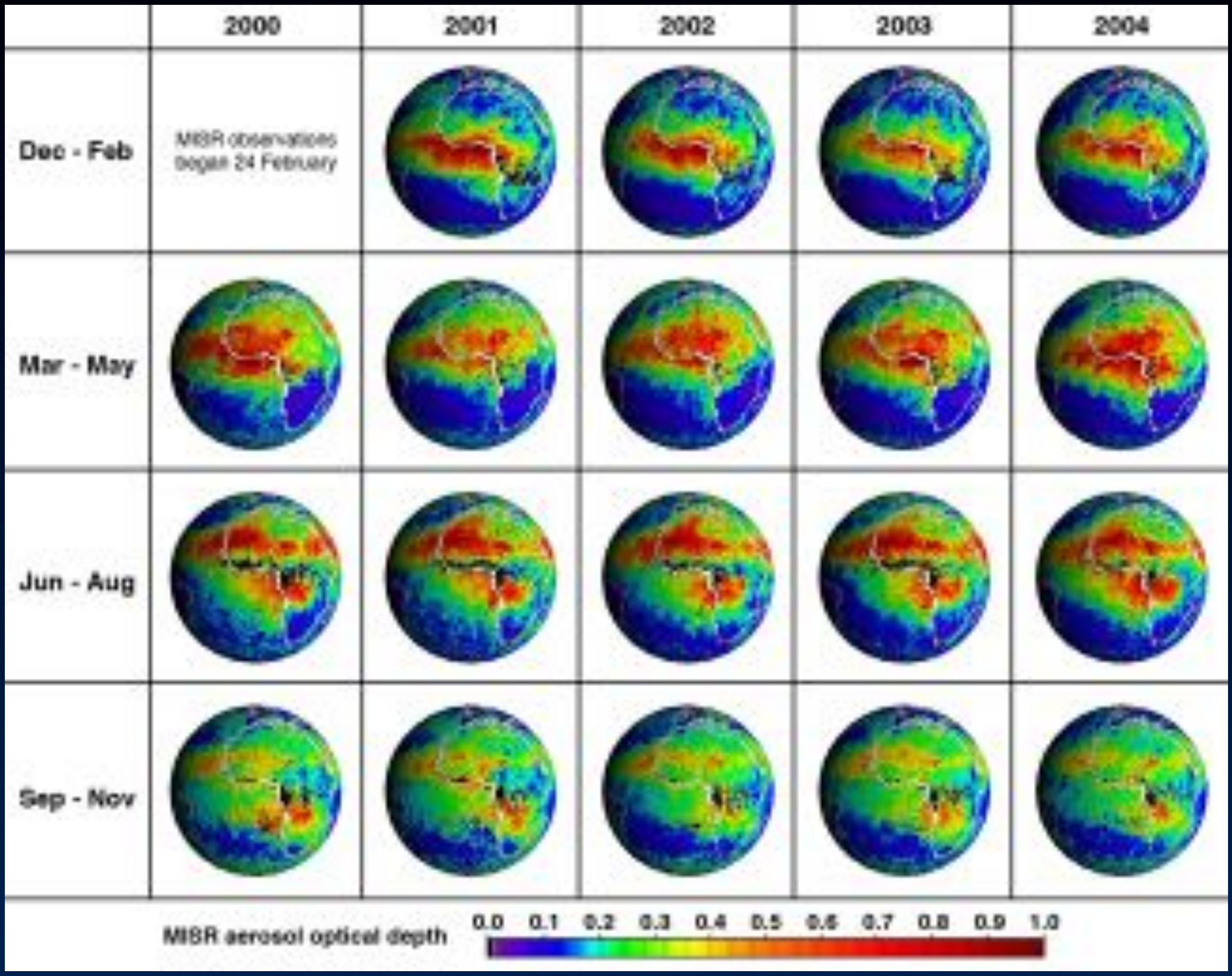

L3 Gridded Surface (MIS09)

Radiative and biogeophysical parameters

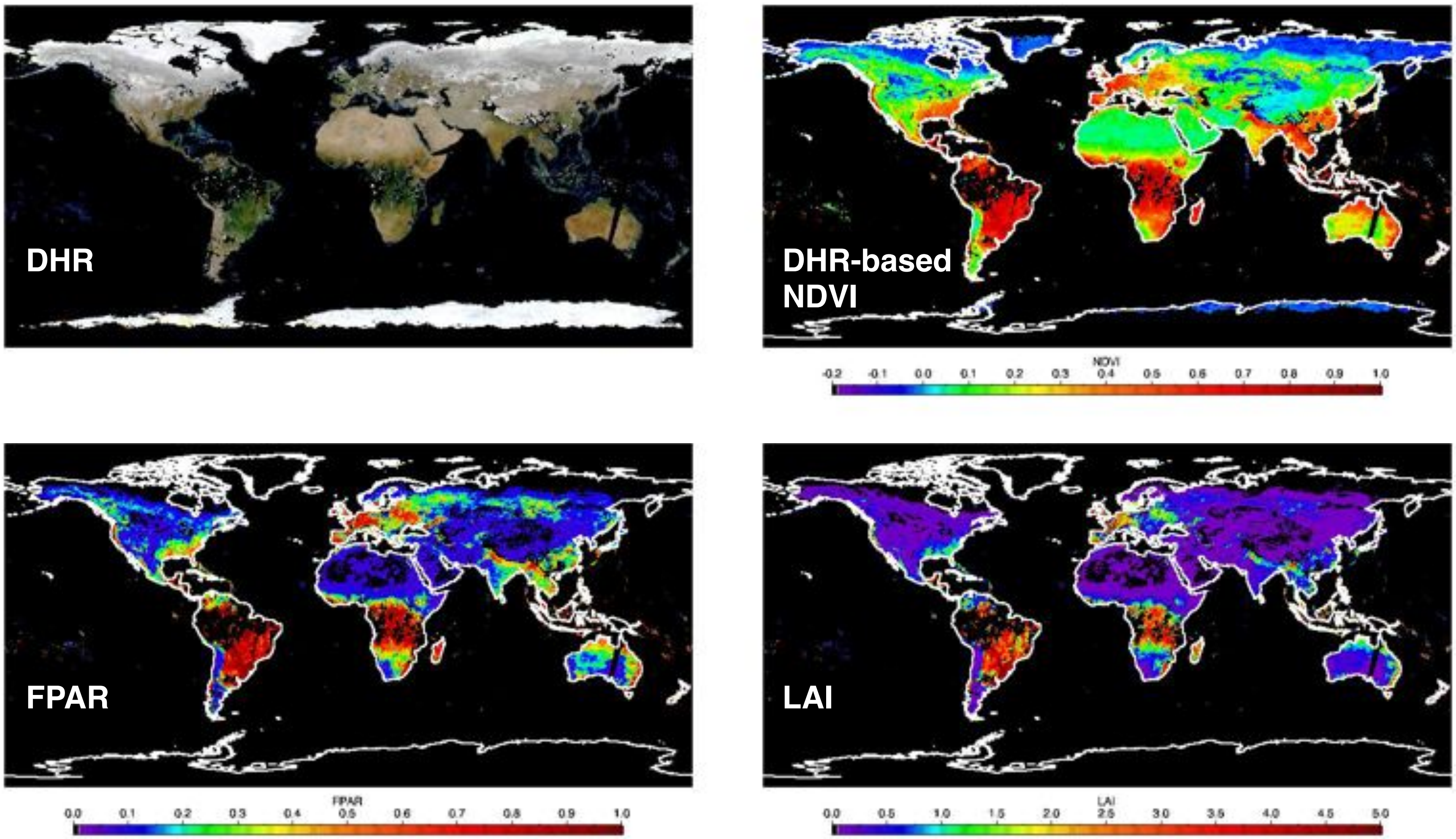

Additional products you might need

Ancillary Geographic Product
--contains latitudes, longitudes, elevations, scene classifiers for each 1.1-km pixel on the Space Oblique Mercator grid

Aerosol Climatology Product
--Aerosol Physical and Optical Properties (APOP) contains characteristics of the component particles used in the aerosol retrievals
--Mixture file contains characteristics of the particle mixtures used

Data maturity levels

Terra data products are given the following maturity classifications:

Beta: Minimally validated. Early release to enable users to gain familiarity with data formats and parameters. May contain significant errors.

Provisional: Partially validated. Improvements are continuing. Useful for exploratory studies.

Validated: Uncertainties are well defined, and suitable for systematic studies.

Mapping of data product maturity to version numbers found at:
http://eosweb.larc.nasa.gov/PRODOCS/misr/Version/version_stmt.html

Where to get help and information

LaRC DAAC User Services
larc@eos.nasa.gov

Langley Atmospheric Sciences Data Center DAAC
http://eosweb.larc.nasa.gov

MISR home page
http://www-misr.jpl.nasa.gov

We welcome your feedback and questions!
"Ask MISR" feature on the MISR web site